Fakultät für Medizin

Institut für Virologie

The role of non-parenchymal liver cells in early hepatitis B virus and hepatitis C virus infection

Xiaoming Cheng

Vollständiger Abdruck der von der Fakultät für Medizin der Technischen Universität München zur Erlangung des akademischen Grades eines

Doctor of Philosophy (Ph.D.)

genehmigten Dissertation.

Vorsitzender: Univ.-Prof. Dr. Roland M. Schmid

Betreuerin: Univ.-Prof. Dr. Ulrike Protzer

Prüfer der Dissertation:

1. Univ.-Prof. Dr. Mathias Heikenwälder

2. Univ.-Prof. Dr. Markus Gerhard

Die Dissertation wurde am 21.01.2015 bei der Fakultät für Medizin der Technischen Universität München eingereicht und durch die Fakultät für Medizin am 20.03.2015 angenommen.

Abstract

The human hepatitis B virus (HBV) and hepatitis C virus (HCV) belong to different families. However, both exhibit high species specificity and liver tropism. They can lead to acute and chronic infection and are major risks for hepatocellular carcinoma. Although the virus life cycles in hepatocytes have already been characterized in detail, the roles of liver non-parenchymal cells in early virus infection remain elusive.

HBV was detected in liver macrophages, Kupffer cells, after perfusion of human liver tissue. The first part of the study presented was aimed to identify the exact transcytosis pathway of HBV from Kupffer cells (KCs) to hepatocytes. Confocal microscopy revealed that HBV localized into recycling endosomes within the macrophages. They co-localized with lipoprotein derived free cholesterol and Niemann–Pick C1 (NPC1), a protein involved in cholesterol transport. Association of intracellular trafficking of HBV with cholesterol was further confirmed by treating cells with an inhibitor of the cholesterol transport, which blocked HBV recycling to the plasma membrane in parallel to inhibition of cholesterol effllux. Furthermore, under pulse chase conditions, ApoA-1 or HDL contained in human serum induced HBV re-secretion into the cell culture supernatant in association with cholesterol export. Finally, after co-culturing HBV loaded KCs with primary human hepatocytes (PHHs), HBV trans-infection of hepatocytes was detected. Taken together, in the first part of the study we found that HBV utilized the cholesterol transport machinery to transcytose through liver macrophages and infect hepatocytes in trans.

The second part of the study focused on the interaction of HCV with non-parenchymal liver cells during the early infection. To mimic the physiological situation, an *ex vivo* human liver perfusion model for HCV was established. Using this model, firstly, permissiveness of perfused liver tissue to HCV infection was evidenced by increasing numbers of HCV genomes released into the perfusate during 48h perfusion. Secondly, a time course analysis by immune staining showed that KCs but even more prominently liver sinusoidal endothelial cells (LSECs) took up HCV at the early time points. Hepatocytes only became positive for HCV after prolonged perfusion. Thirdly, 48h after initial exposure to HCV, analysis of hepatic gene expression of perfused human liver tissues by qRT-PCR showed induction of interferons (IFNs).

To test whether the sequential uptake of HCV in human liver tissue also reflected trans-infection, HCV loaded KCs were co-cultured with Huh7.5 cells for three days. The results supported that HCV could trans-infect hepatocytes via binding to DC-SIGN on KCs as well as L-SIGN on LSECs. To test if KCs and LSECs contributed to the early IFN induction observed in *ex vivo* perfused liver, primary human KCs and primary murine LSECs were exposed to HCV *in vitro*. HCV exposure induced NF-κB activation and enhanced IFN-expression already after 6h. To disclose the sensory pathway resulting in this induction, wild type mice and TLR3-deficient mice were inoculated with HCV. Only wt mice but not TLR3-deficient mice showed an induction of pro-inflammatory cytokines in the liver, confirming that the innate immune activation was TLR3 dependent.

From these data we concluded that HCV particles entering the liver are efficiently sequestered by KCs and LSECs. This may contribute to efficient hepatocytes infection in trans via SIGN molecules binding on one side and on the other side leads to a TLR3-dependent innate immune activation.

Abbreviation

ABC	ATP-binding cassette transporter
Abs	Antibodies
AcLDL	Acetylated low density lipoprotein
Apo	Apoprotein
BSA	Bovine Serum Albumin
CHB	Chronic Hepatitis B
cLD	cytosolic Lipid Droplets
DC-SIGN	Dendritic Cell-Specific Intercellular adhesion molecule-3-Grabbing Non-integrin
DHBV	Duck Hepatitis B Virus
DMSO	Dimethylsulfoxide
EMCV	Encephalomyocarditis Virus
ER	Endoplasmic Reticulum
ERAD	ER-Associated Degradation
GSHV	Ground Squirrel Hepatitis Virus
h.p.i	hour post infection
HBcAg	Hepatitis B core Antigen
HBeAg	Hepatitis B e Antigen
HDL	High Density Lipoprotein
HHBV	Heron Hepatitis B Virus
HIV	Human Immunodeficiency Virus
HSC	Hepatic Stellate Cell
IDL	Intermediate Density Lipoprotein
IFN	Interferon
IRES	Internal Ribosomal Entry Site
IRF	Interferon regulatory factor
KC	Kupffer Cell
LAMP-1	Lysosomal Associated Membrane Protein 1
LPS	Lipopolysaccharide

LSEC	Liver Sinusoidal Endothelial Cell
L-SIGN	Liver/lymph node-Specific Intercellular adhesion molecule-3-Grabbing Non-integrin
LuLD	Luminal Lipid Droplet
LVP	Lipoviral Particle
MAF	Membrane Associated Foci
MDM	Monocyte Derived Macrophages
MLV	Murine Leukemia Virus
NBD	NNitrobenzoxadiazole
NPC1	Niemann–Pick C1
NTCP	Sodium Taurocholate Co-Transporting Polypeptide
NTR	Non-Translated Region
PHH	Primary Human Hepatocyte
PRR	Pattern Recognition Receptor
rcDNA	relaxed-circular DNA
RdRp	RNA-dependent RNA polymerase
REM	Replication Enhancing Mutation
RGHV	Ross Goose Hepatitis Virus
RIG-1	Retinoic Acid-Inducible Gene 1
RT	Reverse Transcription
SMA	Smooth Muscle Actin
SNP	Single Nucleotide Polymorphism
STHBV	Stork Hepatitis B Virus
TAG	Triacylglycerol
VLDL	Very Low Density Lipoprotein
VP	Viral Particle
WHV	Woodchuck Hepatitis Virus

1. Introduction

1.1 The liver

1.1.1. Gross anatomy and function of the liver

The liver is the largest solid organ in the body and weighs about 1400 g in females and 1800 g in males. It lies on the right side of the abdomen and anatomically composed of two lobes. The liver has a unique dual blood supply: 80% is delivered through the portal vein, which drains the spleen and intestines; the remaining 20%, the oxygenated blood, is delivered by the hepatic artery[1].

The liver is a vital organ that fulfills diverse but closely connected functions, for example: 1. Detoxification: liver removes and excretes body wastes and hormones as well as drugs and other foreign substances[2]. 2. Production: liver is responsible for the production of several vital protein components of blood plasma like prothrombin, fibrinogen, and albumins[2]. 3. Immune regulation: liver produces immune cytokines against invading pathogens. The liver also has other important but less immediate functions including production of biles to aid in digestion, storing substances like certain vitamins, minerals, and sugars[2].

1.1.2. Microanatomy and cells of the liver

The liver is a complex three-dimensional structure that can be divided into subunit of lobules. The center structure of a lobule is the terminal hepatic venule (“central vein”) and the periphery is delineated by portal triads. Structures within these tracts include bile duct and ductules, hepatic artery, portal vein, lymphatic vessels, nerve fibers, and a few inflammatory cells. Blood flow from portal vein to central vein in channels named sinusoids. The areas between those vessels are filled with parenchymal and non-parenchymal cells[2].

Hepatocytes are the parenchymal cells of the liver. They occupy almost 80% of the total liver volume and are the chief functional cells in the liver. They are polygonal in shape and their plasma membranes are separated by tight junctions into sinusoidal–basolateral and canalicular–apical domains. Hepatocytes are arranged in plates and are shielded from blood in the sinusoids by liver endothelial cells[2, 3].

Liver sinusoidal endothelial cells (LSECs) constitute the lining wall of the hepatic sinusoids. They are characterized by the presence of fenestrations *in vivo*, which could filtrate blood passing through to allow free diffusion of small molecules (≤ 10nm) from sinus into the space of Disse[4]. LSECs show huge endocytic capacity for many ligands including glycoproteins, immune complexes and transferrin[5, 6]. LSECs may function as antigen-presenting cells in the context of both MHC-I and MHC-II restriction with the resulting development of antigen-specific T-cell tolerance[7]. They are also active in the secretion of cytokines, nitric oxide, and distinct extracellular matrix components[6].

Kupffer cells (KCs) are liver specific macrophages. They are ameboid in shape and predominantly distributed in the lumen of hepatic sinusoids adhering to the surface of LSECs[8]. KCs can clear particulate and foreign materials from the portal circulation and in turn, produce inflammatory mediators. They are also involved in lipoprotein clearance as well as bilirubin production[9].

Hepatic stellate cells (HSCs) are located in the space of Disse between the LSECs and hepatocyte plates. They account for 5%–8% of the cells in the liver and have several important functions like vitamin A storage, extracellular matrix production and contraction or dilation of the sinusoidal lumen in response to endothelin. A characteristic feature of HSCs is that when the liver is injured due to viral infection or hepatic toxins, damaged hepatocytes and immune cells can secret signal molecules causing trans-differentiation of HSCs into activated myofibroblast-like cells[10-12].

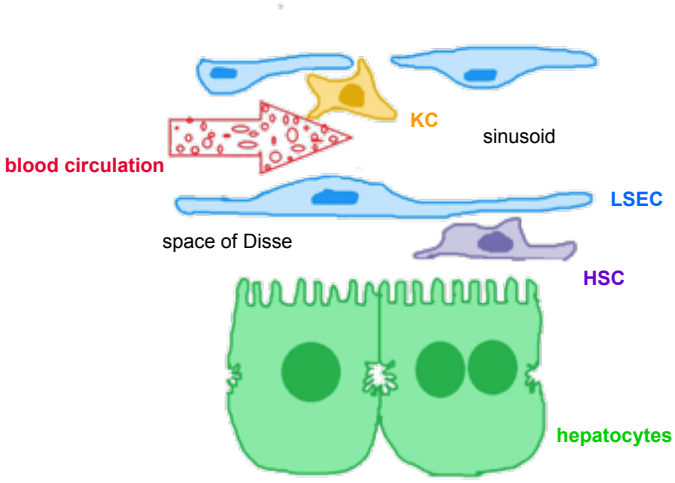

Figure 1.1. A schematic drawing depicting the localization of liver cells. Red arrow shape indicates blood flow in sinusoid. Space of Disse is the compartment between endothelial cells and hepatocytes. LSEC, liver sinusoidal endothelial cell; KC, Kupffer cell; HSC, hepatic stellate cell.

1.2. Cholesterol transport

The liver plays a central role in the regulation of cholesterol levels in the body. It dose not only synthesize cholesterol for export to other cells, but also removes cholesterol from the body by converting it to bile salts. Furthermore, the liver synthesizes the various proteins involved in transporting cholesterol throughout the body[13, 14].

1.2.1. Extracellular cholesterol transport

Cholesterol is highly hydrophobic. Its extracellular transportation in the blood circulation is mediated via lipoproteins, which are particles contains both lipids and proteins. The hydrophobic lipid core is rich with triacylglycerols (TAG) and cholesterol esters. The outer layer is composed amphipathic phospholipids and unesterified cholesterol and distinct amphipathic proteins called apoproteins (Apo)[15].

Lipoproteins are classified according to their density. The lowest density lipoproteins are the chylomicrons followed by very low density lipoproteins (VLDL), intermediate density lipoproteins (IDL), low density lipoproteins (LDL), and high density lipoproteins (HDL). The densities of these lipoproteins are related to the relative amounts of lipids to proteins in the complex. The higher the protein contents the higher the density of the lipoprotein.[16]

Chylomicron and VLDL are two forms of triglyceride rich lipoprotein (TRL). Chylomicron is synthesized by enterocytes from exogenous lipids absorbed in the small intestine[17]. During circulation through human body, TAGs are removed by the peripheral tissues. As the tissues absorb the fatty acids, the chylomicron particles progressively shrink until they are reduced down to cholesterol enriched remnants. The depleted or remnant chylomicrons, containing the dietary cholesterol, eventually reach the liver where they are cleared from the circulation by binding of their ApoE to receptors presented only on the surface of hepatic cells[18]. Subsequently, the bound remnants are taken up by the hepatic cells via endocytosis and then catabolized in the lysosomes[19].

The VLDL is essential in the endogenous lipid-transport pathway. It is secreted by the liver. As the transport of VLDL particles progresses, the core of lipid is reduced and the proteins and phospholipids on the surface are transferred to the HDL[18, 20]. Eventually, a high proportion of the VLDL remnants (or IDL) are converted to LDL with further loss of TAG.

The LDL is the principle plasma cholesterol carrier and serves as a cholesterol source for most tissues of the body[20]. LDL binds to specific cell receptors located on the plasma membrane of target cells, which is then followed by endocytosis and degradation of the lipoprotein to its primary components.

The HDL is synthesized de novo in the liver and small intestine, as primarily protein-rich disc-shaped particle[21]. It can obtain cholesterol by extraction from cell surface membranes using the ATP-binding cassette (ABC) transporter. Alternatively, the entire HDL particles can enter the hepatocytes through an ApoA-1 receptor interaction, where they undergo facilitated transfer of cholesterol within the cell[19-22]. The primary function of HDL is to remove excess cholesterol from periphery tissues to the liver so that the cholesterol can be metabolized into bile salts[21].

Importantly, those lipoproteins are in a constant change in composition and physical structures in the circulation while the peripheral tissues take up the lipid components and the remnants will return to the liver[15, 23].

1.2.2. Intracellular cholesterol transport

Cholesterol is an essential constituent in mammalian cell membranes and also serves as precursor for synthesis of steroid hormones and bile acids[14]. There are two

sources of cellular cholesterol. De novo synthesis of cholesterol can take place in all nucleated cells in human and the endoplasmic reticulum (ER) harbors enzymes essential for cholesterol processing[24]. Another source of cholesterol is extracellular lipoprotein. After their internalization via receptor-mediated endocytosis, they are transported to acidic endosome where cholesterol esters are hydrolyzed and free cholesterol is released[15, 19].

Free cholesterol derived from de novo synthesis or released from lipoprotein can target the plasma membrane for integration and become available to extracellular acceptors or they may redistribute to equilibrate the intracellular cholesterol pool. They may also go through esterification in the ER for longer time storage[25, 26].

Cholesterol delivery between those different sites is mediated by non-vesicular and vesicular mechanisms. Non-vesicular mechanism presumably uses cytosolic lipid transfer proteins, direct membrane contacts or combinations, which largely remained unclear. Vesicular mechanism means trafficking along cytoskeletal route via endosomal systems. In the endocytic pathway, the internal membrane of recycling compartments and the internal vesicles of multivesicular bodies harbor majority of the cholesterol. The recycling endosomes can transport the cholesterol directly to the plasma membrane. Alternatively, Niemann–Pick C1 protein (NPC1 and NPC2), which is located on the late endosome membrane can mediate cholesterol efflux out of the endosomal system before further maturation of late endosomes into lysosomes [27]. This is supported by the observation that deficiency of NPC protein leads to the accumulation of LDL-derived unesterified cholesterol in late endosomes[28]. The NPC phenotype can also be reproduced by treatment of normal cells with steroids like progesterone or with hydrophobic amines (class II amphiphiles) like U18666A[29]. On release from the endosomal system, cholesterol is delivered to other membranes, such as the plasma membrane, ER, recycling endosomes and mitochondria.

When there is excessive free cholesterol inside the cell, a key process to prevent cholesterol retention is cholesterol efflux, which is a process regulated by ABC transporter proteins[22, 30, 31]. It is suggested that triggered by binding of lipid-poor ApoA-1 to ABCA1, phospholipids and cholesterol are transferred to ApoA-1 to generate nascent HDL[32]. And ABCG1 cooperates with ABCA1 by further adding cellular lipids to the nascent particle, which results in the maturation of HDL[31].

1.3. Hepatitis B virus

1.3.1. Classification and origin

Hepatitis B virus (HBV) belongs to the family of *Hepadnaviridae*. Within the family are two genera: the orthohepadnavirus genus and the avihepadnavirus genus. The former infects mammals and is represented by HBV (Hepatitis B Virus), which targets humans and is the prototype member of this famlily. The other member of this genus includes viruses such as woodchuck hepatitis virus (WHV) that causes hepatitis in woodchucks[33], woolly monkey HBV[34] and orangutan-HBV[33], which infect non-human primates. The latter genus of HBV infect birds, including the duck hepatitis B virus (DHBV) isolated from Pekin duck[35], Heron hepatitis B virus (HHBV) that is responsible for hepatitis in herons[36], Ross goose hepatitis virus (RGHV) and stork hepatitis B virus (STHBV)[37].

The Hepadnaviridae viruses share the following characteristics in common. For example, they have a tropism for liver cells; The double stranded DNA genome consists of a long negative strand and a short incomplete positive strand of a variable length; They produce subviral particles and generate persistent infection and replicate through pregenomic RNA (pgRNA) template via reverse transcription with their own DNA polymerase[37].

HBV is an old world virus. Competing models of HBV origin have been proposed since 1990s based solely on sequence and geographic distribution analyses of extant HBVs[38]. The main obstacles in chasing the origin and development of HBV include the difficulties in estimating the real mutation rates in long time scale and a completely lack of genomic endogenizations in extant avian, rodent and primate's hosts. Until recently, endogenous hepadnaviruses was discovered in the genome of the zebra finch[39, 40], which has not been documented as extant HBV host. And this discovery has revealed that the evolutionary origin of hepadnaviruses is more than 63 million years older than previously known[41]. And in parallel with this finding, birds are suggested to be the ancestral hosts of Hepadnaviridae, and mammalian hepatitis B viruses probably emerged after a bird–mammal host switch[40].

1.3.2. Epidemiology and transmission

HBV infection is a global health problem. It is estimated that >2 billion people worldwide have been infected with HBV. And around 360 million individuals are chronically infected and at risk of serious illness and death, mainly from liver cirrhosis and hepatocellular carcinoma (HCC)[42].

Prevalence of chronic HBV infection and the HBV transmission patterns vary geographically. High endemicity areas include developing regions with large population such as South East Asia, China and sub-Saharan Africa. About 70 to 90% of the population becomes HBV-infected before the age of 40, and 8 to 20% of people are HBV carriers [43]. The usual mode of transmission is vertical at the time of birth from a chronically infected mother or horizontal in early childhood from bites, skin lesions or unsanitary habits[44]. In intermediate prevalence areas (Mediterranean countries, Japan, Central Asia, Middle East, and Latin and South America), 2% to 8% of the given population is HBsAg positive and between 10–60% of the population have evidence of infection [43]. In these areas, mixed patterns of transmission exist, including infant, early childhood and adult transmission. The prevalence of HBV is low in most developed areas, such as Western and Northern Europe, Australia and North America. In these regions, the HBV carrier rate is less than 2%, and less than 20% of the population is infected with HBV[43]. Adult horizontal transmission is the most common route. The most frequently reported risk factors are injection drug use, sexual activity and healthcare employment [45, 46].

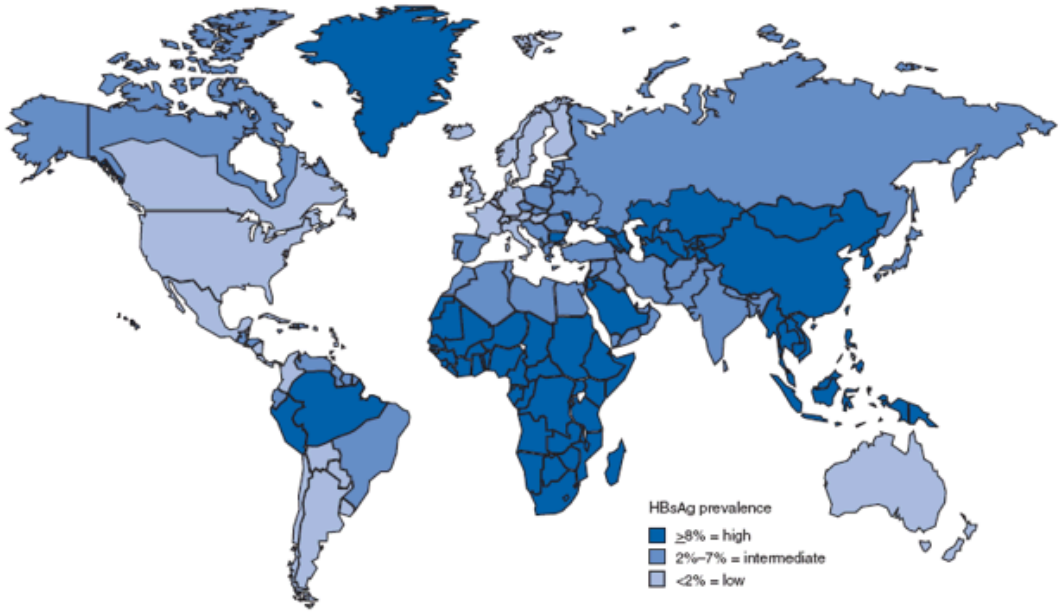

Figure 1.2. Global distribution of chronic hepatitis B infection (2006). Estimates of prevalence of hepatitis B surface Ag (HBsAg) worldwid. Regions colored in dark blue show the highest prevalence with more than 8% of the population infected, followed by intermediate prevalence (2-7%) and low endemic areas presented in lighter colors. Modified from Center for Disease Control and Prevention, US[47].

1.3.3. Pathogenesis and treatment

1.3.3.1. Pathogenesis

HBV infection leads to a wide spectrum of clinical presentations in both acute and chronic disease. During the acute phase, manifestations range from subclinical hepatitis to anicteric hepatitis, icteric hepatitis, and fulminant hepatitis[48, 49]. During the chronic phase, manifestations range from an asymptomatic carrier state to chronic hepatitis, cirrhosis, and hepatocellular carcinoma[50].

Many studies suggest that HBV infection is not cytopathic to hepatocytes[51-53]. Experiments in chimpanzees have shown that virus specific T cells are responsible for eliminating infected cells and thus also become a determinant influencing the onset and course of liver disease[54, 55]. Successful HBV specific T cell responses terminate HBV infection in the host and lead to the recovery of hepatitis B[56]. Vice versa, persistence of HBV infection is resulted from insufficient T cell response, which could be caused by failure of T cell response induction, or counteraction of virus against T cell response[57]. Further more, chronic HBV infection often accompanied with long term of immune-mediated liver injury, which is characterized by continuous

cycles of low-level liver cell destruction and regeneration that over time will cause fibrosis, cirrhosis and probably hepatocellular carcinoma (HCC)[53, 58]. Besides immune status, the overall clinical outcome of HBV infection is also affected by the age at infection, the level of HBV replication and the status of co-infection with other virus, etc[59].

1.3.3.2. Treatment

The goal of therapy for chronic hepatitis B (CHB) is to improve quality of life and survival by preventing progression of the disease to end-stage liver disease like cirrhosis and HCC[60]. This goal can be achieved if HBV replication can be suppressed with an effective treatment. The current approved treatment of HBV has been centered on interferon and nucleos(t)ide analogues. They suppress HBV replication but each with their own disadvantages[61, 62].

IFN has been used in the treatment of CHB for many years[63, 64]. It has the following advantages. First, IFN has direct antiviral effects includes inhibiting synthesis of viral DNA[51] and leading cccDNA degradation in the host cell through ISGs[65]. Second, IFN modulate the cellular immune response against HBV infected hepatocytes by increasing the expression of class I histocompatibility antigens and by stimulating the activity of helper T lymphocytes and natural killer lymphocytes[66]. Third, IFN also exert an anti-proliferative effect and an anti-fibrotic effect to alleviate the pathogenic progression of the inflamed liver[64, 65, 67]. However, the major limitations of IFN-based therapy are its significant side effects, low response rate of treated patients[64, 68].

Nucleos(t)ide analogue is a group of HBV inhibitor represented by lamivudine (LMV), adefovir dipivoxil (ADV), entecavir, telbivudine, and tenofovir disoproxil fumarate. They mainly act by inhibiting HBV polymerase activity, which lead to decrease in viral replication and viral particles release. Since they could not clear virus from infected host, persistent viral suppression would need life-long treatment[69, 70]. However, long-term treatment with nucleos(t)ide analogues has been found to be associated with progressively increasing rates of viral resistance because of emergence of resistant HBV mutant strains[71, 72].

To achieve more satisfactory treatment outcome, a series of anti-viral agents targeting different steps of HBV life cycle is under development pipeline. For example, Myrcludex-B is a synthetic lipopeptide consisting of the authentically myristoylated

N-terminal 47 amino acids of the preS1 domain of the large viral envelope protein (L protein). It targets specifically hepatocytes and efficiently blocks de novo HBV infection both *in vitro* and *in vivo*[73-75]. A phase 0/1 clinical study to evaluate the safety, tolerability, pharmacokinetics, and immunogenicity of single ascending doses of Myrcludex-B in healthy volunteers is ongoing. DV-601 is an immune based therapy. It comprises recombinant HBsAg and HBcAg and aims at promoting stimulation of virus specific T cell[76, 77]. ARC-520 is a siRNA-based agent targeting transcription of cccDNA thus reduces the expression and release of new viral particles[78]. Those emerging antivirals will provide additional and improved choices for optimized regimen development [77].

1.3.4. Molecular Virology

1.3.4.1. Structure of HBV particles

There are three types of viral particles secreted by HBV infected host cell: infectious Dane particle and non-infectious subviral particles with sphere or filament shape[37].

The Dane particle is a 42 to 47 nm spherical structure with lipid-containing envelope that consists of small (S), medium (M) and large (L) surface protein[37]. Inside the envelope is an icosahedral capsid with a diameter of ~28 nm assembled by 120 dimers of HBV core protein[77]. The capsid harbors a single copy of the partially double-stranded DNA genome, which is covalently linked to the viral reverse transcriptase (RT) at the 5'end of the complete strand[79, 80].

The subviral particles are produced by budding of HBV envelope proteins from cells without participation of capsids[37]. They usually reach a 10,000-fold higher concentration than Dane particles in patients' serum and have been speculated to serve as decoys for the host's immune system [81] (Figure 1.3).

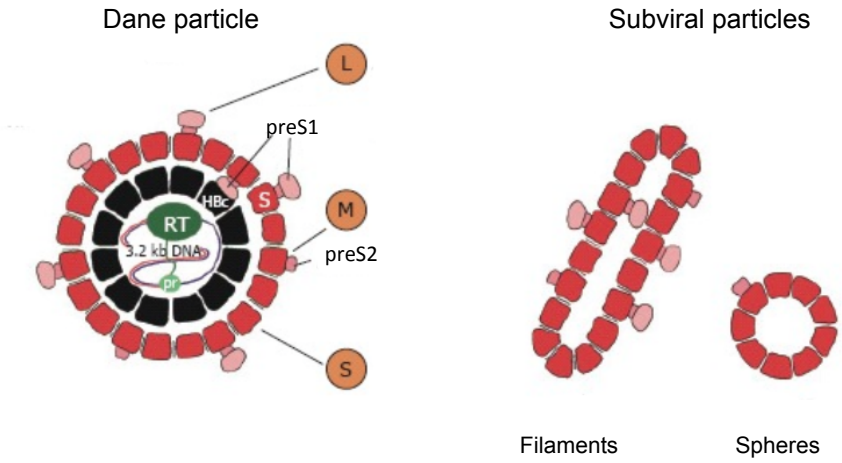

Figure 1.3. Structures of HBV particles. The infectious Dane particles with a diameter of ~42 nm are composed of a host derived lipid bilayer with integrated HBV surface proteins (L-, M- and S-protein). This envelope covers the nucleocapsid, composed of viral core proteins. The nucleocapsid harbors the 3.2 kb HBV DNA genome, covalently linked via the terminal protein to the viral polymerase. The non-infectious subviral particles (SVP), filaments and spheres, contain neither viral capsids nor viral DNA. Modified from Glebe,D and Urban,S[81].

1.3.4.2. Organization of HBV genome

HBV genome in the capsid is typically organized as a relaxed circular partially double-stranded DNA (rcDNA) of around 3.2 kb[82, 83]. Minus-strand DNA is complete and spans the entire genome, while the plus-strands extend to about two-thirds of the genome length and has variable 3' ends[84]. HBV genome is organized into four open-reading frames (ORF) that produce all the viral products. The longest ORF encodes the viral polymerase (ORF P). The envelope ORF (ORF S) is located within the ORF P in a frame-shifted manner. Partially overlapping with the ORF S are the core (C) and the X ORF. Because of the highly overlapping sequences between ORFs, a mutation in any area of the genome can have far-reaching consequences for viral replication and protein production[83, 84]. Transcription regulatory regions are present within ORFs and are active following the conversion of rcDNA into a covalently closed circular DNA form, called cccDNA[85].

Four mRNA products are transcribed from minus-strand DNA using host cell RNA polymerase II. They are 3.5kb pregenomic RNA that encode precore, core, polymerase protein, as well as forming the template for reverse transcription; 2.4kb RNA encoding L protein; 2.1kb RNA encoding M and S proteins; 0.7 kb RNA encoding X protein (Figure 1.4)[86].

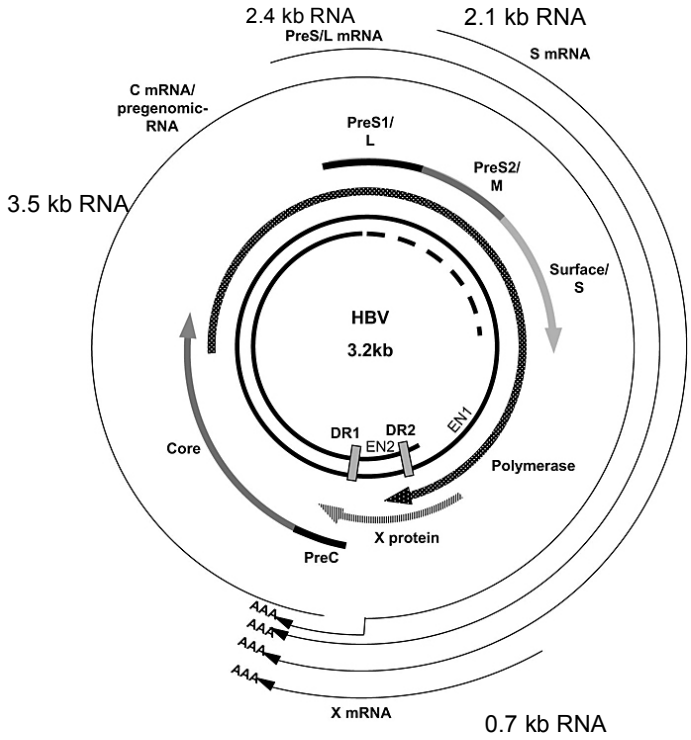

Figure 1.4. Genome of HBV. Centrally is the partially double stranded DNA. The virus has 4 highly overlapping open reading frames shown in shadowed bars. Transcription of all four viral mRNAs begins at different sites, and uniquely ends at a common poly A site. Modified from Kay,A and Zoulim,F[84].

1.3.4.3. HBV proteins

HBV surface protein is usually referred as hepatitis B surface antigen (HBsAg). They are essential for envelopment of capsid. Three types of surface proteins named large (L), middle (M), and small (S) are expressed by HBV. They are encoded by ORF S, which is divided by three in-frame AUG start codons into the following domains: PreS1, PreS2 and S. The L protein encompasses the PreS1 domain (108 or 119 aa depending on the genotype), the PreS2 domain (55 aa) and the S domain (226 aa); the M protein encompasses the PreS2 and S domain and the S protein consists of the S domain[87].

HBV core protein is also known as hepatitis B core antigen (HBcAg). As mentioned earlier, they participate in nucleocapsid formation. HBcAg is encoded by ORF C and encompasses either 183 or 185 amino acids depending on the genotype of the virus[80]. The primary sequence of core protein can be divided into assembly domain and protamine domain. The former covers the N-terminal 149 or 151 aa (depending on the genotype) and is sufficient for the self-assembly of capsids. The latter covers the C-terminal 34 aa, which is essential for the encapsidation of the pregenome / HBV P polymerase complex[88, 89].

As indicated in figure 1.4, a second product derived from the Pre-C/C ORF is HBeAg. It is an accessory protein of HBV, which is not essential for replication but important for natural infection[88]. This antigen has been used clinically as an index of viral replication, infectivity, severity of disease, and response to treatment[90, 91]. It is produced after cleavage of a 212 amino acid precursor encoded by Pre-C/C ORF starting from the first initiation site[37].

HBV encodes its own polymerase (Pol) that contains 842 or 843 amino acids in most of genotypes[37]. This enzyme displays both a DNA polymerase activity that can copy either DNA or RNA templates and a ribonuclease H (RNase H) activity that cleaves the RNA strand of RNA-DNA heteroduplexes. It initiates HBV genome replication from reverse transcribing pregenomic RNA template inside nucleocapsid. Once the DNA minus-strand is synthetized, RNase H degrades the RNA template and HBV Pol starts the synthesis of plus-strand DNA, leading to the formation of relaxed-circular form of the HBV genome[86, 92, 93]. The translation initiation codon of Pol lies internally on pregenomic RNA[37].

HBx protein is a 17 kDa non-structural protein. Expression of full-length HBx protein is essential for viral replication *in vitro* and a critical component of the infectivity process *in vivo*[94, 95].

1.3.5 HBV life cycle

1.3.5.1. HBV entry and intracellular transport

HBV entry into host hepatocytes starts from reversible attachment of the virion to cell surface proteoglycans. This step is energy-independent and is with low affinity and specificity[96]. After the primary attachment, the virus particle is transferred to a more

specific receptor, which largely defines HBV host specificity and hepatocyte tropism. The identity of HBV receptor has remained enigmatic for long time because of the lack of reliable infection system *in vitro*. It was until 2012 that sodium taurocholate cotransporting polypeptide (NTCP) was found to be functional receptor for HBV entry[97 98, 99]. .NTCP is a member of the solute carrier family 10 (SLC10) and the major bile acid uptake system in human hepatocytes. It localizes to the basolateral membrane of hepatocytes. Though exogenous overexpression of hNTCP could confer HBV permissiveness in non-infectable HepG2 or Huh7 cells[99 100, 101]. It cannot reverse the insusceptibility of mouse hepatocyte to HBV infection[102]. Thus, It is unknown if molecules other than NTCP also contribute to HBV entry.

Virus-receptor binding is then followed by cellular internalization, which has been reported to involve caveolae-, clathrin- or macropinocytosis-dependent endocytosis, depending on the cell types and experimental systems[103-106].

Following endocytosis, HBV must travel through complex cytosol environment toward nucleus for genome replication. So far, details about the intracytosolic trafficking event are still largely unknown. Microtubules systems are suggested to be the driving motor for virus trafficking. One recent report based HepaRG cells proposed that Rab5 (early endosome) and Rab7 (late endosomes) are crucial for HBV intracellular transport and genome uncoating, while Rab9 (trans-Golgi related vesicles) and Rab11 (recycling endosome) has limited involvement in this process[107].

After fusion of viral and cellular membranes in endosomes, HBV genome is liberated from the capsid to traverse through nuclear envelope to the site for multiplication[108]. Viral polymerase, viral capsid and host heat shock proteins as Hsc70 or Hsp90 have been reported to aid the translocation of HBV genome via interaction with nuclear pore complex (NPC) [109]. In 2010, *Schmitz et al.* reported that nucleoporin 153 (Nup153), a protein of nuclear basket, was an essential trigger for viral genome release via interaction with HBV capsid and host nuclear transport reporter importin-beta[110].

1.3.5.2. HBV replication

Upon translocation of rcDNA to the nucleus, virus replication could be initiated. And this process can be broadly divided into three stages[85, 111]: 1. rcDNA to cccDNA conversion. The viral Pol that linked to 5' end (-)-strand DNA will be removed. The

incomplete (+)-strand will be modified and repaired to full length. And both (-)- and (+)-strand DNA will be covalently ligated to form cccDNA. Host cellular repair enzymes are likely to be involved during this process but how these are achieved remains poorly understood. 2. From cccDNA to pgRNA. Using (-)-strand of the cccDNA as a template, pgRNA is transcribed by cellular RNA polymerase II. It is composed of the entire genome length plus a terminal reduncancy containing the ε signal that is critical for HBV Pol binding[112]. 3. Reverse transcription of pgRNA. pgRNA and Pol form complex and recruit HBc dimers via interaction with HBc protamine domain. Once pgRNA and Pol are being encapsidated, Pol-ε interaction will initiate reverse transcription. The first DNA nucleotide that is covalently linked to P protein will be extended into a complete (-)-DNA, and (+) strand DNA synthesis ensues, giving rise to a new molecule of rcDNA. Newly formed rcDNA can re-enter into the nucleus and convert to cccDNA, thus amplify the cccDNA pool, which serves as an HBV reservoir responsible for persistent replication[86, 113-115].

1.3.5.3. HBV release

Besides recycling, mature capsid can also be enveloped with viral surface proteins in the endoplasmic reticulum (ER)-Golgi compartment and released from the cell[116]. The expression level of envelope proteins was reported to regulate particle release and cccDNA amplification. The lack of envelope protein expression increases cccDNA levels, while co-expression of the envelope proteins favours viral secretion[117]. And a more recent study showed that HBV could activate the ER-associated degradation (ERAD) pathway to reduce the levels of HBV envelope proteins, which possibly served as a mechanism to control the level of viral particles in infected cells and tuning the balance of cccDNA amplification to facilitate the establishment of chronic infections[118]. Efficient export of HBV virions from hepatocytes have been suggested depend upon hepatocyte polarity and involve the machinery of multivesicular body and lipid raft [119, 120].

1.3.6. Experimental models for HBV

1.3.6.1. Cell culture systems

HBV is hepatotropic virus. Primary human hepatocyte (PHH) used to be the only HBV susceptible cell and remains the golden standard for HBV infection study *in vitro*[119]. The major drawback of this model is its limited resources and high batch-to-batch variation. Besides, PHH tend to loose their differentiation status within days after plating thus loose the susceptibility to HBV infection very fast, which further hinder its usage[121, 122]. The first HBV permissive hematoma cell line, HepaRG, was established in 2002[122]. Differentiated HepaRG cells exhibits a mixture of hepatocyte-like and biliary-like epithelial cells, with the former closely resemble PHH in terms of morphology, specific hepatocyte function and permissiveness to HBV infection. Never the less, only a subset of those cells (10% to 30%) can be infected. And after viral inoculation, the conversion of the input rcDNA into cccDNA was demonstrated to be slow and inefficient [123, 124]. After the introduction of HBV entry receptor hNTCP in 2012, hNTCP expressing human hepatoma cell line (e.g. HepG2-NTCP, Huh7-NTCP) were rapidly produced and proven to support the whole life cycle of HBV[99 100, 101].

In addition, cell lines in which the viral genome is expressed from chromosomally integrated viral cDNA usually have more consistent and high level of HBV particle production[124]. Compared to the aforementioned infection model, these HBV expressing cell lines are more advantageous in HBV life cycle study in aspect of replication, translation, assembly and release of viral particles[125, 126].

Besides, DHBV infection in duck hepatocytes have also contributed greatly to elucidation of HBV life cycle[127].

1.3.6.2. Animal models

HBV naturally infects human only, but can also experimentally infect chimpanzees. After injection of serum from HBV patient, chimpanzee develop acute infection and hepatitis[128]. It is an extremely valuable model to study host immune response, viral pathogenesis and pre-clinical evaluation of antiviral therapy. However, usage of chimpanzee has encountered major restraints due to ethical aspects, low availability and high cost.

Alternatively, Tupaia, the Asian tree shrew, can be experimentally infected by HBV positive human serum[127]. The woodchuck and Peking duck is the natural host for WHV and DHBV respectively[33, 129, 130]. Those models also contribute greatly to reveal biology of hepatitis B and antiviral drug screening. However, they are all relatively large animals, difficult to handle in captivity or not easily available. They are all of outbred origin and their immune systems have not well characterized.

The requirement of immunologically well-defined and convenient inbred animal models for HBV study has been the driving force for generating HBV mouse model. Though HBV entry receptor has been unveiled, hNTCP could not confer HBV susceptibility to the mouse hepatoma cell lines and rat hepatoma cell line tested[102], which shatters the hope for the establishment of a small animal model of HBV infection in the near future.

Nevertheless, various lineages of transgenic mice harboring either the complete HBV genome or single viral genes have been established. These models provide important insights on specific aspects of HBV replication and the oncogenic potential of distinct viral genes *in vivo*[51, 128, 131, 132]. However, there are several limitation of these transgenic mouse model: they bypass virus entry; though they could secret decent amount of infectious virions, there is no formation of cccDNA; viral elements are recognized as “self” during embryonic development by the host immune system.

Alternatively, adenovirus vectors containing hepadnaviral genomes or hydrodynamic injection of replication-competent HBV genomes have been used to initiate HBV replication in mouse liver[133, 134]. Those systems allow dynamic analysis of immune response during acute infection and convenient manipulation of HBV genome for mutation analysis. However, data interpretation of these model need to be cautious because the potential side effect of adenoviral vector and significant liver damage due to hydrodynamic injection.

Human-liver chimeric mouse represents another type of small animal model. They generally follow the idea to delete mouse hepatocytes and then repopulate the mouse liver with xenografted hepatocytes. One of the most frequently used is uPA-SCID mouse. Urokinase-type plasminogen activator (uPA) expression leads to the death of transgene-carrying hepatocytes, which results in a growth advantage for transplanted cells. Severe combined immune deficient (SCID) background contributes to long time survival of xenogenic hepatocyte. The transplanted human hepatocytes start to

proliferate and forming larger nodules that eventually merge together and replace the diseased liver parenchyma. This system permits studies of whole HBV life cycle and also spreading. But the major drawbacks are the immunodeficiency and being technically challenging [135-137].

1.4. Hepatitis C virus

1.4.1. Classification and origin

The hepatitis C virus (HCV) is an single-stranded RNA virus belonging to the Flaviviridae family[87]. Currently, this family contains 4 genera with HCV being classified as the type member of genus Hepacivirus. The other members of the Hepacivirus genus include the canine hepacivirus (CHV) that infect dogs, and the non-primate hepacivirus (NPHV) that infect horses[138-140].

HCV displays high genetic variability, which is resulted from the error-prone nature of the RNA dependent RNA polymerase, the high viral production rate and the selection pressure from the host immune response[141, 142]. Within a single individual the virus exists as constantly evolving quasispecies. Based on the nucleotide sequences recovered from infected individuals, HCV is classified into seven different genotypes and numerous subtypes[143-145]. The genotypes differ in their nucleotide sequences by 30-35% across the whole viral genomes and the greatest diversity is found within the viral envelope glycoproteins[141].

The evolutionary origin of HCV is still not clear. Non-human primate source used to be the predominant hypothesis[146]. Despite its plausibility in many aspects, the fundamental problem has always been that HCV or homologues cannot be found in ape or monkey species. More recently, the identification of CHV, NPHV and hepacivirus in bats[147] provided another scenario that hepaciviruses might be highly catholic in their host range and is capable of jumping between different species. Further screening of other mammalian species has been suggested to resolve the ultimate origin of HCV[147].

1.4.2. Epidemiology and transmission

With an estimated prevalence of 3% in the world population (around 170 million people), HCV infection heavily burdens public health[148]. In many developed countries, the prevalence of HCV infection is <1.5%. Intravenous or nasal drug use accounts for majority of the newly acquired infection[149]. A medium prevalence (1.5%-3.5%) can be found in areas like South and Southeast Asia, sub-Saharan Africa, Western Europe and so on[150, 151]. The prevalence is considerably much more higher in certain African and Asian countries (>3.5%) [37]. The major reasons could be the lack of transfusion screening system and/or the reuse of contaminated or inadequately sterilized syringes and needles. In particular, Egypt has an up to 20% seroprevalence rate for HCV. This particular high HCV prevalence is the consequence of frequently using unsterilized reused needles and syringes during the treatment of endemic schistosomiasis in mass campaigns (stopped in 1980s)[152]. Other modes of transmission have also been documented such as sexual and perinatal transmission route. However, this occurs less frequent[148, 150, 151, 153].

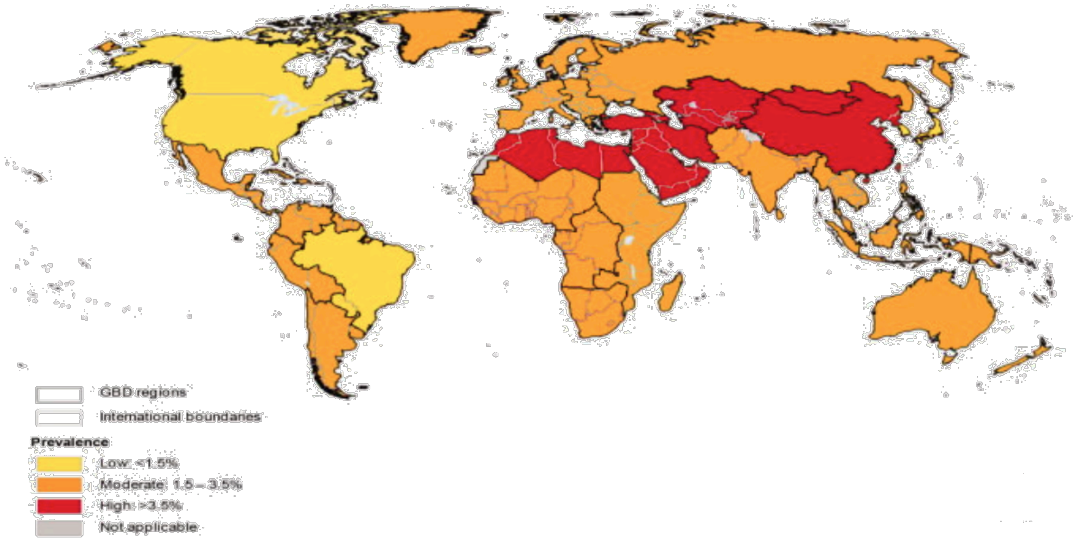

Figure 1.5. Global prevalence of hepatitis C virus infection (2005). Estimates of antibodies to HCV (anti-HCV) seroprevalence by Global Burden of Disease (GBD) region, 2005. Anti-HCV antibodies are a commonly available marker of HCV infection. Regions colored in dark red show the highest prevalence with more than 3.5% of the population infected, followed by morderate prevalence (1.5-3.5%) and low endemic areas (<1.5%) presented in lighter colors. Modified from Mohd Hanafiah, K et al. [154]

1.4.3. Pathogenesis and treatment

HCV is primarily hepatotropic. It is non-cytopathic and its pathogenesis is a complicate phenomenon influenced by a number of virus and host factors including the viral genotype, viral quasispecies diversity, host genetic factor, underlying disease and, importantly, the efficiency of the host immune response[155].

Traditionally, the first 6-month of HCV infection is considered to be the acute phase. The majority of HCV infections are asymptomatic[156]. Up to 50%-80% of acute infections become chronic infection, which is defined by HCV persisting for more than six months. HCV viremia is relatively constant among infected persons with around 10^{12} virions produced daily[142]. Chronic infection is associated with ongoing liver inflammation. Around 20% of the chronically infected patients will develop liver cirrhosis within 20 years of infection. Once cirrhosis is established, the risk of developing an HCC is 1-4% each year[157].

With the emergence of new direct acting antivirals (DAAs), the treatment paradigm for HCV infection enters a new era. Before these new therapeutics options, interferon-α and ribavirin has been the mainstay of treatment, but they are associated with severe side effects and low sustained viral response rates[158]. The new DAAs available now specifically inhibit enzymatic activities of viral proteins like the NS3/4A protease, the NS5A protein or the NS5B RNA dependent RNA polymerase. For example, the NS3/4A inhibitor simeprevir and NS5B inhibitor sofosbuvir have recently been licensed and can reduce the length of antiviral treatment, improve response rates, and allow interferon-free regimens[159].

1.4.4. Molecular virology

1.4.4.1. Structure of HCV particles

The HCV virion is 50-80 nm in diameter and enveloped with a lipid bilayer embedded with E1 and E2 glycoprotein heterodimers[160, 161]. Beneath the envelope resides a nucleocapsid around 30 nm, which contains a single copy of the viral RNA genome[162]. A feature of HCV virion is that it tightly associates with host lipoproteins and lipids to form lipoviral particle (LVP), which results in low and heterogeneous buoyant densities of infectious virus particles[161]. LVP in infected patients vary from particles produced from cell culture in their properties like buoyant density distribution and

lipoprotein composition and that is because of the differential lipoprotein producing capability of the host cells[163, 164]. Besides, it has been reported that in Caco-2 and HepG2 cells, which own VLDL synthesis and secretion capacity, overexpression of envelope glycoproteins E1 and E2 led to production of E1–E2 containing particles. They are complexed with apoB and might be regarded as HCV-related subviral LVPs[165].

1.4.4.2. Organization of HCV genome

The HCV genome is a single positive-stranded RNA of approximately 9600 nucleotides. The coding region is flanked by 5' and 3' highly structured non-translated regions (NTRs), which are essential for the protein translation initiation and genome replication[166].

The 5'-NTR comprises the first 341 nucleotides and is highly conserved among different HCV isolates[167]. This region consists of numerous stem-loop motifs and can be divided into four highly structured domains numbered I to IV. Domains I and II are both essential for HCV RNA replication[168]. Domains II, III and IV of the 5'-NTR, together with the first 24–40 nucleotides of the core coding region, constitute the internal ribosome entry site (IRES)[169].

The 3'-NTR contains approximately 225 nucleotides and is organized into three domains consisting of a short variable region, a poly (U/UC) stretch that regulates replication and a highly conserved 98-nucleotide X-tail[170, 171].

Besides the 5'-and 3'-NTRs, the NS5B coding sequence contains another *cis*-acting replication element designated as 5BSL3. In this region, a stem-loop, 5BSL3.2, has been shown to be essential for RNA replication[172].

The coding region consists of an ORF that contains 9024 to 9111 nucleotides depending on the genotype. Translation initiation is IRES dependent, which could directly recruits 40s ribosomal unit to the AUG codon and initiates protein translation in a cap-independent manner[166, 169].

1.4.4.3. HCV proteins

Translation of the HCV open reading frame yields a single polyprotein precursor that is co- and post-translationally processed by cellular and viral proteases into the mature structural and non-structural proteins[166].

The structural proteins (Core, E1 and E2) and the p7 polypeptide are processed by the endoplasmic reticulum (ER) signal peptidase[37].

The HCV **core proteins** form the shell of viral nucleocapsid. It is located at the N-terminus of the HCV polyprotein. Maturation of the core protein involves C-terminal cleavage by the aforementioned signal peptidase and, in addition, the signal peptide peptidase[173]. The matured form of the core protein with 173-179 amino acids has a molecular weight of about 21-kDa and can be roughly separated into the N-terminal D1 and C-terminal D2 domain[174]. The D1 domain is involved in RNA binding and exhibits RNA chaperone properties. The D2 domain is required for proper folding of D1 and association of the core with cytosolic lipid droplets (cLD)[175].

The translation of an alternative reading frame in the core coding sequence can also yield a small protein (~17 kDa), called **ARFP or F protein**. The role of the F protein in the HCV life cycle and/or pathogenesis is not yet known. However, it has been reported that the F protein can stimulate specific immune response and is not required for HCV RNA replication[176, 177].

E1 and E2 glycoproteins are trans-membrane protein and exist as building blocks for viral envelope. They form non-covalently linked heterodimers after maturation and mediate virus entry and membrane fusion[178].

P7 is a small (7 kDa) intrinsic membrane spanning protein. It has been shown that P7 can form oligomer having ion channel activity in artificial lipid membranes, which leads to the assumption that p7 is a viroporin[179]. The protein is dispensable for RNA replication but is essential for productive infection *in vivo*[180].

The non-structural proteins are processed by two viral proteases, the NS2-3 protease and the NS3-4A serine protease.

NS2 is a 24-kDa protein participating in the cleavage at the NS2/NS3 junction of the polyprotein. The protease activity also requires the N-terminal one third of NS3[181]. NS2 is reported to be indispensible for RNA replication[182]. However, it is critical for

assembly and the post-assembly maturation step of HCV in cell culture infection system (HCVcc), independent of its catalytic activity[183, 184].

NS3 is a multifunctional protein with an N-terminal serine-type protease domain[185] and a C-terminal RNA helicase/NTPase domain[186]. Both the NS3 serine protease and the helicase activities require NS4A as a cofactor[187].

NS4A is the smallest HCV encoded protein (6 kDa) with a central transmembrane domain, which could non-covalently associate with NS3[188]. The NS3/4A protease is responsible for the polyprotein cleavage in the region downstream of NS3, which is essential for viral RNA replication complex formation[189]. The RNA helicase domain is capable of unwinding RNA-RNA duplexes in an ATP-dependent manner, which might be required for removing stable RNA secondary structure during replication and/or dissociation of RNA double strand replication intermediates[190]. Furthermore, the NS3/NS4A serine protease also cleaves the MAVS and TRIF adaptor proteins, blocking IFN synthesis triggered by pattern recognition receptors (PRRs) at the early stage of infection[191].

NS4B is a highly hydrophobic 27kDa integral membrane protein tightly associated with the ER membrane. It is responsible for formation of membranous web or membrane associated foci (MAF), which are specialized membrane derived vesicles serving as a scaffold for the HCV replication complex[192].

NS5A is a phosphoprotein that can be found in basally phosphorylated (56kDa) and hyperphosphorylated (58kDa) forms. It is separated into three subdomains (DI to DIII) by low complexity sequence I and II[193]. DI has RNA binding property and is essential for RNA replication; most of DII is dispensable for the viral replication cycle in cell culture, whereas DIII can interact with core and is required for HCV assembly[194-197].

NS5B is an RNA-dependent RNA polymerase (RdRp), which promotes synthesis of both, the positive strand RNA and the negative strand intermediate in the absence of other viral or cellular factors *in vitro*[198]. A specific interaction between NS5B and the 3'UTR has been reported[199]. The enzyme lacks a proofreading function, which contributes to the high genetic variability of HCV[145].

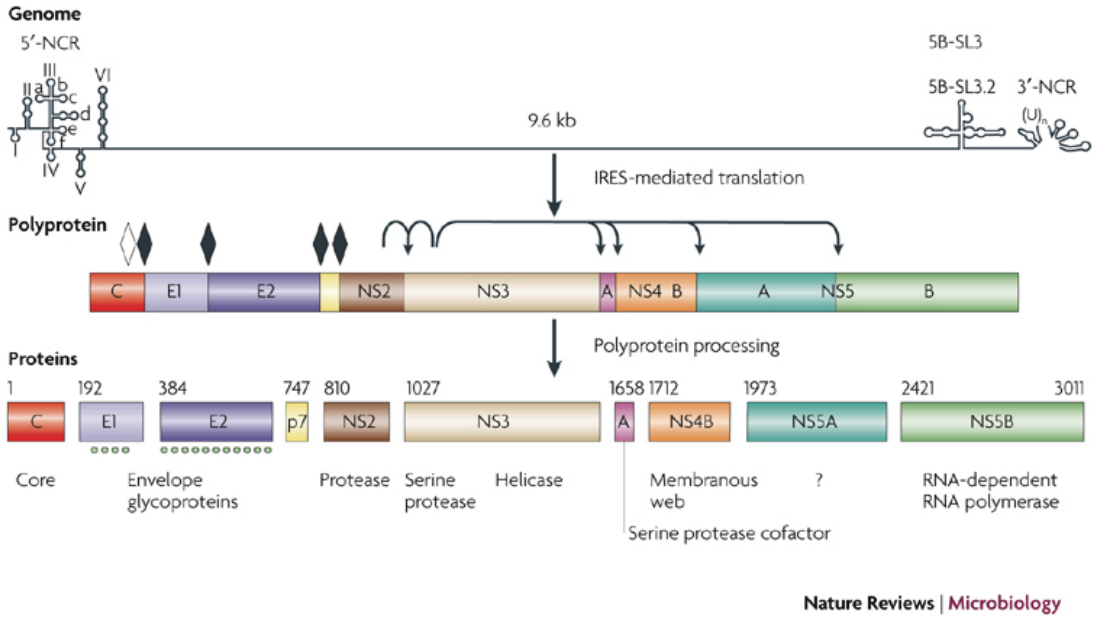

Figure 1.6. HCV genome organization and polyprotein processing. Upper: Scheme of HCV genome with simplified RNA secondary structures in the 5'- and 3'-NTRs as well as the stem loop 5BSL3.2. Middle: Polyprotein precursor yielded by IRES dependent translation. Solid diamonds indicate cleavage via ER signal peptidase. Open diamond indicates additional processing by signal peptide peptidase. Arrows indicate processing by HCV NS2-3 and NS3-4A proteases. Lower: Produced HCV mature structural and non-structural proteins. Amino-acid numbers are shown above each protein (HCV H strain; genotype 1a; GenBank accession number AF009606). Modified from Moradpour D, Penin F and Rice CM, 2007[166]

1.4.5. HCV life cycle

1.4.5.1. HCV entry

HCV close to hepatocyte tend to bind low-density-lipoprotein receptor (LDLR) and glycosaminoglycans (GAGs) present on heparan sulfate proteoglycans via both E2 and virion-associated apoE[200-202]. This initial attachment helps to concentrate virus on the cell surface and is followed by virus binds to specific entry factor(s) with high affinity. A growing number of such cellular molecules have been identified including CD81, SRB1, Claudin-1 (CLDN1), occluding (OCLN), EGFR, NPC1L1 and more recently transferrin receptor 1 (TrR1)[203-209]. These receptors have varied physiological function and distribution region in polarized hepatocytes. How they contribute to HCV entry in a temporally and spatially ordered manner is still not fully elucidated. One of the current models is: HCV LVPs attach to target cell surface by interacting with GAGs, LDLR and SRB1. The cholesterol transfer activity of SRB1 might then serve to dissociate virus particles from their associated lipoproteins, and the interaction with

SRB1 exposes the CD81-binding determinants on the HCV E2 glycoprotein[210, 211]. The CD81-bound HCV particles laterally migrate to tight junctions and interact with CLDN1. This cell surface trafficking relies on several signal transduction pathways, including EGFR and downstream RAS GTPase signalling, as well as RHO GTPases, which remodel cortical actin[205]. The interaction of HCV-CD81 with CLDN1 then induces clathrin-mediated endocytosis[212]. Although the tight junction protein OCLN is also essential for HCV entry, its precise role in this process is currently unknown[206]. The recently reported TfR1 is suggested to act after CD81 and involved in virion internalization[203]. In addition to infection with cell-free virus, direct cell-to-cell transmission is identified *in vitro* and probably also occurs *in vivo*[213]. Those two routs utilize largely overlapping receptors[214].

Following endotytosis, clathrin coated pits fuse with early endosome and the acidic pH in the endosome triggered fusion of viral envelope with the endosomal membrane[215]. In that way, HCV genome is released and viral translation and replication is started[215].

1.4.5.2. HCV replication

HCV RNA translation is initiated via HCV IRES within 5'UTR and utilizes host ribosomal machinery in the ER[37]. Produced viral protein induces the formation of membranous web that constitute the sites of HCV RNA replication[192]. RNA synthesis is catalyzed by the viral RdRp activity of NS5B and supported by other viral NS proteins. Numerous cellular factors have also been identified with potential roles in HCV RNA replication. For example, cycolphilin B can stimulate RNA binding capacity of NS5B and the microRNA miR-122 can enhance the stability of uncapped HCV RNA[216-218]. After synthesis of a negative-sense RNA intermediate, multiple positive-sense progeny RNAs are generated. HCV replication is thought to occur rapidly after virus entry as negative-strand templates are detectable at 2-4 hours after introduction of RNA into cells[219].

1.4.5.3. HCV assembly and release

Virus assembly and release is a tightly regulated process coupled to host cell lipid synthesis[37]. It is not yet completely elucidated because the overall assembly

efficiency is low *in vitro* and *in viv* as well as HCV virions resemble close to (V)LDL paticles, which further preclude a firm detection of the rare event[220]. However, two general principles of HCV assembly have been suggested. In both cases, mature core protein translocates from the ER to cLD surface after cleavage, but the sites of assembly are different. In the first model, the initial core-cLD functions to concentrate core protein and then, via interaction of core with viral proteins like NS5A[197] and/or NS2[183], core is released back to assembly sites at the ER and transfer of the RNA from the ER-resident NS5A complexes triggers nucleocapsid formation. In the second model, assembly occurs on cLD, which is associated with the viral core. RNA is delivered to the cLD surface accompanied by NS5A, whose N-terminal residue is sufficient for cLD targeting[221, 222]. Both scenarios are facilitated by the close proximity of cLD and ER[220]. Newly formed nucleocapsids are then suggested being transferred to luminal lipid droplets (luLDs), which are precursors of VLDL particles residing on lipid rich microdomains of the ER[223, 224]. HCV envelopment and maturation could take place in luLDs, but the whole process is still poorly known[220]. The release of mature LVPs is proposed to be linked with the endosomal sorting complex required for the transport (ESCRT) pathway[225].

1.4.6. Immune responses to HCV

Host immune response is a crucial determinant for the outcome of HCV infection, e.g. viral clearance versus viral persistence. The immune response against HCV involves both, innate and adaptive immunity[226].

1.4.6.1. Innate immune responses to HCV

Innate immune responses are the first immunological barrier against viral infections. Studies on experimentally HCV infected chimpanzee revealed a very early activation of innate immunity reflected by an induction of IFN-stimulated genes (ISGs) within days post infection[156, 227]. This induction is presumably due to the host recognition of viral macromolecular motifs, known as pathogen-associated molecular patterns (PAMPs), by cellular pathogen PRRs. So far, the precise nature of HCV derived PAMP as well as the route they get to PRRs are still in debate. Several targets have been proposed. For example, endosomal Toll like receptor-3 (TLR3) has been reported to recognize the virus replication intermediates double-stranded RNA[228, 229].

Cytosolic retinoic acid-inducible gene 1 (RIG-1) was reported to sense HCV poly-U/UC sequence in 3'UTR[230]. Cytosolic protein kinase R (PKR) was characterized as non-traditional PRRs contributing to HCV sensing by binding to IRES region[231]. Pathogen recognitions trigger down stream signaling pathways, which leads to production of IFN[232, 233]. IFN is the central link to set up antiviral states. It drives expression of hundreds of ISGs[234] and activates and regulates the cellular components of innate immunity such as natural killer (NK) cells[235].

Despite the early activation, innate immunity is ineffective in HCV clearance as indicated by stable viremia for several weeks until the emergence of cellular immune response[236, 237]. The incapability of innate immunity could be explained by attenuated IFN response at multiple levels by HCV. For example, the HCV NS3/4A interferes with both TLR and cytosolic HCV sensing by cleaving and inactivating essential components in the signaling cascades, thereby blocking IFN induction[238, 239]. HCV infection can inhibit cap-dependent protein translation via phosphorylation of eukaryotic translation initiation factor 2 (eIF2) but does not influence IRES dependent viral translation[240]. In addition, binding HCV E2 protein to CD81 has been reported to alter NK cells function that is directly involved in combating HCV infection[241, 242]. In patients who develop chronic infections, innate immunity activation varies considerably between individuals[243]. Though it has been widely accepted that patients with high baseline levels of ISGs are poor responders to IFN-a-based therapies, the mechanisms behind are only poorly understand[244].

1.4.6.2. Adaptive immune responses to HCV

The definitive barrier to control HCV infection is the adaptive immunity. This response can be categorized as humoral and cellular immune response[245].

Virtually all HCV-infected individuals develop antibodies (Abs) against HCV, which has protective effect for the host against HCV as has been identified in chimpanzees that HCV infectivity could be neutralized by *in vitro* treatment with Abs[246]. However, only a small fraction of Abs is neutralizing-antibodies (nAbs), which could be subjected to interference by the remaining non-neutralizing antibodies (non-nAbs)[247]. In addition, the majority of Abs have been mapped to the envelope glycoproteins E1 and E2[248], which have a high mutational rate, limiting their effects in preventing reinfection [249, 250]. Besides, HCV can also spread via direct cell-to-cell transmission,

thus evading neutralization by neutralizing antibodies[251]. In summary, humoral immune response may contribute to host defense against HCV, but its role in the clearance of infection is a controversial issue.

Cellular adaptive immune responses are thought to have the greatest impact on HCV eradication[252]. The main components in cellular immune response are $CD4^+$ helper and $CD8^+$ cytotoxic T lymphocytes. They are detectable until 8–12 weeks in both self-resolving or chronically evolving hepatitis C patients[253]. Patients with acute-resolving HCV infection usually display broad CD4+ responses with better T cell proliferation and cytokine production than patients with chronic evolving infection[254-256]. In chronic HCV infection, HCV-specific CD8+ T cells are still detectable, but they often have a dysfunctional phenotype, e.g. they are impaired in their effector functions such as production of antiviral cytokines, cytotoxicity and proliferation[257, 258]. The main reasons for CD8+ T cell dysfunction are reported as following: 1) expression of inhibitory receptors, leading to CD8+ T cell exhaustion and ultimately CD8+ T cell depletion; 2) appearance of viral escape mutations which abrogates recognition of viral antigens by HCV-specific CD8+ T cells[259, 260]; 3) absence of HCV-specific CD4+ T cell responses in chronic HCV infection, which most likely further contributes to CD8+ T cell failure[261, 262], and 4) additional mechanisms of T cell dysfunction which may include the action of regulatory T cells, impaired priming of virus-specific T cells and suppression by inhibitory cytokines[263].

1.4.6.3. Host genetic factors influencing immune responses to HCV

Host genetic polymorphisms related to immune response account for some of the heterogeneity in infection outcome[264].

Single nucleotide polymorphisms (SNPs) upstream of the *IL28B* locus have been identified to correlate with response to IFN therapy and infection outcome[265]. These SNPs associate with altered mRNA expression of *IL28B* gene, which encodes the antiviral cytokine IFNL3[265, 266].

Certain HLA class I and II alleles are associated with a high rate of viral clearance. For example, patients that are positive for the class I alleles HLA-A3, or HLA-B57 have increased chance for spontaneous HCV clearance. It has been reported that patients with HLA-B27 have more robust CD8+ T cell response because of more efficient binding of epitope located within the HCV polymerase (NS5B)[267].However,

due to ethnic differences, the association between HCV infection and polymorphic HLA system remains is not clearly understood[268, 269].

1.4.7. Experimental models for HCV

1.4.7.1. Cell culture systems

Ever since HCV has been successfully cloned in 1989[270], continuous efforts have been made to culture the virus *in vitro* by inoculating patient sera or transfection with cloned viral RNA. Productive viral replication has been reported in primary human hepatocytes, hepatoma cell line and lymphocytes. In all cases virus replication was variable and very low[182, 271-273].

HCV Replicon System: In 1999, high level HCV replication was achieved with subgenomic replicon system in human hepatoma cell (Huh7) under selection pressure [182]. The prototype replicon is a bicistronic RNA of genotype 1b named Con1. In this system, the first cistron encodes a neomycin resistance gene under the control of the HCV internal ribosomal entry site (IRES). The second cistron expresses genes for NS3-NS5B, which is initiated by IRES from encephalomyocarditis virus (EMCV). All genes are driven by T7 promoter. Following *in vitro* transcription using T7 RNA polymerase, the replicon RNA is transfected into the human hepatoma cell line Huh-7. Afterwards, cell lines containing high amounts of self-replicating HCV RNAs could be obtained under G418 selection[182]. Using this system, it was observed that selected replicon cells that have been cleaned of HCV infection by IFN or anti-HCV drug treatment support viral RNA replication much better compared to naive Huh-7 cells[274, 275]. Using such “HCV cure” method, several highly permissive cell clones such as Huh-7.5[274] or Huh-7-Lunet[172] have been established. With respect to replication enhancing mutations (REMs), they have been identified throughout the HCV coding region (NS3-5B), but clustered around NS5A, NS3 and NS5B[276-278]. The exact mechanisms involved in cell culture REMs are still not fully understood, but most of them have been shown to affect the phosphorylation status of NS5A[275]. The advancements in the understanding of the replicon system through viral REMs and highly permissive cell clones has led to the development of replicons with different HCV genotypes[279] and reporter replicon harboring selectable reporter genes applicable for high throughput screening[280].

HCV Retroviral Pseudoparticles: HCV pseudoparticle (HCVpp) is a surrogate model developed to study the early stages of viral life cycle[281, 282]. This system is generated by co-transfection of 293T cells with expression vectors encoding HCV E1 and E2, the gag-pol proteins of either murine leukemia virus (MLV) or human immunodeficiency virus (HIV) and a retroviral genome encoding a reporter gene[281]. As a result, HCVpp harvested from 293T supernatant consists of retroviral capsid harboring reporter gene, which is enveloped by lipid bilayer embedded with unmodified HCV E1/E2 glycoproteins. The unmodified HCV envelope proteins confer HCVpp receptor binding and cell tropism[283]. Entry of these particles leads to the delivery of the retroviral capsid into the cytoplasm of the target cell and subsequent expression of reporter gene. Since HCVpp are replication deficient and support only a single infection event, quantification of the reporter gene expression directly reflects the productive entry events[283]. Therefore, this system offers opportunity to investigate virus receptor interactions or screening for potent virus entry inhibitors[281, 282]. However, a limitation of the HCVpp system is that these particles are produced in a non-liver cell line (293T) and assembled in post-Golgi compartments and/or the plasma membrane as retroviruses, thus the particles are deficient of close association with lipoproteins compared to wildtype virons[283]. They are not suitable for studies on virus neutralization antibodies and interaction of virus with lipid receptors including LDL-R, SR-BI, and NPC1L1.

Infectious HCV particles derived from cell culture: In 2005, three research groups reported that wildtype JFH-1 or chimeras based on JFH-1 replicated efficiently in Huh-7 cells and produced infectious HCV particles[284-286]. Those particles are termed HCVcc (cell culture-grown) and they support complete HCV life cycle *in vitro*. While the JFH1-based infection system belongs to genotype 2a, many efforts have been made to generate molecular clones from other genotype. As a result, an increasing panel of HCV genomes capable of recapitulating the complete viral replication cycle in cell culture has become available[275, 287].

1.4.7.2. Animal models

Only human and Chimpanzee are permissive for HCV infection. Studies in chimpanzees have led to the discovery of HCV and provided a wealth of knowledge regarding the mechanism of HCV infection, replication, and both innate and humoral

antiviral immune responses[270]. However, chimpanzee differs from human in that their course of infection is milder; chronic carriers do not develop cirrhosis or fibrosis and only one chimpanzee has been reported to have developed HCV-related HCC[288]. Furthermore, due to same reasons listed before (section 1.3.6.2), usage of chimpanzee in HCV research has been banned.

Tupaia has been shown to be susceptible for infection of HCV, besides aforementioned HBV (section 1.3.6.2). It was demonstrated that serum or plasma derived from HCV infected patients could establish effective replication and virion synthesis in primary tupaia hepatocytes[289]. And more recently, it was reported that tupaia inoculated with patient derived HCV developed mild inflammation and viremia during the acute infection, which was followed by liver steatosis, cirrhotic nodules and tumorigenesis[290]. Tupaia, therefore, is a promising and effective model for the ongoing study of HCV. A disadvantage of this model is that, unlike humans infected with HCV, these animals rarely maintain sustained viremia[290].

Immune deficient mice grafted with human hepatocytes, the so-called chimeric mouse models, represent a type of small animal model that can be robustly infected with HCV[291]. There are several kinds of this type, like the uPA-SCID mouse[292] and the $Fah^{-/-}Rag2^{-/-}$ $IL2rg^{-/-}$(FRG) model[291]. However, because these mice are immune deficient, they have impaired utility for studies of immune responses against virus infection.

In order to create a mouse model permissive to HCV infection with uncrompromised complex immunity, humanize mice that were genetically engineered to express HCV-specific entry factors including CD81, occludin, SRB- I, and CLDN1 are developed[293, 294]. Because this model is based on immune competent mouse, viral replication and persistence of infection was limited. But it facilitates studies of passive immunization or vaccination strategies meant to prevent acute infection of HCV before or after virus exposure[295, 296].

Other HCV mouse models include mice that express transgenes encoding HCV protein elements. They do not permit natural steps of viral life cycle, but have contributed to understanding of HCV pathogenesis mediated by viral proteins[297].

1.5. Aim of study

Both HBV and HCV are blood-borne viruses and they specifically target hepatocytes. While the viruses' life cycles in hepatocytes have been characterized in detail, how they target the hepatocytes as well as their interactions with non-parenchymal liver cells on the way to the hepatocytes have been poorly studied.

The overall aim of this study was to investigate: 1) The mechanisms involved in efficient targeting of HBV to the hepatocytes. 2) The role of non-parenchymal liver cells in early HCV infection.

The first part of study was based on previous observation that HBV was preferentially sequestered by KCs in *ex vivo* perfused human liver pieces[298]. Since it has been reported that inoculation with a single virion of HBV in chimpanzees or its duck virus analogue in ducklings is sufficient to establish a productive infection *in vivo* [299, 300], the question how HBV overcomes the scavenging of KCs and subsequently target hepatocytes efficiently was raised.

In the same study of *ex vivo* perfusion, it was also shown that in the presence of human serum, HBV was associated with triglyceride rich lipoproteins (TRL)[298]. As it is well acknowledged that macrophages are very potent in lipoprotein uptake and cholesterol recycling[30, 301]. A hypothesis that HBV transcytose through KCs following cholesterol recycling pathway was proposed in the beginning of the study.

To investigate this hypothesis, THP-1 differentiated macrophages, monocyte derived macrophages (MDMs) and Kupffer cells (KCs) as well established macrophage models were used. Concentrated HBV stock from HepG2.2.15 culture supernatant was used in biochemical assays and fluorescence labeled HBV particles were used in confocal microscopy for providing information on the intracellular localization of viral particles (VPs) as well as the potential interactions with host targets. Finally, to test the assumption of transinfection, a macrophage/hepatocyte co-culture system was established.

The second part of this study dealt with the aim to investigate the interactions of liver non-parenchymal cells with HCV in the early infection. To answer the question about which type of non-parenchymal cells could potentially interact with HCV, a time course analysis of the virus location in perfused liver was carried out. Following the identification of the main non-parenchymal cells showing HCV localization at the

investigated time points, the following questions were asked: 1). Does the sequential uptake of HCV reflect a transinfection pathway of the virus *in vivo*? 2). Does uptake of virus by non-parenchymal cells contribute to the early activation of innate immunity? And which sensing pathway is involved? To address the first question, co-culture system of KCs and Huh7.5 could be utilized to test transfection. To answer the second question, cytokine expression in *in vitro* cultured primary non-parenchymal cells, *ex vivo* perfused human as well as *in vivo* perfused mouse livers were analyzed after virus exposure.

2. Experimental part I:

HBV transinfects hepatocytes by transcytosis through Kupffer cells following the cholesterol transport pathway

2.1. Results

2.1.1. Intracellular trafficking of HBV is associated with free cholesterol transport

A previous study from our group illustrated that HBV is associated with TRL in patient's serum[298], and it is known that TRL-components can efficiently recycle after cellular uptake[14]. In this part of the study, I aimed at studying if intracellular transport of internalized HBV was in close association with TRL or a component derived from TRL. Viral particles (VPs) labeled with Alexa Fluor®594 (HBV^{594}) were therefore used for visualization of HBV transport.

First, the location of HBV^{594} in relation to lipoprotein derived cholesterol was investigated.

Isolated primary Kupffer cells (KCs) were incubated for 1h with TRL containing fluorescence labeled cholesterol (NBD-cholesterol) as well as HBV^{594} in the presence of 10% human serum. Subsequently, cells were washed and further cultured with medium containing human serum for 2h followed by fixation for confocal imaging. As shown in figure 2.1.A, HBV^{594}-positive vesicular structures (red) were observed in the cell co-localizing with NBD-cholesterol positive structures (green).

As lipid poor ApoA-1 could efficiently target cellular free cholesterol to induce cholesterol efflux for formation of mature HDL[302, 303], ApoA-1 was used as a marker to track lipoprotein derived cholesterol. To investigate the co-localization of ApoA-1 and HBV, KCs were incubated with HBV^{594} in the presence of human serum for 1h. Cells were then fixed and stained using an antibody against ApoA-1 (Figure 2.1.B). Vesicular structures positive for both HBV^{594} and ApoA-1 were observed, with signals from HBV^{594} mainly localizing in compartments positive for ApoA-1.

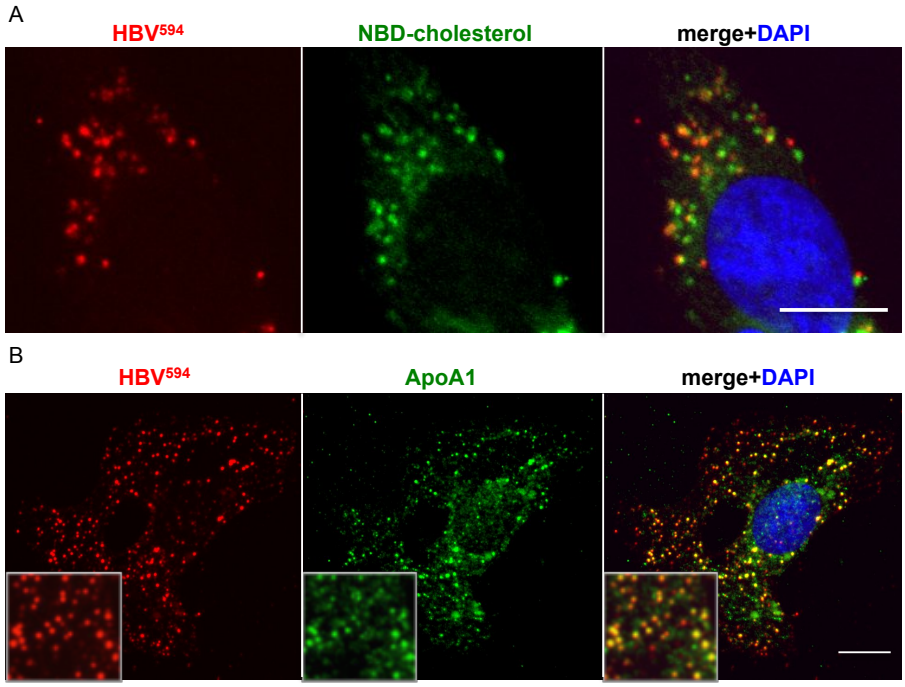

Figure 2.1. Co-localization of HBV^{594} with free cholesterol in KCs. (A). KCs were incubated for 1h with HBV^{594} and 5μg/ml NBD-cholesterol labeled TRL in medium containing human serum, and subsequently washed and further cultured for 2h prior to visualization. The experiment was done in cooperation with Dr.Knud Esser. (B). KCs were loaded with HBV^{594} for 1h in the presence of human serum prior to staining using antibody against ApoA-1. Scale bars = 10 μm. Representative pictures are shown.

As monocyte derived macrophages (MDMs) are much more convenient to get and have less fluorescence background than primary Kupffer cells, these cells were used for visualization of intracellular free cholesterol. Free cholesterol was stained by the fluorescent filipin, which can selectively bind to cholesterol but not to cholesterol esters[304].In the following imaging studies, MDMs were pre-treated with 50µg/ml acetylated LDL (AcLDL) for 24h to elevate the intracellular cholesterol levels before VP were added. In figure 2.2, cells were exposed to HBV^{594} for 1h before culturing with virus free medium for further 4h. The detected cholesterol distribution was comparable to what has been described before, showing strongest signals in the perinuclear region and at the plasma membrane[305, 306]. The perinuclear area is the site of the ER, where excess exogenous free cholesterol is delivered for esterification, and the plasma membrane is naturally rich in free cholesterol and also the site for cholesterol efflux[306]. In between those regions, many filipin positive vesicles could be distinguished. Those could be organelles enriched with cholesterol in the endocytic

pathway. Distribution of internalized HBV followed the same pattern as free cholesterol. They were in association with free cholesterol positive vesicles, which led to dispersed localization in periphery area and an accumulation in perinuclear area. As it is shown in “i” and “ii”, the abundance of yellow pixels illustrates that HBV^{594} co-localized with free cholesterol.

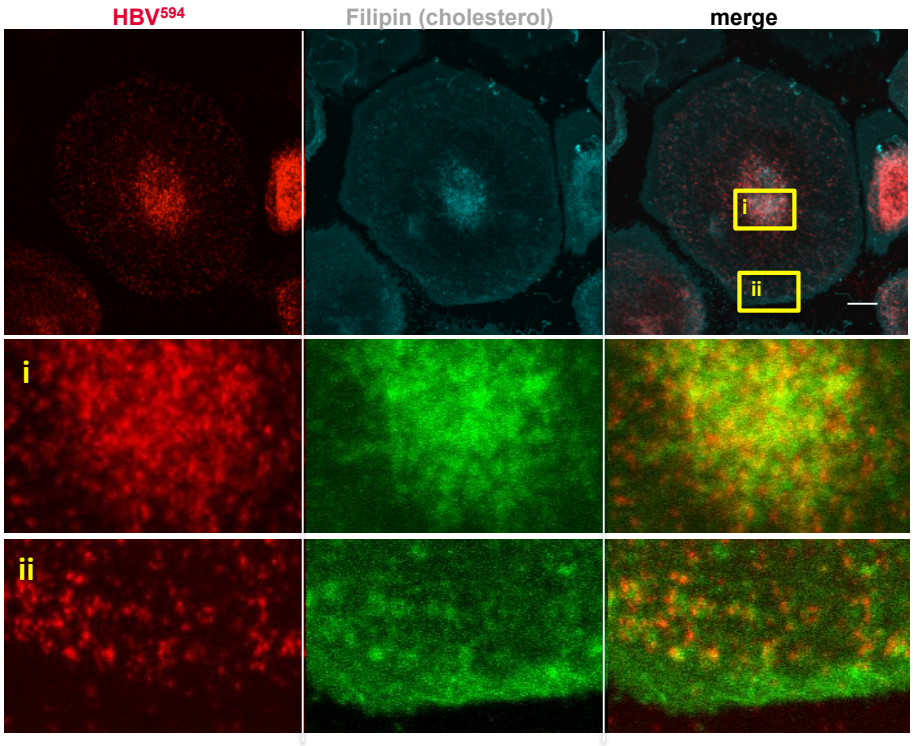

Figure 2.2. Co-localization of HBV^{594} with cholesterol in MDMs. MDMs were pre-incubated with medium containing 50 μg/ml acLDL for 24h, and then loaded with HBV^{594} for 1h. After intensive washing, cells were further cultivated for 4h with acLDL containing medium. Filipin staining was done as described in chapter materials and methods. Cholesterol stained by filipin is shown in the upper panel in cyan to indicate its UV fluorescence, while the red color shows the fluorescence of HBV^{594}. The panel “i” and “ii” are derived from the yellow-boxed areas illustrated above. Filipin staining is changed into green for visualizing co-localization with fluorescent HBV^{594} in red. Scale bar = 10 μm. One representative picture is shown. Experiments were done in cooperation with Dr.Knud Esser.

Because of the co-localization of internalized HBV with free cholesterol and cholesterol targeting protein ApoA-1 in cytosolic vesicles, it seemed that HBV transport is associated with the intracellular cholesterol transport pathway.

Lipoproteins, for example TRL, are taken up by cells via receptor mediated endocytosis. After entering the endosomal system, free cholesterol is released in acidic endosomes via hydrolysis. This lipoprotein derived cholesterol can then be delivered to other compartments including the plasma membrane and the

endoplasmic reticulum[14, 29]. Niemann-Pick C1 (NPC1) protein is an endosome enriched transmembrane protein that is essential in intracellular cholesterol transport. Its deficiency leads to accumulation of cholesterol in lysosomes[28]. To test if HBV^{594} also relies on NPC1 for transportation, immune staining of NPC1 with HBV loaded MDM was done. As shown in figure 2.3, the majority of HBV^{594} concentrated in NPC1 positive compartments implying that HBV transportation may be linked to NPC1.

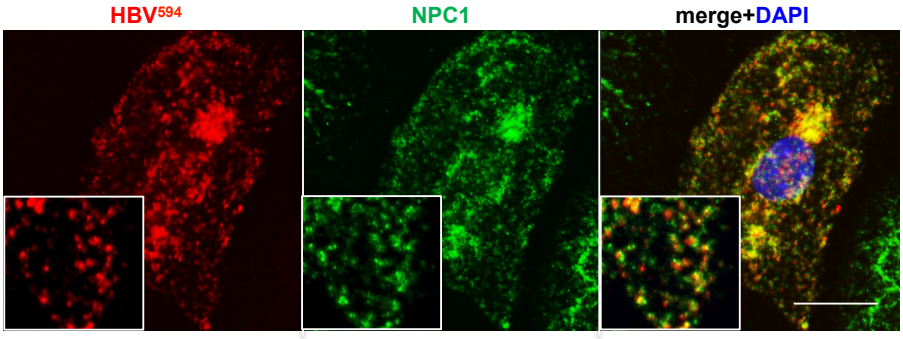

Figure 2.3. HBV^{594} concentrates in NPC1 positive compartments. MDMs were pre-incubated with medium containing 50 μg/ml acLDL for 24h, and then loaded with HBV^{594} for 1h. After intensive wash, cells were further cultivated for 4h with acLDL containing medium prior to fixation and staining against NPC1. Scale bar = 10 μm. One representative picture is shown. Experiments were done in cooperation with Dr. Knud Esser.

To confirm that HBV intracellular trafficking and free cholesterol transport are functionally linked, HBV^{594} loaded MDMs were treated with U18666A, which is a drug arresting intracellular cholesterol transport, resulting in the perinuclear accumulation of intracellular cholesterol in late endosomes/lysosomes[29]. To visualize the effect of U18666A on free cholesterol transport, free cholesterol was labeled with filipin. The influences on HBV^{594} and cholesterol cellular localization were examined by confocal microscopy. Results are shown in figure 2.4. It became obvious that U18666A treated cells accumulated free cholesterol in perinuclear regions compared to untreated cells. In parallel, the HBV signals in perinuclear regions were enhanced under treatment of U18666A. To quantify the changes caused by drug treatment, the ratio of fluorescence intensity volume of the perinuclear region to the periphery region in both the filipin and the HBV channel was determined. The relative fluorophore content of the different regions investigated was calculated by multiplying the area of the region with its corresponding average fluorescence intensity. The results in turn represented the total amount of the target in this region (HBV^{594} or cholesterol). It was confirmed,

as shown in figure 2.4.B, that U18666A treatment led to an enhanced ratio between perinuclear to peripheral levels of both, free cholesterol and HBV^{594}.

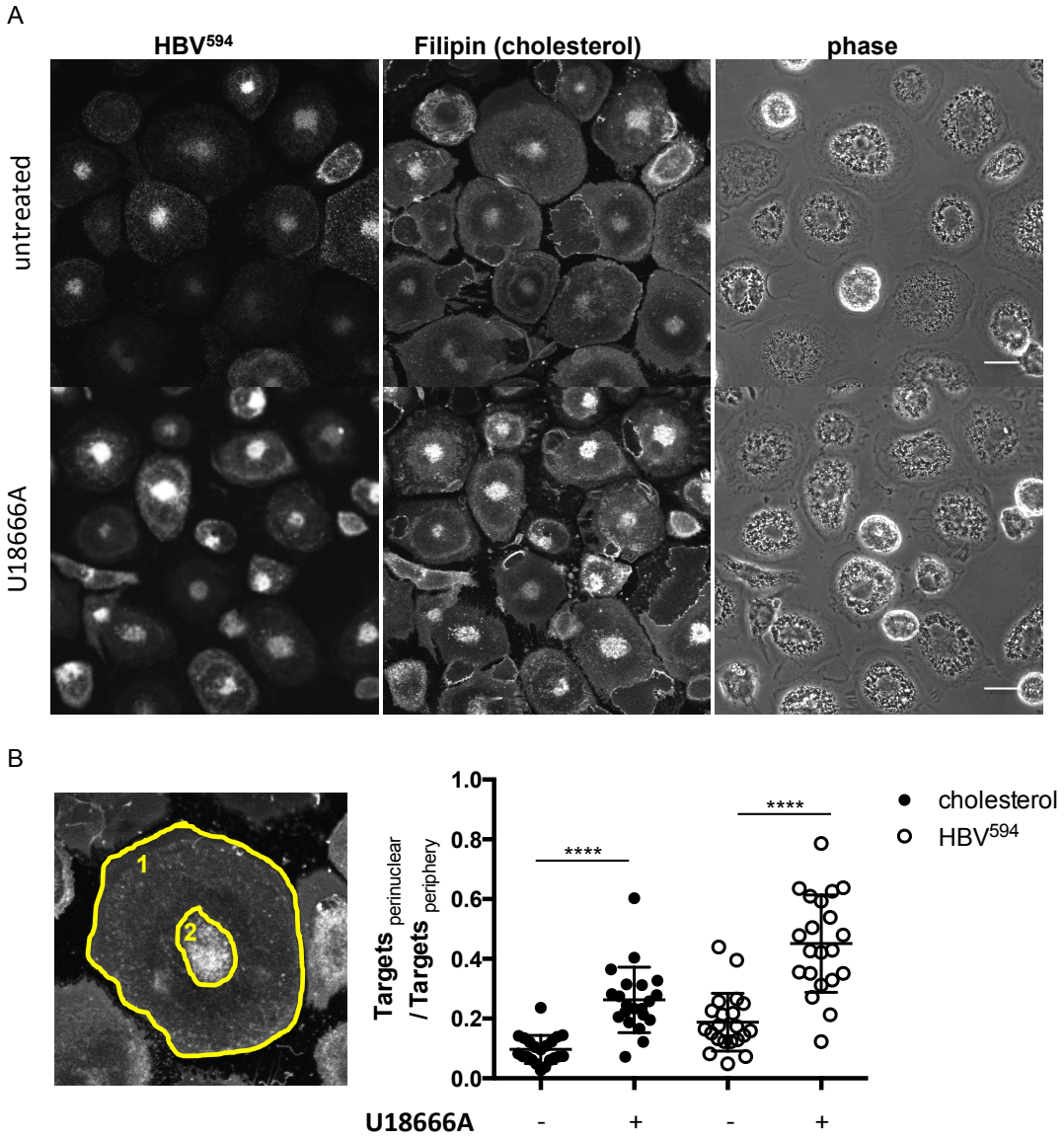

Figure 2.4. U18666A treatment causes accumulations of both, free cholesterol and HBV in perinuclear regions. In the presence or absence of 5 mM U18666A, MDMs were pre-loaded with 50 μg/ml acLDL for 24h, washed, exposed to HBV^{594} for 1h and then further cultured with medium free of virus but containing acLDL. Subsequently, the cells were stained with filipin and analyzed by confocal microscopy. (A). Representative images of cells treated (lower panel) and untreated (upper panel) with U18666A. HBV^{594} (red fluorescence) and filipin (UV fluoresecne) are shown in white for better visualization of intensity change. Scale bar = 10 μm. (B). Left: illustration of how perinuclear and periphery regions were defined using filipin stained cell: The inner circle "2" shows the boundary for the perinuclear area, the outer circle "1" defined the limit for the peripheral area. Right: Fluorescence intensity volume ratios between perinuclear region and periphery regions under different conditions. Each dot represents one randomly selected cell. Means±SD of one representative experiment are shown. **** P <0.0001. $I_{fluorescence}$: fluorescence intensity; A: area. Experiments were done in cooperation with Dr. Knud Esser.

Hereby, we concluded that internalized HBV did not only localize to compartments enriched for free cholesterol in macrophages, but they also hijacked the transportation pathway of intracellular free cholesterol.

2.1.2. HBV is transcytosed through macrophages utilizing cholesterol transport pathway

2.1.2.1. HBV localizes to recycling endosomes

It has been documented that in macrophages recycling compartments harbor most of the cholesterol in the endocytic pathway, while the cholesterol content of lysosomes appears to be low[27]. In particular, after internalization, intracellular lipoprotein derived cholesterol can be delivered by recycling endosome and target the plasma membrane for efflux, especially if extracellular cholesterol acceptors like HDL, ApoA-1, etc. are available [14, 29, 306]. As it was demonstrated before that trafficking of internalized HBV is linked to free cholesterol transport, we hypothesized that HBV might also locate to recycling endosomes for resecretion.

To visualize the intracellular compartmentalization of HBV, HBV^{594} loaded THP-1 macrophages were stained by antibodies against lysosomal-associated membrane protein 1 (LAMP1) or Rab11 for labeling of lysosomes or recycling endosomes, respectively. Fluorescence-labeled recombinant HBV surface protein ($rHBsAg^{594}$) was used as control. Analysis using confocal microscopy showed that after differentiation, macrophages contained matured lysosomes as indicated by strong staining of LAMP-1 (green, Figure 2.5). The internalized $rHBsAg^{594}$ distributed in similar pattern as LAMP-1, and even more intriguingly, some clusters of $rHBsAg^{594}$ were completely surrounded by LAMP1, suggesting they had been fused with lysosomes. In contrast, HBV^{594} distributed as punctate signals like described in section 2.1.1 and did not co-localize with LAMP1, suggesting that, unlike $rHBsAg^{594}$, HBV^{594} did not enter into the lysosomes. Co-localization was quantified using Mander's coefficient. Only M_{red} (fraction of red overlapping with green) is shown and the co-localization coefficient is 0.9 for rHBsAg and 0.3 for HBV.

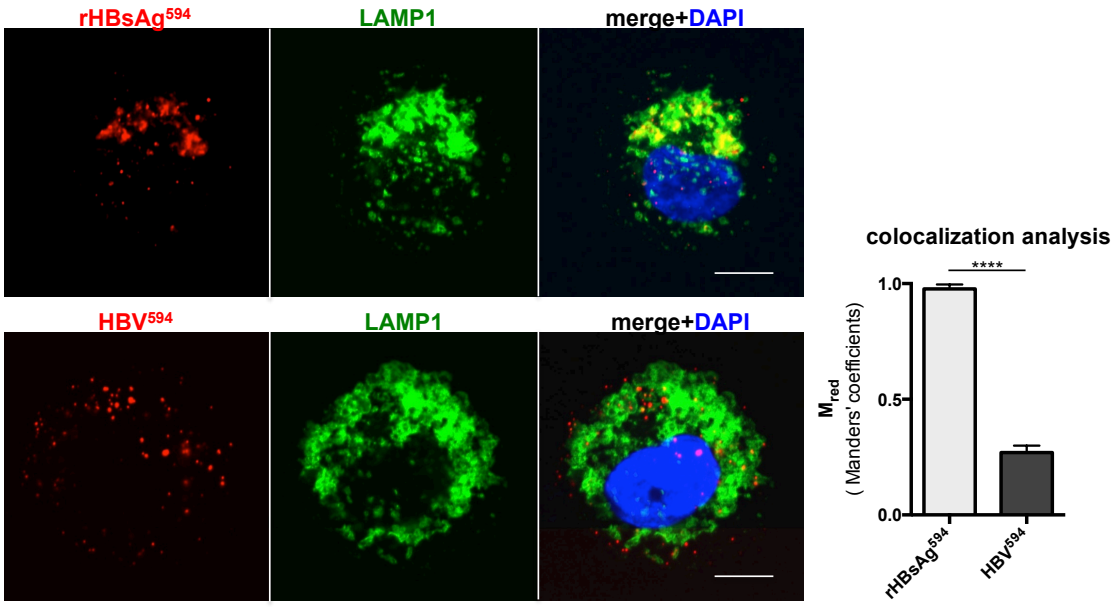

Figure 2.5. In macrophages HBV does not localize to lysosomes after 1h pulse incubation. THP-1 macrophages were incubated with rHBsAg^{594} or HBV^{594} for 1h prior to staining with antibodies against LAMP1. Scale bar = 10 μm. Co-localization of three randomly selected views of each group was analyzed using Manders' correlation method. M_{red} (fraction of red overlapping with green) was calculated using JACoP plugin of ImageJ. Means±SD of four random view of one representative experiment are shown. ****p<0.0001

To be sure that the lack of co-localization of HBV^{594} with LAMP1 was not an occasional phenomenon due to the chosen time point after 1h pulse incubation, the cells were further chase incubated with virus free medium for 16h and analyzed by LAMP1 staining. As shown in figure 2.6.A, HBV^{594} did not co-localize with LAMP1, which illustrated that HBV did neither enter into lysosomes after prolonged incubation. To investigate if HBV located to recycling endosomes after this time period, cells were exposed to HBV^{594} or rHBsAg^{594} for 1h, chase cultured for 16h and stained for Rab11. The imaging data (Figure2.6.B) showed that HBV^{594} partially co-localized with Rab11, especially in the area close to the plasma membrane. In contrast, rHBsAg^{594} did not show any co-localization with Rab11. When co-localization quantification was done, the Manders' coefficient of red channel (M_{red}) for HBV^{594} and Rab11 was around 0.5 while the M_{red} for rHBsAg^{594} and Rab11 was close to zero. Those observations demonstrated that after internalization by macrophages, HBV was able to avoid entering into lysosomes but efficiently target recycling endosomes.

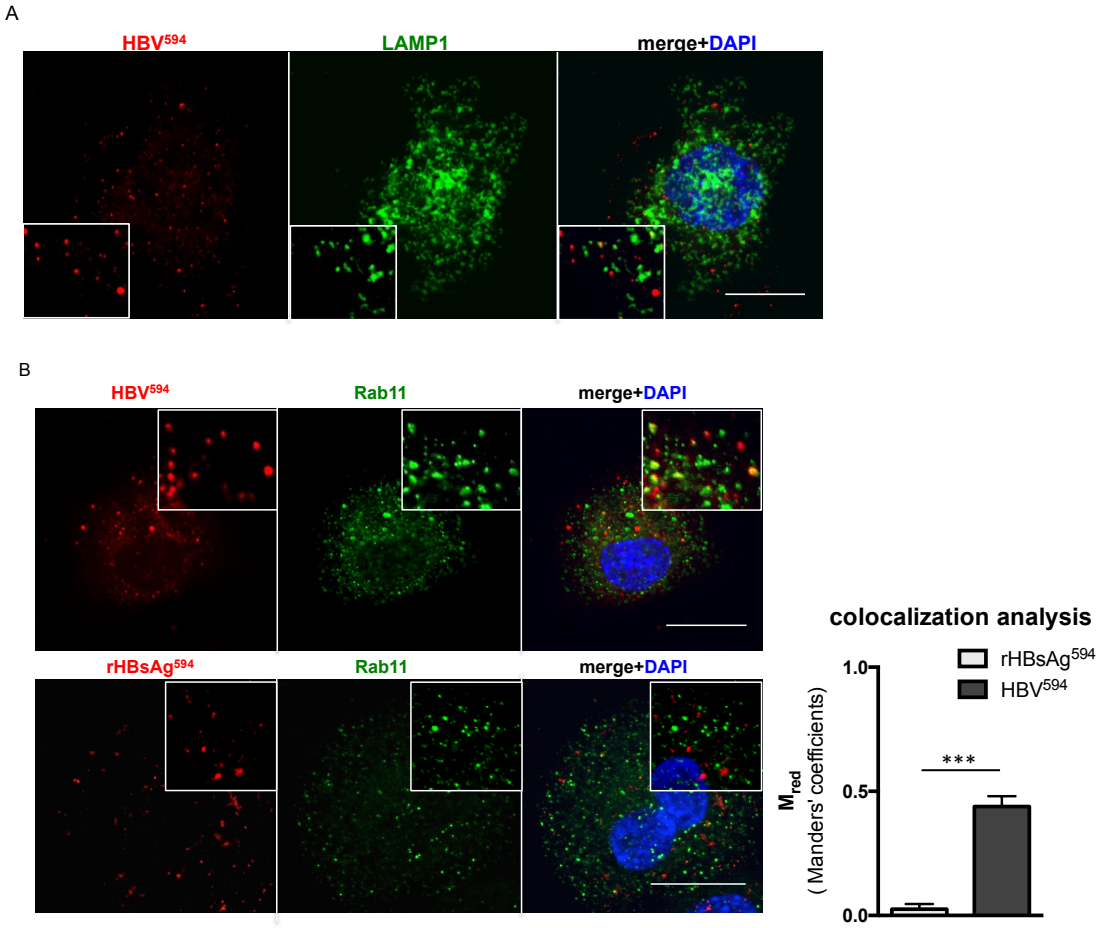

Figure 2.6. HBV^{594}, but not rHBsAg^{594}, escapes lysosomes and concentrates within recycling endosomes after 16h chase incubation. THP-1 macrophages were incubated with HBV^{594} (A and B upper panel) or rHBsAg^{594} (B lower panel) for 1h and chased for 16h. After washing, cells were fixed and stained using antibodies against LAMP1 (A) or Rab11 (B). Scale bar = 10 μm. Quantification of co-localization was done for Rab11. Means±SD of four random view of one representative experiment are shown. ***p<0.001

To investigate HBV localization to recycling endosomes in a more dynamic way, a time course analysis of HBV^{594} localization in relation to Rab11 positive recycling endosomes was performed. THP-1 macrophages were incubated with HBV^{594} for 1h followed by chase incubation with virus free medium for 15min, 2h or 5h. The results are shown in figure 2.7. After 15min, only some HBV^{594} co-localized with Rab11, while after 2h there were clearly increased co-localization events. Interestingly, after 5h incubation, less HBV^{594} retained inside the cells but almost 100% co-localized with Rab11. These observed increasing co-localization events of HBV to Rab11 suggest that after internalization via early sorting endosomes and following the maturation of the early endosomes, HBV gradually located to recycling endosomes.

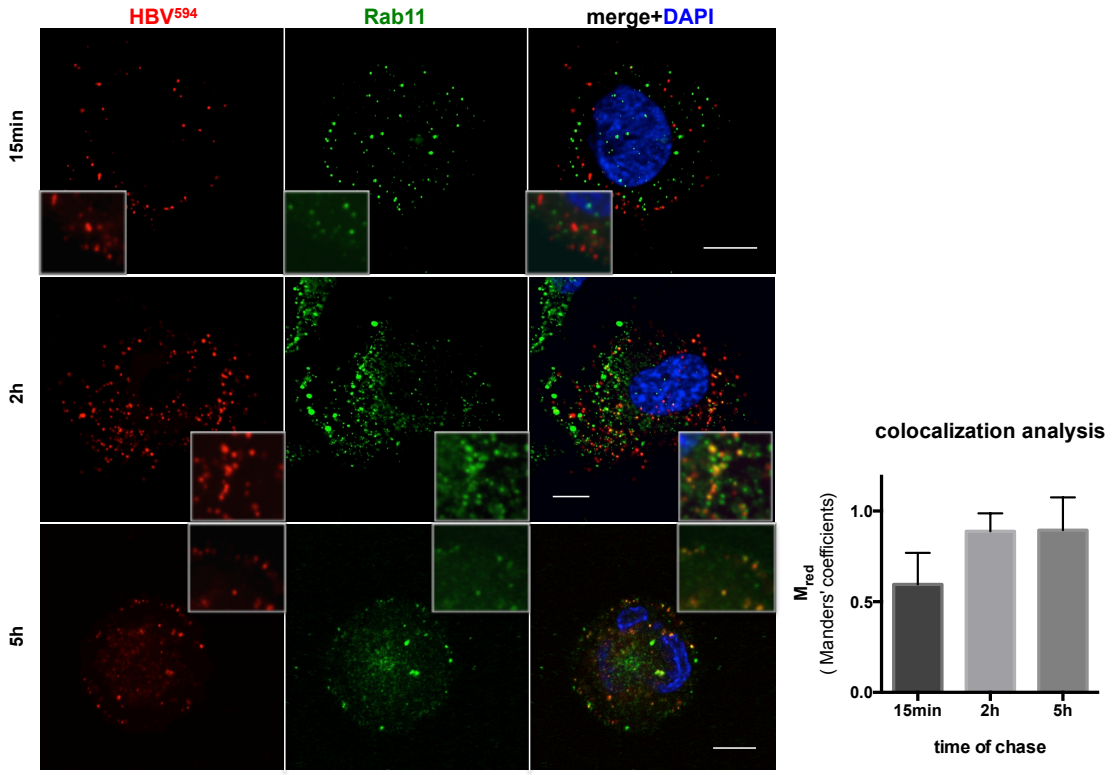

Figure 2.7. Kinetic of HBV association with recycling endosomes. THP-1 macrophages were incubated with HBV^{594} for 1h and chased for 15min, 2h or 5h as indicated on the left. After washing, cells were fixed and stained using antibodies against Rab11. Representative pictures are shown. Scale bar = 10 μm. Co-localization quantification of HBV^{594} with Rab11 was done as described before. Means±SD of three random views of one representative experiment are shown.

So far, the data obtained strongly supported that HBV was delivered to recycling endosomes in the macrophage in parallel with free cholesterol. It is known that human serum containing HDL and ApoA-1 is a strong inducer for cholesterol efflux [307], it was of interest to analyze, if human serum has any effect on HBV and Rab11 co-localization. For this purpose, HBV^{594} loaded THP-1 macrophages were chased for 1h with medium containing 10% human serum. Co-localization of HBV^{594} and Rab11 was compared under conditions with and without human serum. As shown in figure 2.8, in the presence of human serum (lower panel), HBV^{594} had a higher incidence of co-localization with Rab11. Quantification using Manders' approach revealed a significant increase of co-localization coefficient suggesting that human serum components could drive HBV localization to recycling endosomes.

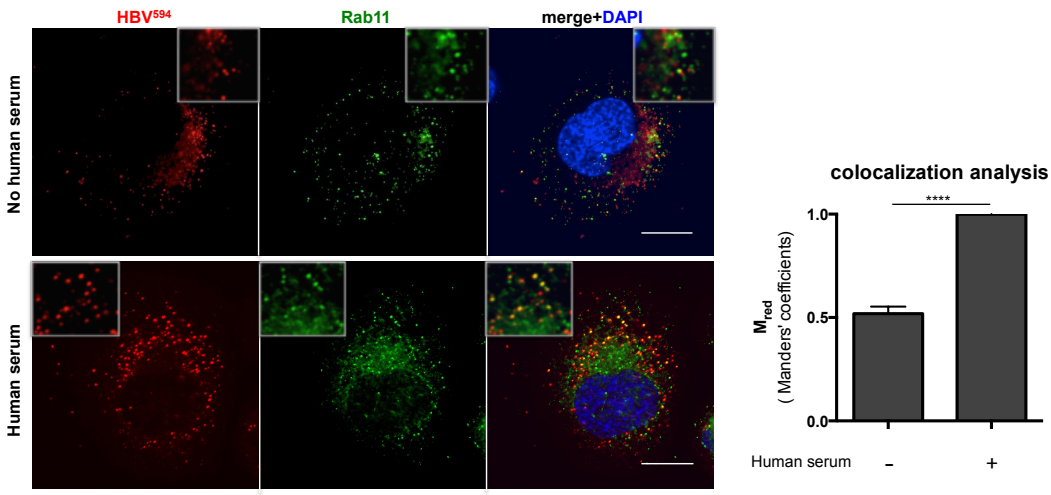

Figure 2.8. Human serum can enhance HBV's location to recycling endosomes. THP macrophages were incubated with HBV^{594} for 1h and chased for 1h using medium containing no or 10% human as indicated on the left of the images. After washing, cells were fixed and stained using antibodies against Rab11. Scale bar = 10 μm. Co-localization quantification was done as described before. Means±SD of one representative experiment are shown. ****p<0.0001

To strengthen the data obtained with THP-1 macrophages that HBV located to recycling endosomes in liver macrophages, primary KCs were utilized. As before, cells were loaded with HBV^{594} for 1h and chase cultivated for 16h. Afterwards, Rab11 staining was performed. As shown in figure 2.9, HBV^{594} also co-localized with Rab11 in KC. This confirmed that in macrophages including Kupffer cells, HBV was delivered into recycling endosomes.

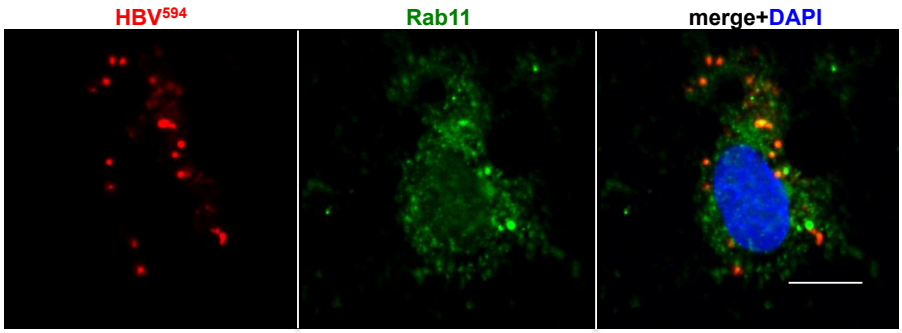

Figure 2.9. In Kupffer cells, recycling endosomes concentrate HBV. Isolated KCs were incubated with HBV^{594} for 1h and further chased for 16h before staining of Rab11. One representative picture is shown. Scale bar = 10 μm.

Taken together, the observations in this part proved that HBV, after entering into the endocytotic pathway, were concentrated in recycling endosomes and successfully avoided lysosomes in macrophages.

2.1.2.2. Extracellular cholesterol acceptors induce HBV re-secretion

The data illustrated so far support that within macrophages, HBV associated with intracellular free cholesterol and also utilized recycling endosomes for transportation. It has been documented that human serum or serum components like ApoA-1or HDL, by acting as cholesterol acceptors, can induce cholesterol transport to the plasma membrane for efflux[303, 308]. In this part, it was investigated whether those substances can also induce HBV re-secretion. For this purpose, macrophages were pulse incubated with medium containing 10^8/ml HBV for 3h to allow virus uptake. After intensive washing, cells were further chase cultured with virus and serum free medium supplemented with different cholesterol acceptors or serum. After overnight chase incubation, the supernatants were collected for HBV or cholesterol analysis.

Figure 2.10 shows the data from THP-1 macrophages. The cells in the negative control have not been exposed to HBV, thus the readout reflects the background value of the HBsAg ELISA assay. The mock control cells have been incubated with HBV, but chased with medium supplemented with BSA only. Here, HBsAg was determined to be close to the negative control. In contrast, significant higher HBsAg was detected in the supernatant from cells chased with medium containing 10%human serum or 25µg/ml ApoA-1 (Figure 2.10.A). In another experiment (Figure 2.10.B), when 200µg/ml HDL was supplemented to the chasing medium, HBsAg in the supernatant was also significantly higher than the mock control. In both experiments (Figure 2.10.A,B), human serum showed the most potent capacity in increasing HBsAg content. To prove that it was not only the virus surface proteins but also mature virions that were secreted during the chase, supernatant collected from mock and human serum chased cells were subjected to DNA extraction and subsequently HBV-DNA qPCR analysis. Absolute quantification showed that around 10^6 copies/ml of HBV genomes were secreted into the chasing medium containing human serum. In contrast, there were much less HBV genomes (≈10^5/ml) in mock control. These data illustrate that human serum or serum components like ApoA-1 and HDL can induce re-secretion of HBV virions from macrophages.

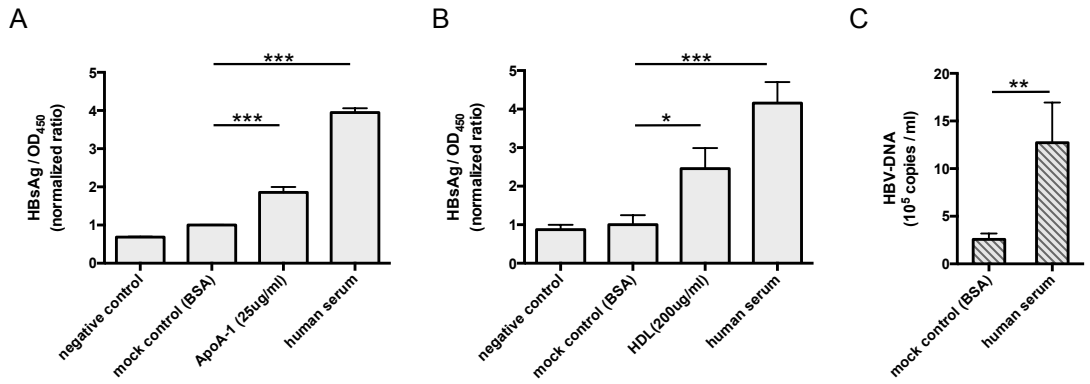

Figure 2.10. Human serum or serum components (ApoA-1 or HDL) induce HBV re-secretion from virus loaded THP-1 macrophages. THP-1 macrophages were incubated with HBV at 37 °C for 3h with exception of the negative control. Following intensive washing, cells were incubated overnight with medium containing 2 mg/mL BSA (mock control) (A-C), 25 μg/ml ApoA-1 (A), 200 μg/ml HDL (B) or 10% human serum (A-C). The next day, supernatants were collected for HBsAg ELISA (A,B) or DNA extraction and qPCR. Means (triplicate) ± SD of one representative experiment of three independent experiments are shown. Where error bars are not visible, they are obscured by the top of the bar or by the symbol. *p<0.05, **p<0.01, ***p<0.001. Experiments were done in cooperation with Dr.Knud Esser.

Furthermore, to access if the observed virus re-secretion was associated with efflux of cholesterol derived from endocytosed lipoproteins, comparable pulse chase assays were performed using THP-1 macrophages as described above with medium containing [^{3}H] cholesterol-labeled TRL in addition to HBV in the pulse phase. After overnight chase, supernatants were analyzed for HBsAg and [^{3}H] cholesterol content by ELISA and liquid scintillation, respectively. As shown in figure 2.11, [^{3}H] cholesterol in the supernatant significantly increased under the incubation of HDL or human serum containing medium, and this correlated with the increase of HBsAg, which suggested that HBV re-secretion occurred in parallel with cholesterol efflux.

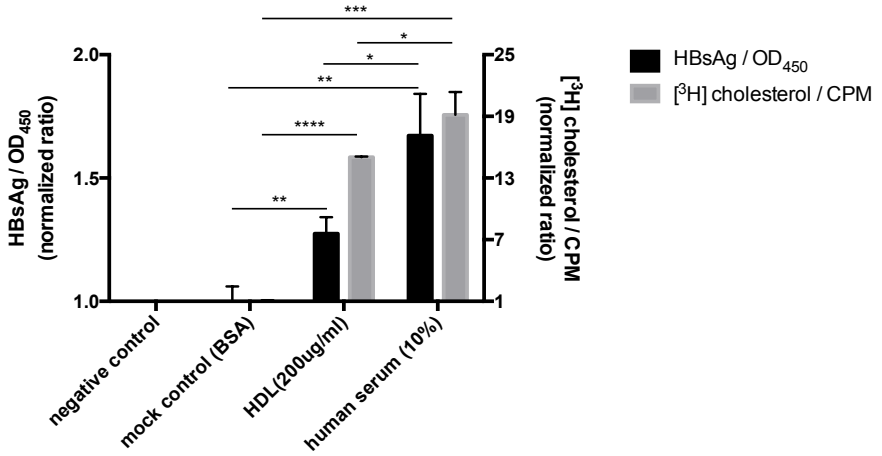

Figure 2.11. HBV re-secretion from virus loaded THP-1 macrophages is associated with cholesterol efflux. THP macrophages were incubated with HBV and [^{3}H]-cholesterol-TRL or no supplements (negative control) for 3h at 37 °C to allow particles uptake. Following intensive washing, cells were incubated overnight with medium containing 2 mg/mL BSA (mock control), 200 μg/ml HDL or 10% human serum (A, B). The next day, supernatants were collected and analyzed for HBsAg by ELISA and [^{3}H]-cholesterol by liquid scintillation assays. Means (triplicate) ± SD of one representative experiment of two independent experiments are shown. *p<0.05, **p<0.01, ***p<0.001, ****p<0.0001. Experiments were done in cooperation with Dr. Knud Esser.

To ensure that virus re-secretion and cholesterol efflux originated from an intracellular pool, not only cell culture supernatant but also cell lysate were collected for analysis in another pulse chase experiment performed with pulse medium containing HBV and [^{3}H] cholesterol loaded TRL. Supernatants were analyzed as described before. From cell lysates, half were used to determine the retained intracellular HBV by HBV-DNA qPCR anaylsis and half were subjected to scintillation assays for [^{3}H]-cholesterol measurement. Results from supernatant analysis confirmed those shown above. Human serum induced higher HBsAg as well as higher [^{3}H] cholesterol contents in the chasing medium (Figure 2.12.A). As a consequence, in cell lysates less HBV and [^{3}H]-cholesterol were retained inside the cells (Figure 2.12.B), confirming that the re-secreted HBV and cholesterol stem from the VP and TRL internalized during the pulse phase.

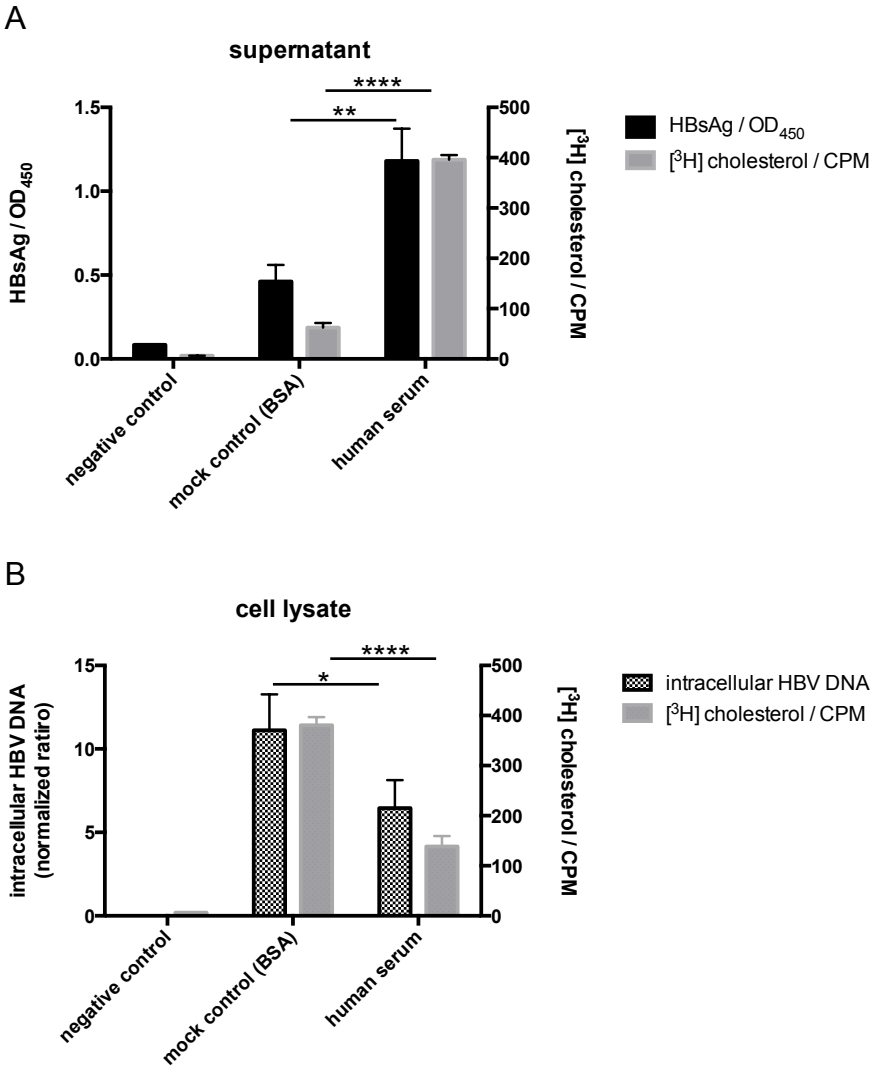

Figure 2.12. Re-secreted HBV and [^{3}H]-cholesterol originate from an intracellular pool. Pulse chase incubation was done similarly as described for figure 2.11. In the end of the experiment, (A) supernant was collected for HBsAg ELISA and [^{3}H] scintillation assay. (B) Cell lysates were prepared as required for DNA extraction. Half lysate was used for DNA extraction and subsequent HBV-DNA qPCR analysis. The other half of the lysate was dissolved in scintillation buffer for [H^3]-cholesterol quantification. Means ± SD of one representative experiment of two independent experiments (triplicates) are shown. *p<0.05, **p<0.01, ****p<0.0001

Besides, MDMs (Figure 2.13.A) and KCs (Figure 2.13.B) were analyzed for HBV re-secretion. Experiments were performed as described for THP-1 macrophages. Comparable to the THP-1 macrophages, the results showed that chase incubation of the HBV loaded cells with medium containing HDL or human serum led to higher HBsAg in the supernatant of MDMs (Figure 2.13.A) or KCs (Figure 2.13.B). This further strengthened the notion that cholesterol efflux inducers can induce HBV re-secretion in liver macrophages.

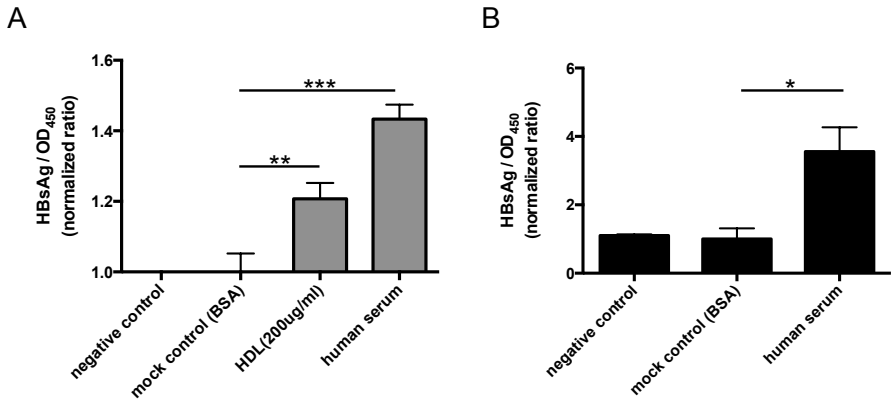

Figure 2.13. Human serum or serum components induce HBV re-secretion from virus loaded MDMs and KCs. MDMs (A) or KCs (B) were incubated with HBV at 37 °C for 3h with exception of the negative control. Following intensive wash, cells were incubated overnight with medium containing 2 mg/mL BSA (mock control) (A, B), 200 μg/ml HDL (B) or 10% human serum (A, B). The next day, supernatants were collected for HBsAg ELISA. Means (triplicate) ± SD of one representative experiment of three independent experiments are shown. *p<0.05, **p<0.01, ***p<0.001. Experiments were done in cooperation with Dr. Knud Esser.

In summary, HBV internalized by macrophages became re-secreted into the cell culture medium, a process defined as transcytosis. Virus transcytosis occured along with efflux of cholesterol derived from endocytosed lipoproteins.

2.1.3. Transcytosis of HBV through Kupffer cells facilitates hepatocyte infection in trans

To test if transcytosis of HBV through Kupffer cells could contribute to infection of hepatocytes in trans, a mix-culture system of KCs and PHHs from the same donor was established. As KCs are much more potent in taking up acLDL than PHH[309], KCs could be discriminated from hepatocytes in this mix-culture system by being acLDL^{488} positive after 6 h incubation (Figure 2.14.A). In the transinfection experiment, KCs were incubated with HBV particles for 6h at 4 °C or 37 °C, which allowed HBV binding only or endocytosis, respectively. Subsequently, KCs were washed intensively to remove free HBV. PHHs were then added to KCs and cells were co-cultured for 12 days (Figure 2.14 B, C). As it is evidenced by the release of HBV antigens into the supernatant (Figure 2.14 B) and HBV cccDNA in cell lysates (Figure 2.14 C), only KCs that were initially incubated with HBV at 37 °C allowing endocytosis led to a productive infection. In contrast, KCs that had been exposed to virus at 4 °C, which only allowed virus binding, did not lead to HBV infection (Figure 2.14.B,C). In pure KC

cultures, no viral antigen was detected although KCs had been incubated with HBV for 6h at 37 °C (Figure 2.14 D). This emphasized again that KCs alone did not support HBV infection, and the detected infection markers in the mix-culture resulted from PHH infection. These data prove that HBV particles transcytose through KCs can trans-infect hepatocytes.

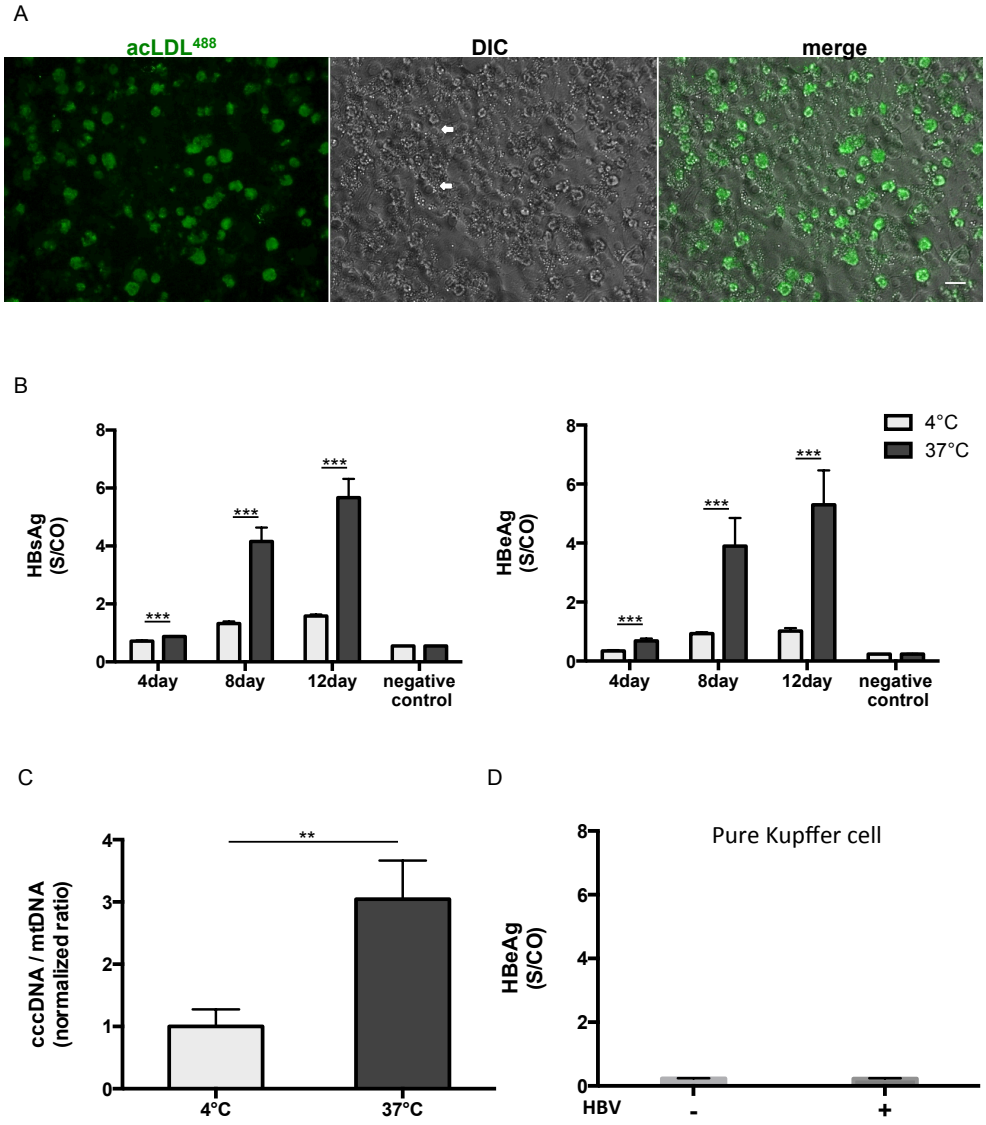

Figure 2.14. HBV transinfects PHH via KCs. Mix-cultured KCs and PHHs were grown as confluent monolayers (A). After incubation with 4 μg/ml Alexa-Fluor 488 labeled acLDL (acLDL^{488}) for 6h, only KCs were fluorescence positive. PHH can be distinguished by their typical round nuclei. White arrows indicate two examples of PHH nuclei. For transinfection experiments (B-D), isolated KCs were incubated with HBV containing medium (1x10^8 genome copies / ml) at either 4 °C or 37 °C to allow HBV binding or uptake. Subsequently, PHHs were seeded (B-C) to KCs and cells were cultured for 12 days (B-C). Supernatants of mix-cultures were collected every 4 days for HBsAg or HBeAg measurements by ELISA (B). Cell lysates were harvested on day 12 for HBV cccDNA qPCR. Supernatant of pure KCs were measured on day 12 for HBsAg (D). Means±SEM of two independent experiments (triplicates each) are shown **p<0.01, ***p<0.0001. Experiments were done in cooperation with Dr. Knud Esser.

2.1.4. Summary

In this part of the study, we found that:

1. HBV endocytosed by macrophages initially concentrated in vesicles enriched for lipoprotein derived free cholesterol.

2. These vesicles were identified to be recycling endosomes. Similar to lipoprotein derived free cholesterol, HBV located to recycling endosomes for intracellular trafficking, which on one hand avoided lysosomal degradation and on the hand allowed HBV re-secretion.

3. The intracellular transportation of HBV occured along the cholesterol transportation pathway.

4. Re-secretion of HBV as well as that of free cholesterol was induced by cholesterol acceptors contained in human serum.

5. Finally, HBV transcytosis allowed hepatocytes infection, defining this process as transinfection.

Thus, it is proposed that *in vivo*, after efficient uptake by sinusoidal KCs, HBV hijacks the cholesterol transport pathway for transcytosis through KCs and to target and infect hepatocytes.

2.2. Discussion

2.2.1. Methods used to evaluate co-localization in present study

In this part of study, confocal microscopy was frequently used for visualizing the localization of HBV[594] in correlation to cellular molecules of interest to investigate the virus association with host cellular machinery (e.g. Figure 2.1,2.2,2.3). It is based on generally accepted idea that the intracellular location of a component is closely related to its role in biological processes. Two components located in the same spatial compartments have higher potential in functional association than components located apart[310, 311].

Co-distribution of HBV[594] with other molecules has been primarily determined by the yellow pixels in superimposed dual-channel images, in which HBV has been pseudo colored in red and the other component in green (e.g. Figure 2.1.). Resulting yellow hotspots reflected combined contribution from each individual probe in the same pixel. Based on the resolution limit of light microscopy, the yellow spots would be insufficient for proving the physical apposition of the HBV and the other target molecule, but it is appropriate to conclude that those two probes were co-distributed in the same cellular compartment, like endosomal vesicles in the presented study[312]. However, the presence of a yellow spot highly depended on the relative fluorescence intensity of each channel, which was affected by factors like quantities of the probe. In the case of HBV[594] and LAMP1 staining (Figure 2.5.), some yellow pixels could be seen in the merged pictures, but HBV[594] was not concluded to co-localize with LAMP1 as the fluorescence overlap of HBV[594] and LAMP1 more likely resulted from broad distribution of LAMP1 in the cytosol.

Merging images of different channels helps to generate visual estimates of co-localization events in two-dimensional, identifying compartments which molecules co-occupy. However, it is not helpful for comparing the degree of co-localization in different experimental groups. To quantify the co-localization, Mander's coefficient analysis was chosen. This coefficient (M) varies from 0 to 1, with 0 reflecting no overlap at all and 1 corresponding to 100% co-localization[313, 314]. For dual-channel images, two M coefficients can be calculated. Taking figure 2.5 as an example,

coefficient M_{red} and M_{green} can be generated. M_{red} indicates the proportion of the red (HBV^{594}) signals coinciding with green (LAMP1) signals over its total intensity. M_{green} would indicate conversely for green (LAMP1). This independent evaluation for each channel is extremely useful when the two components are expected to overlap but to have different intensities[310]. For example, in figure 2.6, HBV^{594} was expected to locate to Rab11 positive recycling endosomes, but there were no rationale to assume that the amount of HBV should parallels the amount of the Rab11 proteins. Co-localization quantification like Pearson's correlation analysis would yield conclusion of low or no co-localization with such non-proportional co-distribution. But Manders' analysis is not affected by the non-proportionality, therefore in this part of my study, Manders' method is more appropriate for quantitatively evaluating co-localization of HBV and rHBsAg with the target molecule (LAMP1 in figure 2.5, Rab11 in figure 2.6,2.7,2.8) than Pearson's method.

However, the limitation of Manders' approach is that its coefficient is very sensitive to noise. To circumvent this limit, M_{red} was calculated with the threshold set to the estimated value of background (Figure 2.5-2.8). Within one experiment, the threshold was set the same for all groups to valid the comparison. But between experiments, the M_{red} was not comparable due to varying background levels.

Taken together, in this part, co-localization was primarily evaluated visually by superposition of fluorescence images, and when the degree of co-localization within one experiment needed to be quantified, additional Manders' co-localization analysis was performed.

2.2.2. Lipoprotein association affects the intracellular fate of HBV in liver macrophages

Our data have suggested that HBV trafficking in liver macrophages is associated with free cholesterol derived from lipoproteins, which are facilitated by recycling endosomes (Results 2.1.1,2.1.2.).

It is known that macrophages are very potent in cholesterol recycling. As "professional phagocytes", macrophages take up cholesterol (via uptake of lipoproteins) at more than average level of any cell type other than hepatocytes, enterocytes and steroidogenic cells[30]. Excess unesterified free cholesterol is toxic to

macrophages and can ultimately lead to cell apoptosis. The key mechanism of defence against cholesterol toxicity in macrophages is cholesterol efflux[315].

Dr. Knud Esser previously showed that HBV in patient serum was associated with triglyceride rich lipoprotein (TRL), which implied that transportation of lipoprotein might affect cellular fate of virus based on the notion that HBV-TRL complexes as multivalent ligands could in principle cross-link with their respective receptors for internalization. Uptake of HBV into liver macrophages could be contributed by receptors mediating TLRs endocytosis, which could lead to an intracellular trafficking route balanced to lipid transportation. As shown in this study, intracellular HBV occupied the same compartment as cholesterol derived from lipoproteins, which was targeted by ApoA-1 (Figure 2.1,2.2,2.3.). Re-secretion of virus co-occurred in parallel to recycling of cholesterol (Results 2.1.2.2.). Similar phenomena have been reported for apoprotein E (ApoE), which resides on the surface of TRL and serves as solvent for hydrophobic lipid moiety [316]. *Heeren et al.* have reported that after TRL internalization, ApoE can escape lysosomal targeting and recycle back to the cell surface following intracellular transport of free cholesterol, which was accompanied by internalization of ApoA-I derived from HDL and its targeting to ApoE/cholesterol-containing endosomes [317, 318 307, 319]. Interestingly, it has been reported that ApoE3 allele has a higher binding affinity than ApoE2 allele to its receptor[320]. Thus, HBV infection should be facilitated in humans carrying the ApoE3 allele. Indeed, ApoE3 has been observed to be overrepresented among patients with HBV-related liver disease, and HBV-infected patients carrying the ApoE3 allele have a lower rate of HBsAg clearance[321, 322].

Without TRL association, the fate of virus particle might be different. As it has been observed in the presented imaging study, recombinant HBsAg produced from yeast (rHBsAg) was initially used to exclude the artifact of HBV fluorescence labeling (Figure 2.5-2.7). The intracellular localization of rHBsAg (Figure 2.5) is observed to be different from HBV (Figure 2.6,2.7), and this could be explained by the lack of human lipoprotein (e.g. TRL) association of rHBsAg due to its yeast origin or lack of large surface protein. To prove that with confidence, a gradient centrifugation of rHBsAg should be done in future.

2.2.3. Kupffer cells contribute to HBV infection in trans, which complements a direct hepaotcyte targeting pathway of HBV

The data described in this study have demonstrated a novel role of Kupffer cells (KCs) in HBV infection—they mediate transinfection of hepatocytes by HBV (Figure 2.14).

On one side, KCs reside in the liver sinusoids and are specialized to perform scavenger and phagocytic functions, thereby removing protein complexes, small particles, and apoptotic cells from blood[9, 323].

So far, there was no study on the uptake of HBV by human KCs *ex vivo* or on the presence of HBV in KCs *in vivo*. Studies using monocyte and THP macrophages have shown binding of HBV (proteins) to these cells[324]. Most of the published studies on the interaction of KCs and HBV focused on the immune regulatory roles of KCs. For example, *Hoesl et al*. reported that KCs contribute to immune activation and anti-viral immunity upon HBV infection[325]. *Wu J et al.* reported that HBV abrogates the pro-inflammatory functions of KCs to evade host immunity[326] and *He L et al.* reported that HBV induced anti-inflammatory cytokine secretion by KCs, which promoted the tolerogenic milieu of the liver[327]. Those seemingly contradictory results could be due to different focus and interpretation of results since always a mixture of cytokines was induced or it could also be due to different experimental conditions used, such as different amount of virus that have been added to cell culture for different time periods, which could result in different receptors binding of HBV to KCs and subsequently different functions of macrophages being triggered[324-326].

The study presented here followed previous observation in our lab, which for the first time revealed the following: in *ex vivo* perfused human liver tissue, in the presence of human serum, HBV was preferentially taken up by KCs after 45min pulse perfusion and entered into hepatocyte only after 16h chase perfusion when KCs became negative for the virus[298]. As the perfused liver maintains a microanatomy structure that closely resembles the *in vivo* situation, the model enabled unveiling the sequential uptake of HBV on the route for hepatocytes targeting, which can be easily overlooked when 2-D cell culture formats are used for studies on host virus interaction.

Based on those data, the study presented here aimed to investigate the roles of KCs in HBV transinfecting hepatocytes as well as the mechanisms involved. For that purpose, *in vitro* cultured macrophage models were used in this study, which led to

the interesting, novel finding that HBV highjacks the free cholesterol transport in macrophages for infecting hepatocytes in trans.

On the other side, HBV infection of hepatocyte occurs with high specificity and extraordinary efficiency. Studies of HBV-infection in chimpanzees and duck hepatitis B virus (DHBV) in ducks revealed that a single virion is sufficient to establish HBV infection when experimentally inoculated[299, 300]. HBV entry in hepatocyte is widely assumed to be directly mediated by hepatocyte specific receptors. In 2012, sodium taurocholate co-transporting polypeptide (NTCP) was identified as a cell and species-specific receptor for HBV. NTCP binding was even considered to be the single entry pathway for HBV infection[97, 98]. However, as hepatocytes are not directly exposed to the blood stream to prevent contact with toxic substances, and particles exceeding 10nm in diameter are limited from free diffusion from sinusoidal lumen to hepatocytes[4, 328], it is questionable how a single virion could overcome the sinusoidal endothelium so efficiently for binding to receptors on hepatocytes. Furthermore and as mentioned before, results from our lab showed, that when HBV entered via the liver sinus, it was preferentially taken up by KCs[298].

Many pathogens are known to be able to exploit physiological pathways to infect target cells in trans. For example, HIV has been described to transinfect $CD4^+$ T cells after being captured by dendritic cells (DC) via DC specific intercellular adhesion molecule-3-grabbing non-integrin (DC-SIGN)[329, 330]. For various hepatotropic pathogens there is also evidence that sinusoidal liver cell populations contribute to infection by facilitating crossing of the sinusoidal barrier. HCV has been shown to be able to bind C-type lectins liver / lymph node-specific intercellular adhesion molecule-3-grabbing non-integrin (L-SIGN) or DC-SIGN presented on the surface of KCs and DCs. Following internalization, HCV is transported via transferrin positive endosomal compartments providing protection from lysosomal degradation and allowing subsequent delivery to proximal hepatocytes[331, 332]. Similarly, for DHBV it was suggested that LSECs removes DHBV from the circulation and that hepatocytes are infected in trans through an active transcellular transport process[333].

Thus, it is not entirely surprising that HBV hijacks a cholesterol recycling pathway for host cell targeting, which is more efficient than direct targeting when the virus first enters the liver from the blood circulation.

To conclude, the presented study disclosed a novel role of Kupffer cells in HBV infection, namely, that the virus could utilize the cholesterol transport machinery of KCs for transcytosis and to transinfect hepatocytes subsequent to internalization by KCs. Such KCs and HBV interactions may contribute to the efficiency of the establishment of HBV infection as well as to the spread of HBV infection both by the capture and delivery of virus to the hepatocytes. Further studies on receptors mediating HBV internalization into KCs may unveil potential targets for designing strategies to combat HBV infections.

3. Experimental part II:

The role of Kupffer cells and liver sinusoidal endothelial cells in early HCV infection

3.1. Results

3.1.1. Characterization of HCVcc (JC1) production and stability

HCVcc describes fully infectious virus derived from cell culture systems owning infectivity *in vivo* as well[285]. Unless otherwise stated, HCV experiments were performed using the HCVcc strain JC1[334]. With the aim to gain a high yield of virus production as well as to know the stability of the virions, some characterization of HCV JC1 was performed. The viral genome was synthesized *in vitro* from the plasmid pFK-JC1 and delivered into Huh7.5 cells by electroporation (EPO). Subsequently, culture supernatants were collected every 24h and stored directly at -80 °C or concentrated by PEG precipitation and then stored at -80°C. Upon use, preserved sample aliquots were thawed and measured directly or incubated at 37°C for different time length before measurement. Absolute genome quantification was carried out using HCV specific Taqman probe based real time PCR, which is calibrated by *in vitro* synthesized standard. HCV infectivity was accessed by limiting dilution assay as described by Lindenbach et al.[284, 286], with modification of staining against NS3 instead of NS5A. The virus production kinetic is shown in Figure 3.1.A. Already one day after HCV RNA EPO, high levels of HCV genome (10^7 copies / ml) were released into the supernatants. The virus production kinetic reached a peak on day 3 post EPO (10^8 copies / ml). In parallel, it was also observed that, counting from the first day after EPO, cells proliferated slower than normal Huh7.5 cells. On day 3 or 4 (varied between productions), when there was the highest virus production, large numbers of cells died (data not shown). This cytotoxicity effect was correlated with a good yield of virus titer. Although it is known that HCV is a non-cytopathic virus, the observed cytopathic effect has been documented in several publications and is attributed to pro-apoptotic effect of HCV at sufficient level[284, 335-337]. After the peak, virus production gradually decreased while the cell number increased and production greatly dropped

when the cells reached confluence due to a lack of nucleotide pool (communication with Ralf Bartenschlager and Jane Mckeating). The stability of HCV infectivity in cell free conditions at 37 °C is shown in figure 3.1.B. Virus $TCID_{50}$ dropped 20% after 1h incubation at 37 °C and 90% after 6h incubation. In contrast, under the same conditions, there was less than 20% change in HCV genome measurement even after 48h incubation.

Taken together, these data suggested that virus production was most efficient between 72 to 96 hours post EPO, which would be most crucial period for preparing highly concentrated stock. In terms of stability, while HCV infectivity was very unstable under 37 °C, HCV genome was rather stable. Therefore, in the following study when virus manipulation was needed, for example labeling, the procedures were managed to avoid 37 °C or higher.

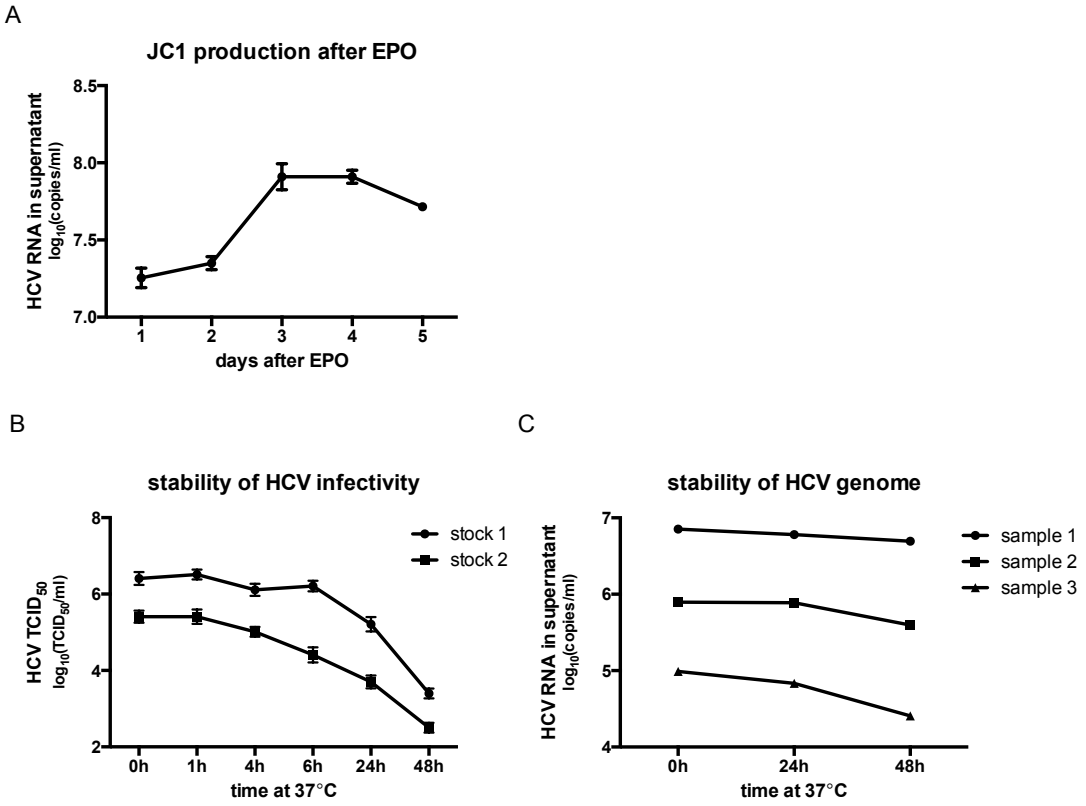

Figure 3.1. HCVcc (JC1) production kinetic and stability at 37 °C. HCV RNA was transcribed *in vitro* from pFK-JC1 with T7 polymerase and electroporated into Huh7.5 cells as described previously[182]. Culture supernatants after electroporation were collected every 24h, concentrated using PEG8000 if necessary and preserved at -80 °C until use. HCV RNA absolute quantification (A and C) and HCV $TCID_{50}$ (B) was performed as described in the section of methods. Means±SD of one representative experiment are shown (sextuplicate for A and triplicate for B and C).

3.1.2. Human liver *ex vivo* perfusion

3.1.2.1. Optimization of the system for longer time perfusion

In a previously in the lab established perfusion system, perfusion was limited to 16 hours[298]. Prolonged perfusion lead to broad cell necrosis, which was very likely due to low O_2 concentration as well as increasing pH value in the perfusate. With the aim of enhancing air exchanging capacity of the system, in the here presented work extra tubing was added. This "air buffer tubing" was with one end inserted into the perfusate container, the other end was connected with a 0.45 nm filter and freely exposed to the air in the incubator. In order to improve the vitality of cells in the perfused tissue, 10 mM sodium pyruvate together with 1 pM EGF was added to the existing perfusate recipe, as this has been reported to protect liver from ischemia reperfusion injury and to support hepatocyte, biliary epithelium and connective tissue regeneration[338, 339]. To test the function of the modified system, non-cancerous human liver tissue leftover from surgery resections were obtained. A small piece was directly fixed for later comparison with the perfused tissue. The remaining pieces were cannulated through portal vein branches and perfused at a speed of 1-3 ml / min / g for 24h with one medium exchange after 12h. Subsequently, tissues were fixed and cyro-perserved, respectively. Due to scarcity of human tissue samples, cryosections of longer perfused tissues as well as functional evaluations of the tissues under perfusion were not possible so far. To examine the integrity of the samples, H&E staining of non-perfused (0h), 1h, 12h and 24h perfused was performed on 5 µm thick cyrosections. Light microscopic evaluation suggested, that the liver architecture was well maintained after 24h perfusion: In issues having been perfused for different time periods the hepatocyte morphology showed the same features in the unperfused sample (0h, Figure 3.2.). The majority of hepatocytes had a single nucleus with one or two prominent nucleoli. Some binucleated hepatocytes could also be found in all samples. The nuclei of hepatocytes have comparable sizes and round shapes in perfused and non-perfused tissues, suggesting that no apoptosis or necrosis occurred in hepatocytes. Thus, it was concluded that the systems optimization was successful and could be used for prolonged perfusion.

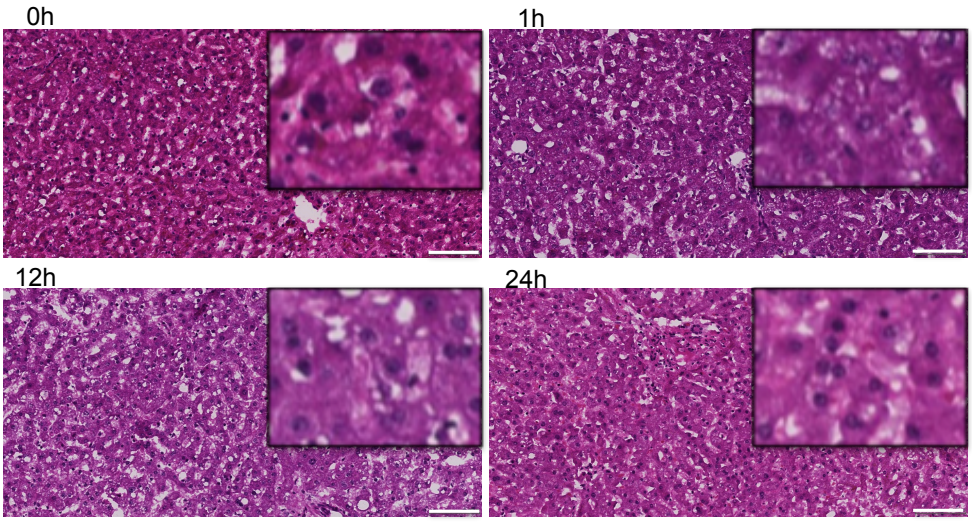

Figure 3.2. Tissue morphology is maintained during perfusion. Human liver tissues were perfused for the indicated time periods prior to fixation and H&E staining. Preventative pictures are shown. Scale bar = 100 μm

3.1.2.2. Establishment of HCV infection

An increasing kinetic of HCV genome in perfusate was achieved

To test if the *ex vivo* perfusion model supports productive HCV infection of the hepatocytes, an 5g human liver tissue was first perfused for 12h with medium containing HCV at 10^7 genome copies/ml (10 genome copies / hepatocyte, which equals 0.1 $TCID_{50}$ / hepatocyte) to allow sufficient virus uptake. Following three times washing with PBS, fresh medium without virus was given for continued perfusion. A second medium exchange (virus free) was performed at 38 h.p.i. (hours post infection) to maintain sufficient nutrient supply in the medium. Perfusate samples were collected for HCV genome quantification at different time points up to 48h. As shown in figure 3.3, from 16 h.p.i. to 37 h.p.i., a 2 log increase of virus genome copies was detected. After the medium exchange, 10^4 copies / ml HCV genome was still detected on 40 and 48 h.p.i. Those data indicated that HCV infection can be established in human liver under perfusion condition.

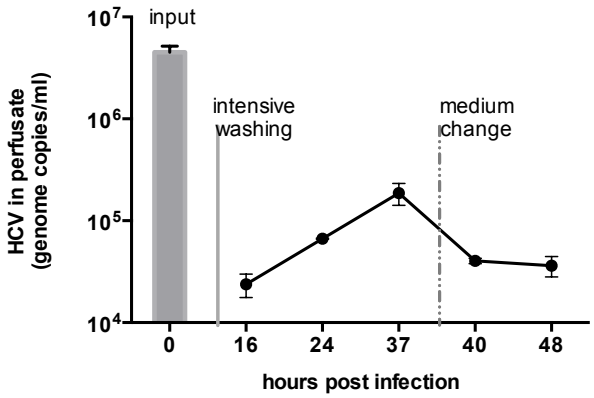

Figure 3.3. HCV infection in perfused human liver tissue. Human liver tissues were perfused with 500 ml medium containing 10^7 genome copies / ml of HCV for 12h. After extensive washing, tissues were perfused with HCV free medium. A second medium change was carried out at about 38 h.p.i. Perfusate was collected at indicated time points for RNA extraction and absolute quantification of HCV genome.

Establishment of strand-specific detection of HCV (-) RNA by qRT-PCR

The kinetic of HCV genome in the perfusate strongly supported that a productive infection was established. To solidly prove HCV replication in the perfused liver tissue, a second readout would be supportive. As HCV has a positive-strand RNA genome, negative-strand HCV RNA only exists when virus is actively replicating. Therefore, establishing an HCV negative strand ((-) strand) specific SYBR Green based qRT-PCR became the aim of the next step.

For this purpose, the highly conserved 5'-UTR region of the viral genome was chosen as amplification target. cDNA synthesis was carried out using a primer targeting the HCV 3'-end with addition of a Tag sequence. Thermoscript™ reverse transcriptase, which enables RT at 60°C, was used to replace the commonly used SuperScript® III reverse transcriptase, which synthesizes cDNA at the temperature range of 42-55°C. Quantitative PCR primers were designed in a way that one primer bound the tag sequence and the other primer bound the HCV specific sequence. Using the tagged HCV specific primer during RT as well as higher RT temperature, the goal was to minimize the potential detection of unspecifically primed cDNA. The qRT-PCR strategy is briefly depicted in figure 3.4.

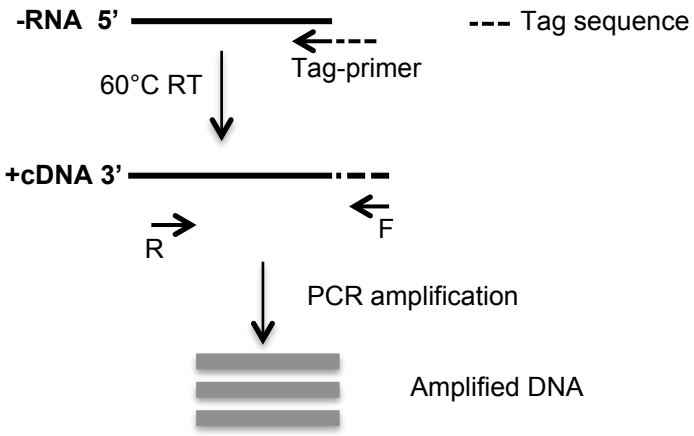

Figure 3.4. Schematic diagram of tagged strand-specific qRT-PCR. A (+) cDNA complementary to the (-) RNA was made using thermo-stable reverse transcriptase (Thermoscript™). The primer used in RT contained a tag sequence in addition to the sequence complementary to the HCV (-) RNA. qPCR amplification of the tagged cDNA was performed using only the tag portion of the cDNA for one of the primers and a HCV specific primer as the opposing primer.

To evaluate the specificity of this method, synthetic (+) RNA was diluted in 10 fold series in cellular RNA extracted from virus free Huh7.5 cells, which was to mimic the real situation. The (-) RNA amplification was performed as described in detail in the chapter of materials and methods. Cellular RNA containing 10^6 copies of synthetic (-) HCV RNA or H_2O were used as positive and negative control, respectively. In the end, all the PCRs had an amplification curve. Specific amplification of positive control produced oligonucleotides having a single melting point at around 88°C (Figure 3.5.A). This is due to the tag sequence introduced into specific cDNA during RT, which resulted in a longer PCR product compared to conventional SYBR Green products. Amplification product of the negative control (H_2O) has a single low melting point at around 81°C (Figure 3.5.F). When using HCV (+) RNA as template, in the existence of 10^7 or more HCV (+) RNA, two types of products with distinct melting temperatures were generated. One was around 88°C and the other was around 81°C. In the presence of 10^6 HCV (+) RNA only products with lower melting temperature was generated (Figure 3.5.B-E). These data suggest that the qRT-PCR strategy used can successfully amplify (-) RNA. With lower concentration of (+)RNA ($\leq 10^6$ copies/reaction), unspecific products could be distinguished from specific products by melting temperature. But with higher concentration of (+)RNA ($\geq 10^7$ copies/reaction), additional unspecific products were generated with the same melting feature as specific products. In the following trial, a higher detection temperature (84°C) was

setted. And under this setup, no false negative strand could be detected for samples containing 10^6 or less (+) HCV RNA.

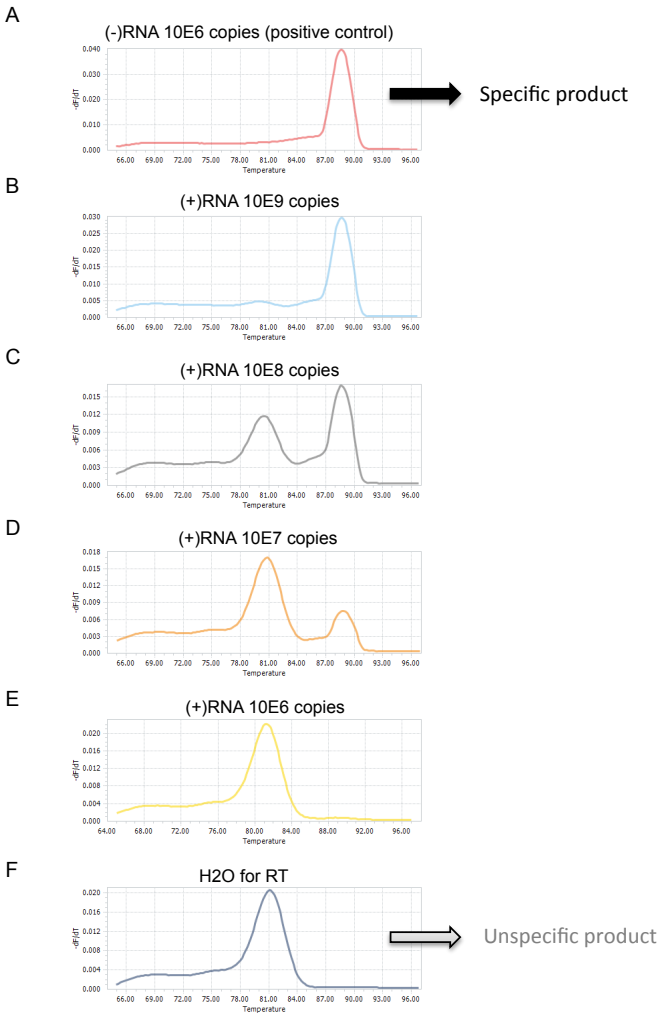

Figure 3.5. Melting curves of HCV (-) RNA qRT-PCR in specificity test. *In vitro* synthesized HCV (+)/(-) RNA or H_2O were diluted in virus free Huh7.5 cellular RNA as indicated above each melting curve picture (A-F), and they were used as templates for RT. Primer HCV-tag-RC1 and Thermoscript reverse transcriptase were used for reverse transcription at 60°C. Ten times diluted cDNA were used for SYBR Green qPCR with primers HCV-tag/ HCV-RC21.

To test the sensitivity of HCV (-) RNA qRT-PCR, serial dilutions of synthetic (-) RNA were prepared in cellular RNA extraction. 10^5copies/reaction of (+) RNA were added to the template to mimic the real situation, in which (-) RNA always co-occurs with (+) RNA. As shown in Figure 3.6, the lower the (-) RNA concentration, the higher the crossing point (Cp) value was. When HCV (-) RNA template was less than 10^5 per reaction the Cp values of HCV specific PCR exceeded 40. Only when HCV (-) RNA was above 10^8, the Cp fell into range of less than 30 representing a very high detection limit for HCV (-) RNA.

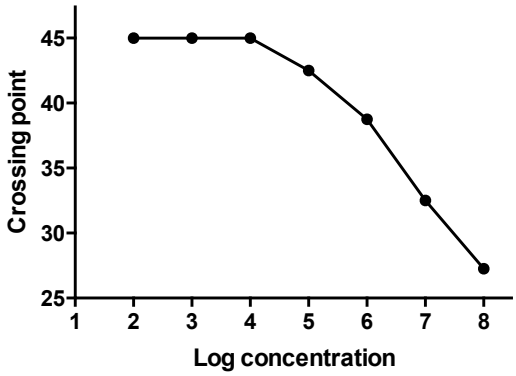

Figure 3.6. Quantification curve of HCV (-) RNA amplification. RT was carried out using 10-fold serial dilutions of synthetic (-) HCV RNA in the presence of 10^5 (+) HCV RNA. Cycle numbers of crossing points were plotted against the logarithmic concentration of the serial dilutions.

Taken together, these studies illustrate that a strand-specific detection of HCV (-) RNA by qRT-PCR is possible using the established protocol, however sensitivity must be improved if a specific detection in samples with low amounts of HCV (-) RNA is required. Taking that into account, it was not surprising that the RNA extracted from *ex vivo* perfused liver tissue failed to give a clear positive result (data not shown) under the current protocol. Further optimization in enhancing the efficiency of RT or qPCR would be helpful.

3.1.2.3. Sequestration of HCV by non-parenchymal cells

To unveil the entry route of HCV in the liver, a time course analysis of virus location in the perfused liver was carried out. Obtained liver tissues were cannulated through portal vein branches and perfused with HCV containing medium for 1h at 1 ml /min / g (pulse phase) (Figure 3.7), which was followed by a continued perfusion with virus free medium at 3 ml / min / g for indicated time length in some experiments (chase phase) (Figure 3.8,3.9). In the end, tissues were fixed and immunofluorescence staining was performed in the cryosections. Antibodies against L-SIGN (CD209-L), smooth muscle actin (SMA) and CD68 were used to label LSECs, HSCs and KCs, respectively. HCV was stained using monoclonal antibodies against E2. Because within hepatocytes, filamentous actin (F-actin) is concentrated along the plasma membrane[340], phalloidin was used to label actin for the purpose of depicting the outskirt of hepatocytes.

After 1h pulse perfusion with HCV containing media, the HCV-E2 signal was mainly distributed along the sinusoids (Figure 3.7.B). Figure 3.7.C shows two examples of L-SIGN positive LSECs. The cell in area “i” had a distinguishable cytosol, which was positive for HCV and surrounded by the L-SIGN positive membrane. The cell in area “ii” represents the typical morphology of LSECs, which is very slim and has no distinctable cellular structures like plasma membrane, cytosol and nucleus. But it is clear that HCV E2 located to L-SIGN positive pixels. To exclude that such a spatial co-distribution of E2 and L-SIGN was an artifact caused by unresolved imaging of two targets that did not co-localize but only in close proximity, which was highly possible if large amount of HCV viral particles were attached to hepatocytes membrane, hepatic stellate cells (HSCs) was labeled against SMA. HSCs reside in the space of Disse between endothelium and hepatocytes [341]. As shown in figure 3.7.D, signals of SMA were one layer more closer to parenchymal area and for all SMA positive pixels E2 were negative, and vice versa. This observation suggested that the HCV virus were spatially separated from hepatocytes and thus confirm that the co-localization of E2 and L-SIGN reflected binding or uptake of virus by LSECs. When L-SIGN positive cells (or cell like structures) were counted for HCV positivity, the result was close to 100% (Figure 3.7.G). When KCs, another liver sinusoidal cell population, were checked, it was found they also efficiently took up HCV from the perfusate. As exemplified in figure 3.7.E, $CD68^+$ cells showed strong E2 staining in the cytosol. Quantification revealed that around 80% KCs were HCV positive. However, at this time point almost no hepatocyte contained any HCV-E2 signal intracellularlly even if neighboring non-parenchymal cells were strongly positive for HCV (Figure 3.7F). Taken together, those data suggested that LSECs and KCs could efficiently sequester HCV from circulation, while hepatocytes were not in the preference of virus entry during the early infection.

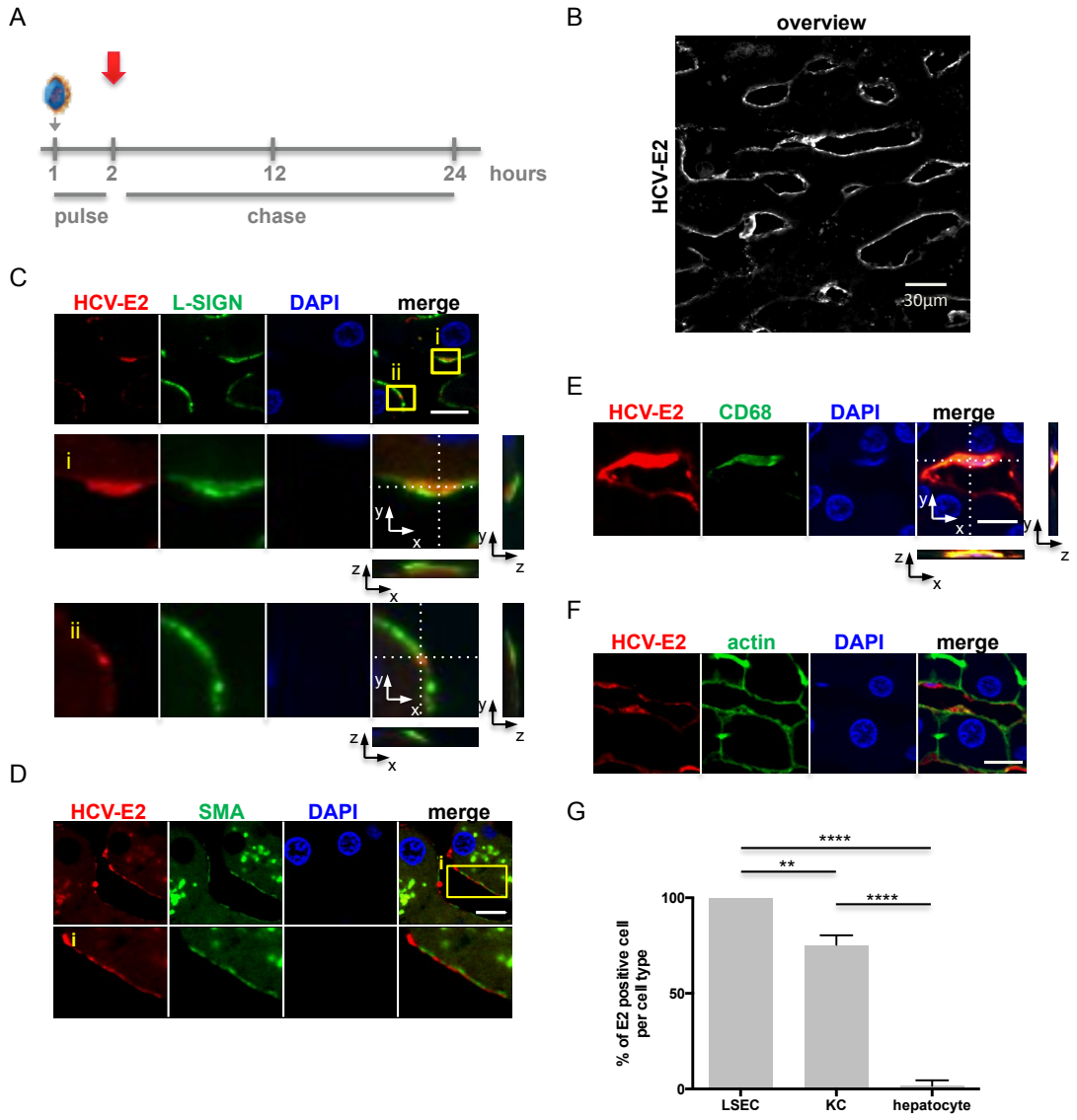

Figure 3.7. Localization of HCV in human liver tissue after 1h perfusion. (A) Scheme of the experimental setup. The red arrow indicates that for this experiment, tissues were directly fixed and processed for cryosection after 1h virus perfusion. (B-F) Immunofluorescence staining: antibodies against E2 were used to stain HCV, antibodies against L-SIGN, SMA and CD68 were used to label LSCEs, HSCs and KCs, respectively. Alexa Fluor® 488 Phalloidin were used to stain actin to depict the outskirt of hepatocytes. Boxed areas are shown enlarged below the main panels separately for each channel. Z-sections taken at dotted line are shown as indicated. (G) Cells of each type were counted and quantified for the incidence of being HCV-E2 positive. Ten random vision fields were counted. Means ± SD of each cell type are shown. ****p<0.0001, ***p<0.001. All scale bars are 10 μm unless indicated differently.

To investigate the further route of HCV, human liver tissue was chase perfused for 11h with virus free medium after the 1h pulse perfusion. As illustrated in Figure 3.8.B, the majority of HCV still distributed along sinuses. Cell type specific quantification showed that around 60% of LSECs were HCV positive (Figure 3.8.E). However, in

contrast to the early time point (Figure 3.7), HCV staining could now be found in parenchymal cells in some areas (Figure 3.8.B). CD68 positive KCs contained weaker HCV-E2 signals in the cytosol compared to KCs after 1h HCV pulse perfusion. Some punctate HCV signals located to the cell membrane (Figure 3.8.B). Quantification revealed, that about 10% of KCs were positive for HCV-E2 (Figure 3.8.E). In hepatocytes, HCV-E2 was found within or on the actin cortex. Quantitatively, about 25% of hepatocytes were positive for HCV-E2. In summary, it was concluded that after further chase, HCV started the entry process to the hepatocytes. The non-parenchymal cells became less positive with HCV, which could be due to virus degradation or hepatocytes targeting.

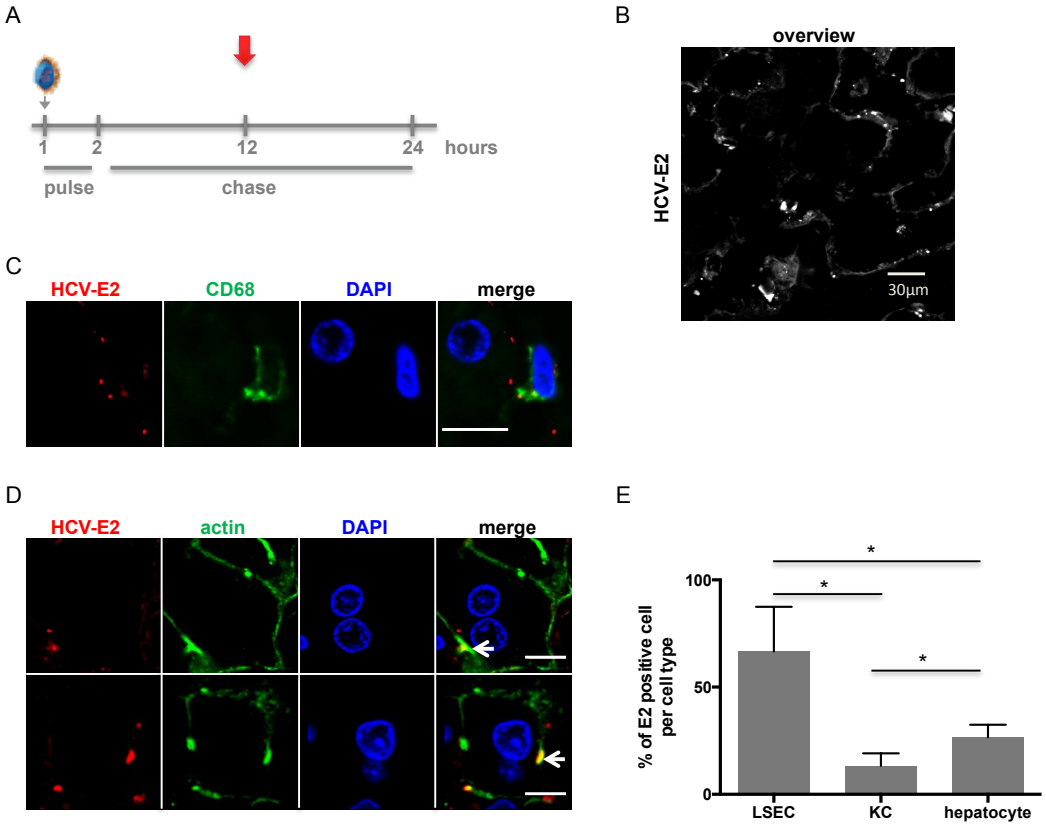

Figure 3.8. Localization of HCV in human liver tissue after 11h chase perfusion. (A) Scheme of the experimental setup. The red arrow indicates that for this experiment, the tissue was fixed and processed for staining after 1h pulse perfusion and 11h chase perfusion. (B-D) Immunofluorescence staining: Similar as before, antibodies against E2 were used to stain HCV, antibodies against CD68 were used to label KCs. Alexa Fluor® 488 Phalloidin were used for actin staining. Boxed areas are shown enlarged below the main panels separately for each channel. Z-sections taken at dotted line are shown as indicated. (E) Cell type specific quantification was done as described before. Ten random vision fields were counted. Means ± SD of each cell type are shown. *p<0.05. All scale bars are 10 μm unless indicated differently.

To check more into detail about HCV's localization during the early entry into the liver, the chase perfusion of an HCV exposed liver piece was enhanced to 23h (Figure 3.9.). Confocal microscopic examination revealed that after 24h, HCV viral particles did not concentrate along sinuses anymore but dispersed into the liver tissue (Figure 3.9.B). Within hepatocytes, HCV could be found much deeper in the cytosol than at earlier time points (Figure 3.9.C). Cell counting showed 50% hepatocytes were positive for HCV-E2. In contrast, LSECs and KCs showed 20% or less percentage of E2 positivity (Figure 3.9.D, E). Those data, together with the data from the above two imaging analyses (Figure 3.7, 3.8), suggested that in an HCV infection event, there was sequential uptake of virus by the liver cells, with LSECs and KCs having the initial contact with HCV and hepatocytes targeting occurred at a later time.

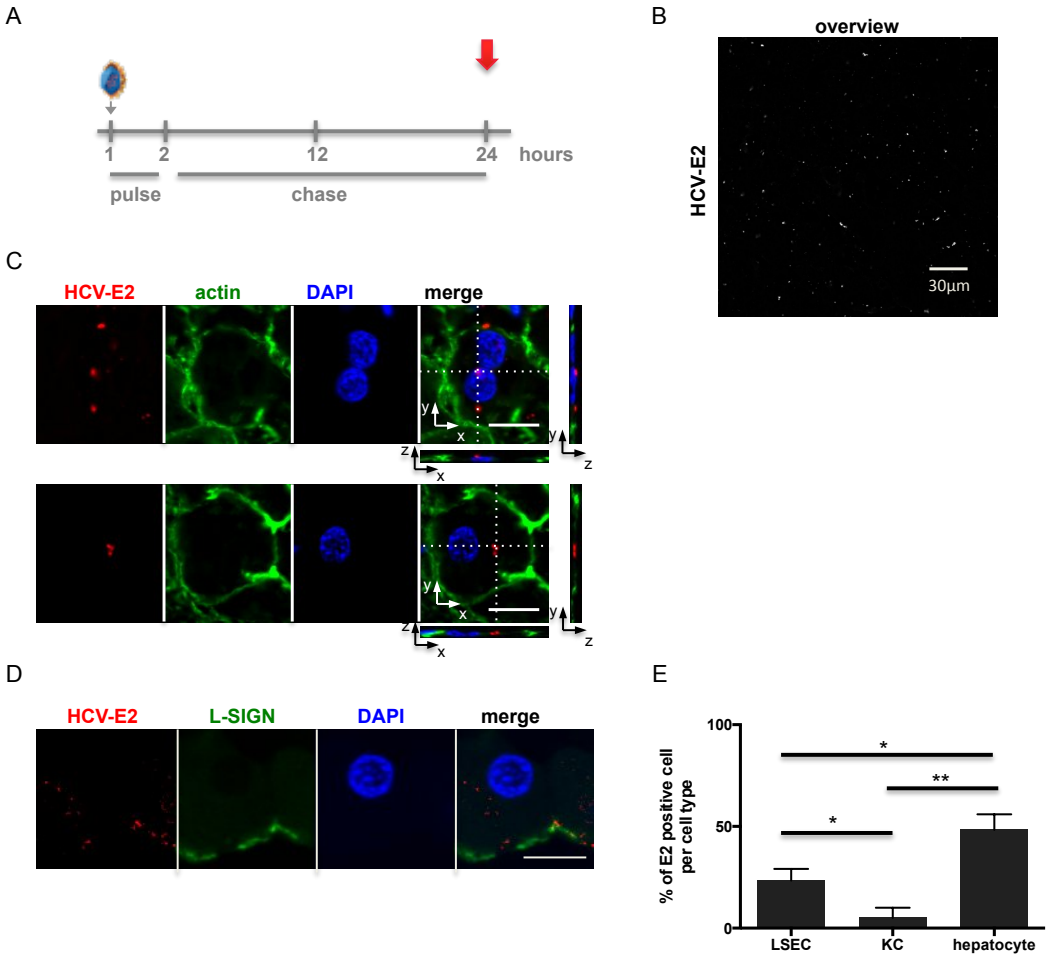

Figure 3.9. Localization of HCV in human liver tissue after 23h chase perfusion. (A) Scheme of the experimental setup. The red arrow indicates that for this experiment, tissue was fixed and processed for staining after 1h pulse perfusion and 23h chase perfusion. (B-D) Immunofluorescence staining: Similar as before, antibodies against E2 were used to stain HCV, Alexa Fluor® 488 Phalloidin were used to label actin, antibodies against CD68 were used to label KCs. Z-sections taken at dotted line are shown as indicated. (E) Quantification of HCV positive cells of each type. Ten random vision fields were counted. Means ± SD are shown. *P<0.05, **P<0.01. All scale bars are 10 μm if not indicated differently.

3.1.2.4. Interferon induction by HCV

It is well acknowledged that HCV can elicit an innate immune response already within the first days after infection *in vivo*[342]. Thus, it was interesting to study if innate immunity in *ex vivo* perfused liver tissue was activated by the virus. Human liver was perfused in the same manner as in the infection experiment (Figure 3.6.). Additionally, liver tissue perfused with mock medium prepared from virus free control Huh7.5 cell culture was used as control. At the end of perfusion, tissues were cut into small pieces and separately lysed for RNA extraction. Expressions of IFN genes as well as HCV

RNA were measured by qRT-PCR. IFN induction was calculated by dividing the target gene expression level after perfusion with the self-non-perfused level. As it is shown in figure 3.10, mock perfusion enhanced IFN expression, ranging from 0.6 fold for IFN-γ, 1.5 fold for IFN-λ to around 2 fold for IFN-α and IFN-β in logarithmic scale. When the liver tissues were perfused with HCV, virus exposure upregulated the expression of IFN-λ and IFN-β 6 and 5.5 fold, followed by IFN-α and IFN-γ, which were induced around 2 and 1 fold, respectively. If subtracting the background induction induced by mock perfusion, the pure induction by HCV was most prominent for IFN-β and IFN-λ, which was a 3.6 and 4.7 fold enhancement, respectively. To characterize the correlation of IFN-β/IFN-γ with HCV, IFN expression and HCV genome in different pieces of the same liver sample were analyzed by Pearson's correlation method. As it is shown in figure 3.10.B, IFN-β expression strongly correlated with HCV genome load (Figure 3.10.B. left), with the correlation coefficient being 0.9978. However, when same analysis was applied to IFN-λ and HCV, no correlation could be found (r=-0.054, p=ns) (Figure 3.10.B. right). So far, it could be concluded that in the liver perfusion model, a HCV specific innate immune response was induced. IFN-β and IFN-λ were the major induced IFN. IFN-β positively correlated with HCV RNA, but no correlation was found for IFN-λ.

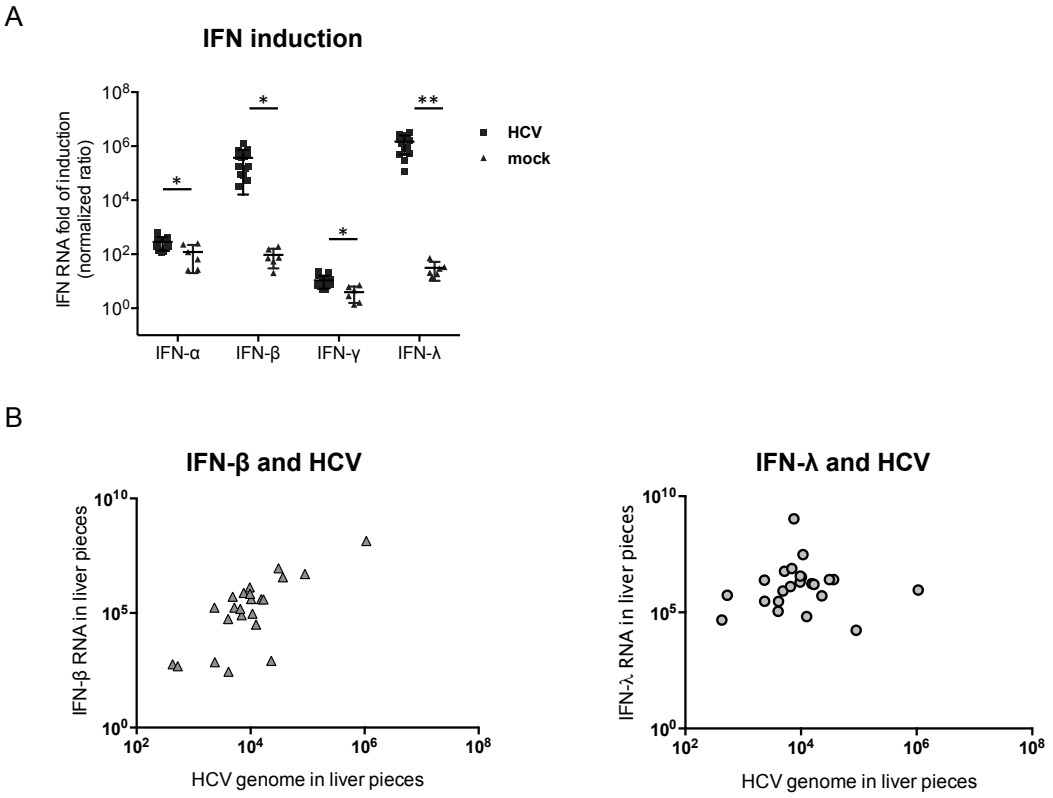

Figure 3.10. HCV induces IFN expression in *ex vivo* perfused human liver tissue. Human liver tissues were perfused with either HCV or mock medium for 12h followed by washing and further virus free perfusion. Tissue pieces before and after perfusion were randomly taken for RNA extraction. Relative quantification of target gene expression was determined by qRT-PCR. (A) Gene expression levels without perfusion were set to one for both HCV and mock perfusion. n_{HCV}=14, n_{mock}=6; *p<0.05, **p<0.01. (B, C) Relative expression of IFN-β/IFN-λ against relative quantification of HCV genomes from the same piece were plotted and subjected to Pearson's correlation analysis. n=24; For IFN-β and HCV, r=0.9978, ****p<0.0001; for IFN-λ and HCV, r=-0.054, p=ns.

3.1.3. Interactions of liver non-parenchymal cells with HCV *in vitro*

3.1.3.1. Binding of HCV to Kupffer cells facilitated hepatocytes infection in trans

It has been reported that HCV can transinfect hepatocytes via macrophages, dendritic cells or endothelial cells *in vitro*, and that process is mediated by virus transcytosis through those non-hepatocytes following binding to their surface DC-SIGN/L-SIGN molecules[331, 332, 343, 344]. In the HCV location analysis described before, a sequential uptake of HCV first by LSECs/KCs and later by hepatocytes was observed, which strongly suggested a transinfection pathway for hepatocyte targeting of virus. However, Prof.Dr.Jane Mckeating in Birmingham has failed to detect transinfection in

mix-cultured primary human LSECs and hepatocytes (communication). Thus, it was of interest to test if KCs could mediate transinfection of hepatocytes *in vitro*. With this aim, a transinfection experiment using mixed cultures of KCs and hepatocytes was set up (Figure 3.11.A). In this experiment, the HCVcc strain that express luciferase upon virus replication was utilized (JC1-luci). Isolated KCs were incubated with JC1-luci at 4°C or 37°C. In another group, cells were pre-incubated with mannan for 30min at 37°C to block the binding sites of DC-SIGNs. JC1-luci was applied afterwards to the KCs at 37°C in the presence of mannan. After 2h virus loading with or without mannan, KCs were washed intensively to remove cell free virus and co-cultured with Huh7.5 cells for 3 days before HCV replication being measured by luciferase assays. In addition, pure Huh7.5 cells incubated with the same MOI of virus were used as positive control. Mix-culture of virus non-exposed KCs with hepatocytes served as negative controls. As shown in figure 3.11.B, Huh7.5 cells cultured with KCs incubated initially with HCV at 37°C had virus infection established, supporting KCs associated virus can lead to productive infection in hepatocytes in trans. And blocking the binding capacity of SIGN molecules on KCs could prevent this infection. Interestingly, KCs incubated with virus at 37°C or 4°C led to comparable levels of virus infection in the 3 day mix-cultured cells, suggesting the that the transinfection mediated by KCs is not dependent on virus internalization into KCs. To conclude, these data suggested that SIGN molecules (DC/L-SIGN) expressed on KCs could capture HCV on the cell surface and mediate the hepatocytes infection in trans.

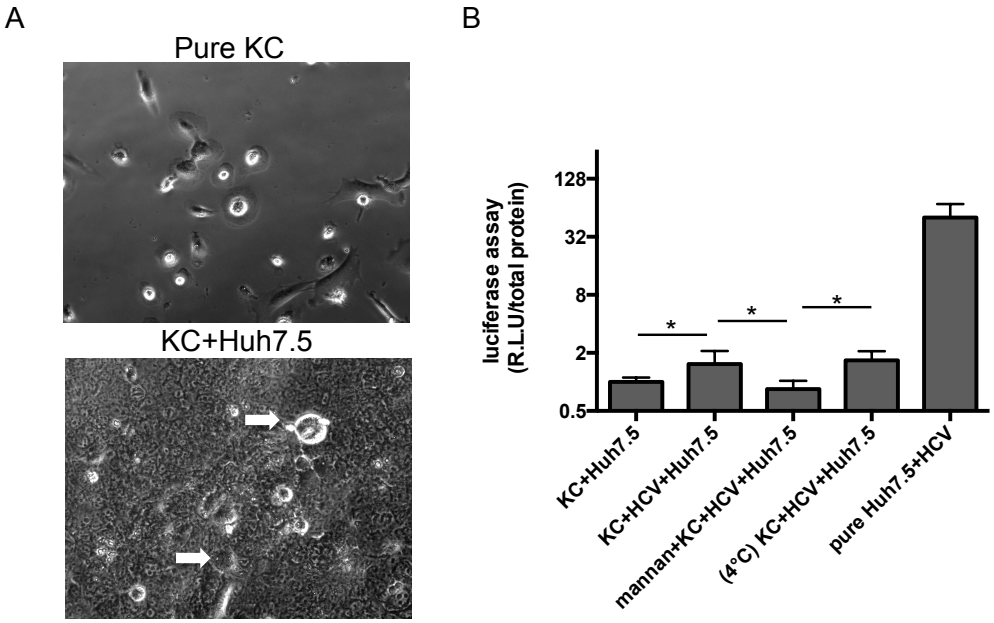

Figure 3.11. Transinfection of Huh7.5 cells by HCV loaded KCs. (A) Light microscopy of pure KCs culture (top) and KC/Huh7.5 mix-culture (bottom). Arrows indicated KCs in mix-culture. (B) KCs were exposed to HCV at 4 °C (indicated) or 37 °C before hepatocytes were added. 20 ng / ml mannan was applied to KCs for 30min before and during virus incubation. Cells were lysed after 3 days of co-culture for luciferase assay. BCA assay was carried out to determine the protein concentration for luciferase readout normalization. Means±SD of one representative experiment are shown (triplicate).

3.1.3.2. Innate immune response against HCV from Kupffer cells and Liver Sinusoidal Endothelial Cells

As KCs and LSECs have vigorously taken up HCV in the ex vivo perfused liver (Figure 3.7, 3.8, 3.9) and high expression of IFNs was induced in the liver tissue after virus exposure (Figure 3.10), it was speculated whether KCs and LSECs had contributed to IFN production. For this purpose, isolated human KCs were incubated with purified HCV at different dose for 6h. For virus purification, culture supernatant from virus producing Huh7.5 cells was ultracentrifuged with a sucrose cushion. Supernatant from control virus-free Huh7.5 cells went through the same procedures for production of a mock control. 50 ng / ml LPS were used as a positive control for cytokine induction. After incubation, cells were lysed for RNA extraction and cytokine qRT-PCR. As it is shown in figure 3.12. A, the cell associated virus genomes were in proportion to the input level. When HCV was added to the cell culture at 0.1 $TCID_{50}$ / ml, IFN-β expression was upregulated around 6 fold compared to the mock control (Figure 3.12.B). As the NF-κB pathway is known to be closely involved in

transcriptional activation of IFN-β[345-347], expression of IL6 and TNF were also checked. 6h after virus exposure, IL6 expression was determined to be 6 fold increased, and with higher dose of virus the IL6 expression was also significantly higher (Figure 3.12.C). TNF was 5 fold enhanced under HCV stimulation at 0.1 $TCID_{50}$/cell (Figure 3.12.D). These data demonstrated that HCV was sensed by KCs, which lead to IFN-β expression and NF-κB activation already 6h after virus exposure.

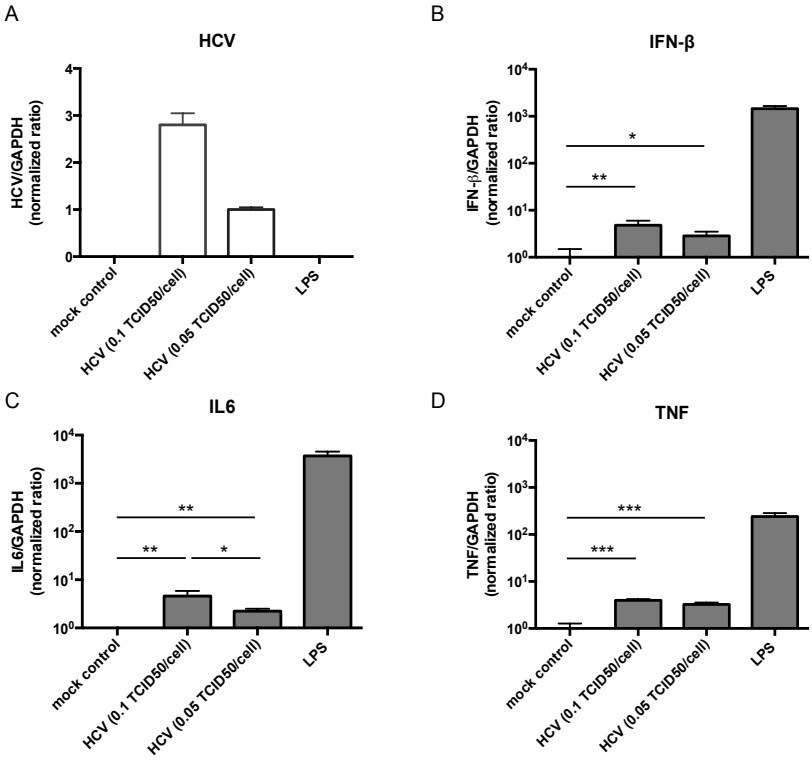

Figure 3.12. *In vitro* stimulation of primary human KCs by HCV. (A-D) *In vitro* cultured human KCs were exposed to virus free mock control, purified HCV at different dose or 50 ng / ml LPS for 6h. RNA extraction and qRT-PCR for relatively quantifying target gene expression under different conditions was performed. Means±SD of one representative experiment of two independent experiments are shown (triplicate values). *P<0.05, **P<0.01, ***P<0.001

To check LSECs' behavior under HCV stimulation, similar experiment as for the KCs were planed for isolated human LSECs. However, as human LSECs could not be isolated in sufficient number, murine LSEC was chosen as alternative model. The rational behind this is that the innate immune system is phylogenetically conserved [348] and the virus does not replicate in human LSECs anyway[349].

To check if murine LSEC is a reasonable model under the current context, it was tested whether or not murine LSECs would efficiently take up HCV.

For this purpose, fluorescence labeling of HCV particles were established. A HCV strain that expresses flag-tag fused E2 membrane protein (JC1-flag) was labeled by integration of the lipophilic dye DiI into the viral envelope. Briefly, culture supernatants from JC1-flag producing Huh7.5 cells were collected. After filtration to get rid of cell debris and concentration to enrich JC1-flag, virions were purified using anti-flag affinity chromatography. The eluted virus enriched fractions were then incubated with DiI. The labeled virus was purified from the labeling mixture by two rounds of size exclusion chromatography. After those procedures, lipoproteins derived from cell culture, which can equally be labeled by DiI, was supposed to be removed by affinity chromatography and the exceeded free DiI was cleaned by size exclusion chromatography. The enriched DiI labeled virus was designated as HCV^{DiI}. To check if the labeling was success and specific, the final stocks were incubated with Huh7.5 cells under different condition for 2h to allow virus entry. As shown by fluorescence microscopy (upper panel, Figure 3.13.), when using purified mock supernatant derived from virus free Huh7.5 cells for labeling ($mock^{DiI}$), no fluorescence could be detected after cell incubation. But when using supernatant from JC1-flag producing cells (HCV^{DiI}), fluorescence signals could be detected in the cytosol of naïve cells, proving that virus had been successfully labeled and that was suitable for visualization. To further confirm the specificity of labeling, a HCV neutralization assay was performed. HCV^{DiI} was preincubated with neutralization antibodies AP33 targeting E2 protein or isotype control antibodies for 30min under cell free condition and then applied to Huh7.5 cells in the presence of antibodies for 2h before microscopy (middle panel, Figure 3.13.). In the presence of HCV neutralization antibody (HCV^{DiI}+nAb) ,which can block virus entry by targeting the E2 protein, fluorescence signals was clearly reduced, while with treatment of antibody isotype control (HCV^{DiI}+isotype control Ab), fluorescencece positive cells could be found as easily as in non treated cells (HCV^{DiI}, upper panel, Figure 3.13). To quantitatively show the fluorescence difference, pixel intensities of four randomly chosen fields were quantifiedplotted (Lower panel, Figure 3.13.), This showed that the intensity of HCV^{DiI} was significantly reduced by HCV neutralization antibodies but not by isotype control, reflecting that the entry of HCV^{DiI} into Huh7.5 cells could be blocked by neutralizing E2. Taken together, these data showed that the establishment of fluorescently labeled HCV^{DiI} was successful and it can be used for testing of virus uptake by murine LSECs.

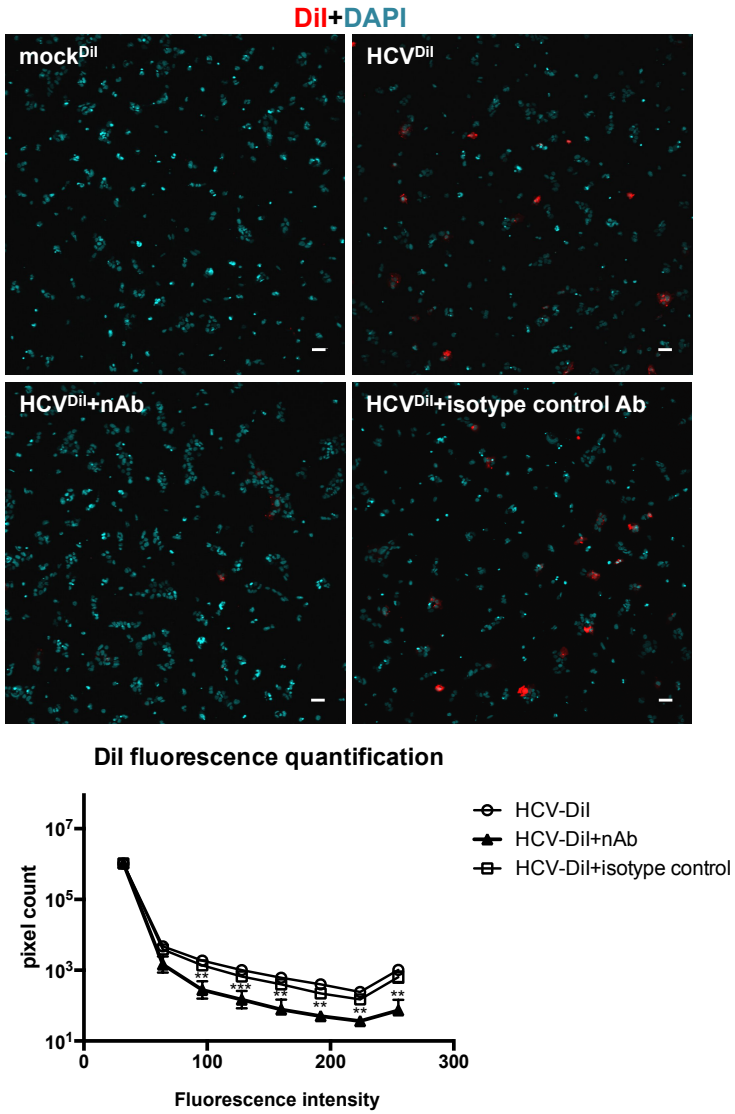

Figure 3.13. Establishment of fluorescence labeled HCV viral particles. Upper: Labeling products derived from virus free cells (mock^{DiI}) or HCV producing cells (HCV^{DiI}) were incubated with Huh7.5 cells for 2h. Middle: HCV^{DiI} was pre-incubated with 25 μg / ml nAb AP33 or same amount of isotype control Ab for 30min at 37 °C before being applied to cells in the presence of Ab for 2h. Scale bar = 10 μm. Lower: Quantification of HCV^{DiI} fluorescence intensities under treatment of no Ab, HCV specific nAb or control Ab. Four randomly chosen microscopic fields from each group were taken for quantification. The grayscale of 0-255 was divided into 8 groups and the total pixels counts in each group were used to plot the figure. Tests were performed between group nAb and isotype control. **P<0.01, ***P<0.001

To know if primary murine LSEC could efficiently take up HCV, isolated murine LSECs were incubated with HCV^{DiI} (0.1 genome copies / cell) for 2h. As shown in figure 3.14, red fluorescent puncta derived from HCV^{DiI} were observed in the cytosol, which proved efficient uptake of virus into cells. In addition, when the cells were pre-treated with cytochalasin D, which could prevent endocytosis by disrupting actin assembly, no HCV^{DiI} could be observed, further confirmed that the observed HCV^{DiI}

from non treated LSECs were rather a result of virus internalization than just derived from HCV bound to the cell membrane.

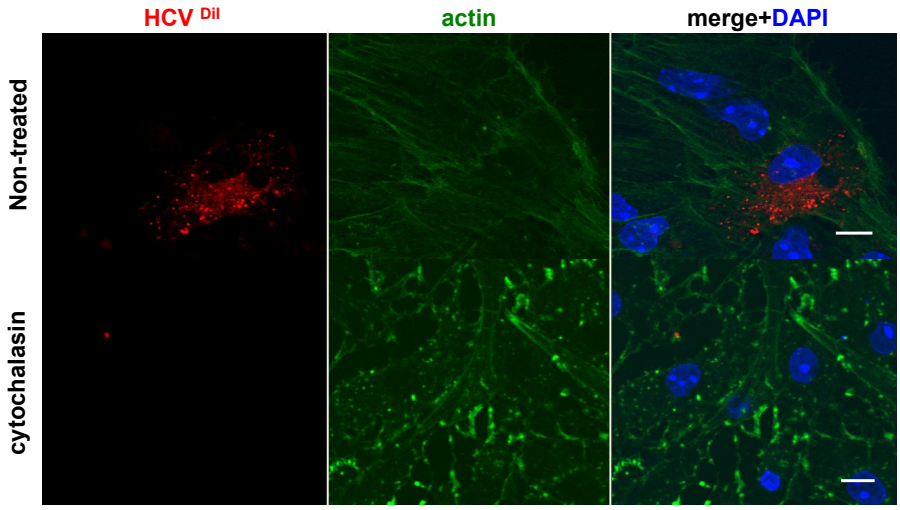

Figure 3.14 Uptake of fluorescence labeled HCV by isolated murine LSECs. Upper: Pure primary murine LSECs were incubated with HCV^{DiI} for 2h. Lower: Cells were pre-treated with 2μM cytochalasin D for 30min. In the presence of treatment, LSECs were incubated with HCV^{DiI} for 2h. Scale bar=10μm

Knowing that murine LSECs can also efficiently take up HCV, it was tested next, whether innate immune response can be activated by HCV. Similarly to the human KCs stimulation assay, murine LSECs were incubated with purified HCV at different dose for 6h before gene expression analysis by qRT-PCR. As shown in figure 3.15, 6h after HCV stimulation of murine LSECs culture, induction of IFN-β, IL6 and TNF expression was already detectable (B-D). Interestingly, when cytocalacin D, which could block virus entry (Figure 3.14.), or bafilomycin, which could disrupt endosome acidification, was applied to the cells, induction of IFN-β was abolished (E). These data suggested that LSECs can sense HCV and activate innate immune defense, which was dependent on virus internalization and endosome maturation.

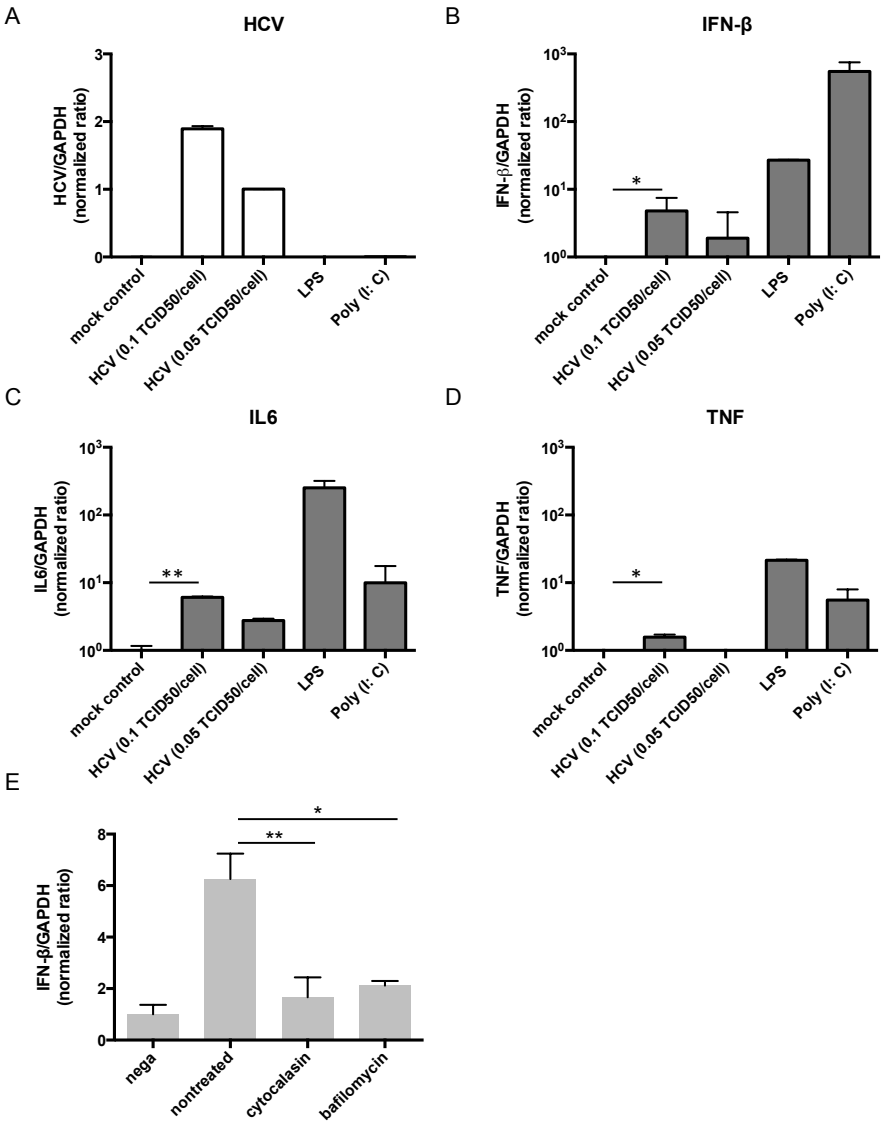

Figure 3.15. *In vitro* stimulation of primary murine LSECs by HCV. (A-D) Isolated murine LSECs were exposed to purified HCV at different dose, 50 ng / ml LPS or 2 μg / ml Poly (I:C) for 6h. (E) Cells were pre-treated with 2 μM cytocalasin D or 1 μM bafilomycin for 30min before incubation with virus while the drugs were still on. Negative cells had no exposure to HCV. After intensive washing to remove the cell free virus, cells were lysed for RNA extraction and relative quantification of target gene expression by qRT-PCR. Means±SD of biological triplicate from one representative experiment are shown. *p<0.05, **p<0.01.

In sum, these data indicated that KCs and LSECs had activated the innate immune defense against HCV, represented by pro-inflammatory cytokines expression, for example, IFN-β.

3.1.4. Involvement of TLR3 in innate immune sensing of HCV

So far, it could be shown that HCV induced potent IFN-β expression in *ex vivo* perfused human liver tissue (Figure 3.10), as well as in isolated human KCs or murine LSECs (Figure 3.12, 3.16). While toll like receptor 3 (TLR3) is known to mediate NF-κB as well as interferon regulatory protein 3 (IRF3) activation, especially with the latter being essential in transcriptional activation of IFN-β[345]. In addition, Dr. Mathias Broxtermann showed that TLR3 was highly expressed and functional in human liver KCs and LSECs[350]. Based on those, TLR3 was speculated to be involved in HCV sensing by KCs and LSECs. As TLR3 is highly conserved from mouse to human and share structural and functional similarities, $TLR3^{-/-}$ mice, which have deficiency in TLR3 expression, provide an option to test this hypothesis.

3.1.4.1. Uptake of HCV by liver sinusoidal endothelial cells in mouse liver

To validate the usage of mouse model in the study of HCV innate immune activation, it was tested first if mouse non-parenchymal liver cells can sequester HCV in the blood circulation. For this purpose, wild type C57BL/6 mouse was inoculated with 10^6 $TCID_{50}$ HCV in a volume of 200 µl. 1h later, mouse was sacrificed for liver isolation. Isolated liver was fixed and prepared for immunofluorescence staining against HCV E2 and the mouse LSEC marker CD146. As it is shown in figure 3.16, HCV-E2 signals co-localized with CD146. This result demonstrated that mouse LSECs could also efficiently collect HCV from blood circulation *in vivo* (Figure 3.16.).

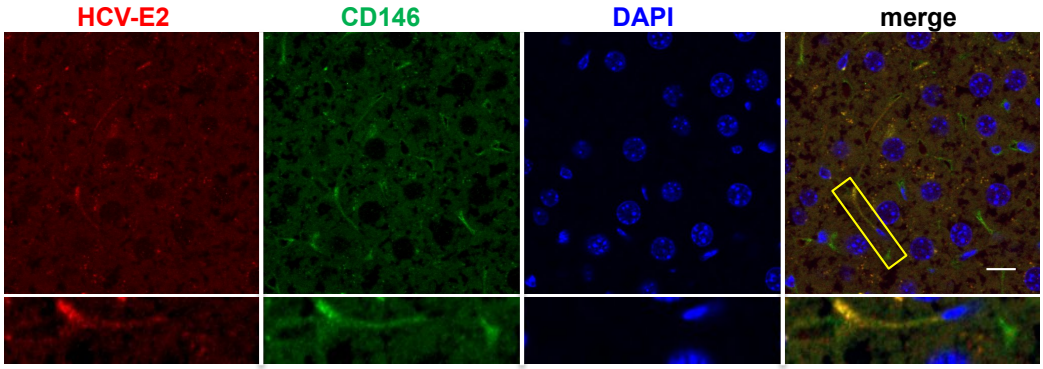

Figure 3.16. Sequestration of HCV by LSECs in mouse liver. C57BL/6 mouse was intravenously injected with medium containing HCV. 1h later, mouse liver was isolated and processed for immunostaining. Antibodies against mouse CD146 and HCV-E2 were used to stain LSECs and HCV, respectively. The lower panel shows an enlarged area from the yellow box above. Representative pictures are shown. Scale bar=10μm

3.1.4.2. TLR3 dependence of hepatic innate immune response against HCV

To test if TLR3 was involved in HCV sensing by liver non-parenchymal cells, control B6 mice (wt) and TLR3$^{-/-}$ mice were equally injected with HCV containing medium or mock containing medium. Wt mice injected with 100 µg poly (I:C) served as positive control for cytokines upregulation. 6h after injection, mice livers were isolated. Tissue RNA was extracted and target gene expression was determined by qRT-PCR. As it is shown in figure 3.17, in wt mice, HCV exposure led to enhanced IFN-α and IFN-β expression, which could be firmly confirmed by significant increase of the IFN stimulated gene 2'5'OAS. Besides, IL6 and TNF were also significantly up regulated after HCV exposure. However, in TLR3 deficient mice, HCV injection did not change the cytokine expression profile. These data strongly supported that the early innate immune sensing was mediated by TLR3.

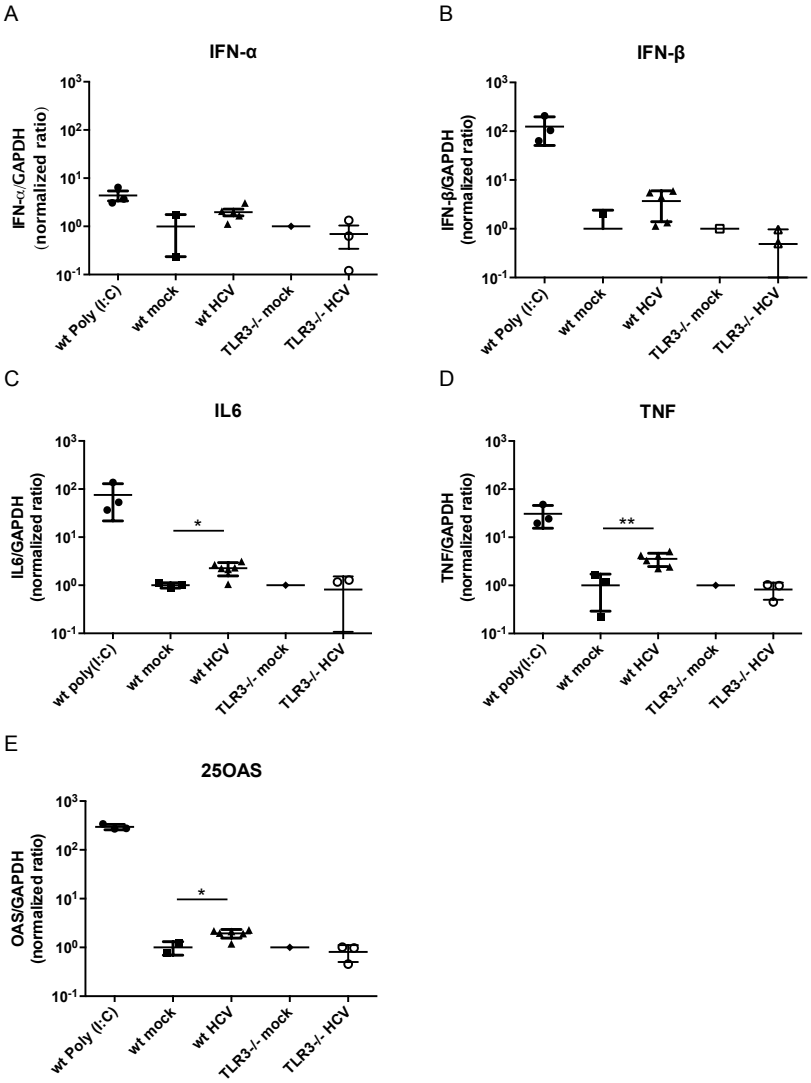

Figure 3.17. Innate immune activation by HCV in mouse livers. (A-E) Wild type or TLR3$^{-/-}$ mice were injected with mock or HCV containing medium. 6h later, liver tissue samples were prepared for RNA extraction. Cytokine expression levels were determined by qRT-PCR. Means±SD of one representative experiment are shown. Wild type: Poly (I:C) n=3, mock n=3, HCV n=5; TLR3$^{-/-}$: mock n=1, HCV n=3.

3.1.5. Summary

In this part of the study, the roles of hepatic non-parenchymal cells in HCV infection have been investigated.

1. An *ex vivo* human liver perfusion model has been optimized and it can support HCV infection. Using this model, it was found that HCV was vigorously sequestered by LSECs and KCs at early time points and hepatocytes became positive with HCV at later time points. Clear IFN upregulation was induced by HCV perfusion, reflecting an activated innate immune response against by HCV.

2. *In vitro* mix-culture of virus exposed KCs with Huh7.5 led to HCV infection in hepatocytes. However, this transinfection was not dependent on virus internalization into KCs.

3. *In vitro* pure culture of KCs and LSECs could exert an innate immune defense against HCV, demonstrated by pro-inflammatory cytokine expression, for example, IFN-β. In addition, innate immune response was dependent on virus internalization and lysosome maturation.

4. *In vivo* perfusion of wt type mice and TLR3 deficient mice with HCV revealed that the innate immune sensing of virus by non-parenchymal liver cells was mediated by the TLR3 signaling pathway.

3.2. Discussion

3.2.1. *Ex vivo* human liver perfusion model for HCV host interaction study

The study presented here has utilized human liver tissue under *ex vivo* perfusion to mimic the *in vivo* situation. The initial usage of *ex vivo* perfusion technique can be dated back to as early as 1960s[351]. With the aim of providing temporary metabolic assistance to patients pending for liver transplantation or with potentially reversible hepatic failure, researchers have investigated using extracorporeal non-human livers under perfusion to shortly provide liver function support to patients [351-353]. In 1972, *Abouna et al.* have reported that patients in fulminant hepatitis got fully recovered from hepatic coma by using 16h extracorporeal baboon liver perfusion[352]. Experiments on functional and morphological characterization of livers from dogs, pigs, and rabbits under *ex vivo* perfusion have been carried out intensively, which showed that livers could maintain their normal physiology, metabolism as well as vital functions under up to 72h *ex vivo* perfusion [354-358].

Applying this concept to human liver tissues, with a modification of using incomplete tissue pieces, sample leftover from clinical hepatic resection becomes valuable model for studying HCV-host interaction. Because HCV infection is highly liver tropical and naturally only supported by human or chimpanzees. However, chimpanzees have been forbidden for their usage in HCV research in many countries[359, 360]. While a robust HCV infectable immunocompetent mice model is still missing, the *ex vivo* perfused human tissue provides a host environment most closely mimic physiological situation. It is of human origin, enables studies on interaction of hepatic cells with virus in their natural occurrence and has the crosstalk of different hepatic cells maintained.

Our group has established *ex vivo* perfusion system for HBV study. Using the old system, human tissue pieces can survive within 16h, after prolonged perfusion, necrosis was found in a large number of hepatocytes and tissue deterioration was irreversible (data not shown). In the beginning of this study, optimization of the system was made by improving the oxygen load and buffering capacity of the perfusate, as

well as adding supplements to better support liver cells function. In the H&E staining of tissue having been perfused for 24h, minor sinusoidal dilatation could be seen but no apparent damage to tissue morphology was observed (Figure 3.2), which is similar to what has been described before [361]. Furthermore, it has been reported that in perfused liver there were two peaks of damage—right before reperfusion and after 4 h of perfusion—as well as two recoveries—immediately following reperfusion and at 6 h of perfusion[362]. In the presented perfusion studies, since no obvious necrosis has been observed along the time of perfusion (Figure 3.2), it was assumed then that tissue "recovery" from cold ischemia was very efficient, which could be due to that partially damaged cells regain the vitality due to new oxygen supply. Using the optimized system, it was found that virus infection could be established *ex vivo* (Figure 3.3). This, at the mean time, provides evidence that the functionality of liver was preserved under *ex vivo* perfusion. Thus it is rational to using this model to study HCV's entry route before hepatocytes targeting in the next step.

However, in the presented study, the vitality evaluation of perfused tissue is so far based on morphological examination of H&E staining. A definitive assessment using enzymatic essays for functional test would be helpful for detailed characterization of liver condition under *ex vivo* perfusion, for example, ATP synthesis, bile secretion measurement and so on.

Despite the benefits of this model, several limitations also exist. Technically, the liver was cannulated through portal vein branches. Due to the variation of the vein branches and retention of clotted blood in some vessels, complete perfusion of the whole piece was difficult. Furthermore, the liver tissues used were often from patients having certain hepatic diseases. Although efforts have been made to use only the pieces that did not have apparent pathological changes, the potential impact of the sample condition to the presented study could not be excluded. In the end, the current perfusion time was limited to 48h, which disables the assays that need longer culture time. Further optimizations for maintaining liver functions over even longer perfusion time would be highly useful.

3.2.2. HCV sequestration from the circulation by non-parenchymal cells

In previous liver perfusion studies on HBV from our group, KCs appeared as the main cells preferentially taking up HBV in the early infection[298]. However, in this presented

study of HCV, it was observed that not only KCs but also LSECs efficiently sequestered virus from the circulation after short time perfusion.

KCs are liver residential macrophages located in the lumen of sinusoids[9, 323] and LSECs are liver specific endothelial cells forming the wall of sinusoids[5, 6, 363]. Both cells are in the frontline of contacting blood materials passing through the liver sinus. Historically, KCs were considered as the only cell population responsible for the clearance of particles from the blood based on the observation that intravenous injected bacteria or vital stains such as carmine were largely accumulated in KCs[364-366]. Investigations on clearance of virus from blood showed that poliovirus, influenza virus, tobacco mosaic virus and etc. are efficiently absorbed by liver macrophages once intravenously injected[367, 368]. In 1972, with a clear discrimination of LSECs from KCs via electron microscopy study[369], the contribution of LSECs in endocytosing particulate materials from blood started to amend. In the 1980s it was discovered that intravenously injected radio-labeled hyaluronan in the rabbit was eliminated from blood at great speed by LSECs[370, 371]. A reevaluation of clearance of lithium carmine from blood in rat revealed that it was predominantly by LSECs that the administered carmine has been taken up[328]. Recently, *Ganesan et.al*. have reported that in the mouse it was LSECs but not the KCs that cleared the bulk of blood-borne human adenovirus.

In the case of HCV, it has been noticed that in HCV patients who accept liver transplantation, the virus load showed a sharp decrease during the eight to twenty-four hours after graft reperfusion. So it has been speculated that hepatic scavenger cells from the new graft may be involved in virus sequestration from the circulation[372]. But no solid evidence for any of the cell type has been obtained so far. In the presented study, taking advantage of the *ex vivo* perfused human liver tissue that maintains the physiological hepatic microanatomy, it was possible to study the preferential uptake before the hepatocytes targeting of the virus. The microscopy data from liver tissue perfused with HCV for 1h clearly demonstrated that the bulk of HCV virions have been internalized by LSECs and KCs (Figure 3.7.).

To perform the “scavenging” function, the cells have to carry receptors enabling the virus binding. And depending on the receptor binding property of the virus, KCs and LSECs might function in a manner peculiar to each individual virus. In terms of HCV, E2 protein of the virus envelope has been reported to bind to L-SIGN or DC-SIGN

molecules on the cell surface[344]. And both types of lectin receptors have been reported to be expressed on LSECs and KCs[331]. It occurs very likely that both receptors were mediating HCV uptake by sinusoidal cells[331, 332, 344, 349, 373, 374].

3.2.3. From non-parenchymal cells to hepatocytes targeting

HCV virus is known to infect primarily hepatocytes. The data obtained in this study showed that in human liver perfusion model, HCV was efficiently accumulated by LSECs and KCs before entering into hepatocytes (Figure 3.7,3.8,3.9).

In the liver, LSECs and KCs constitute the lining cells of the sinus, hepatocytes are not directly exposed to agents that pass the liver in the bloodstream. When infectious agents following blood circulation get to liver, there are three possible ways in which they could pass the endothelium and reach hepatocytes. Firstly, they might pass through fenestrae in LSECs and reach hepatocytes directly. However, the size limitation for such free diffusion was reported to be below 10nm[4, 375]. Secondly, pathogens may reach hepatic cells by "growing through" non-parenchymal cells – a strategy that can be used by non-hepatocyte specific viruses like ectromelia virus[376]. Thirdly, pathogens may reach hepatocytes by being taken up by KCs/LSECs and then passively or actively passed through to hepatocytes - in the way that has been described for Malaria sporozoite[377].

HCV disseminates via blood and targets primarily hepatocytes[159]. With a diameter of 50-60nm, it is very unlikely that HCV is following the first free diffusion pathway for directly hepatocytes targeting. In support of this assumption, it has been reported that when high dose of polio virus (10^8 pfu) were intravenously injected into mice, after 1h the virus could only be detected in LSECs and/or KCs, but not hepatocytes[378]. The size of poliovirus is only around 30nm, which is smaller than HCV. With bigger viral particles, it was even more difficult as has been reported for influenza virus[378].

The second pathway is questionable for HCV as well, as the virus is believed not to replicate efficiently in non-hepatocytes. However, a number of studies have shown HCV infection of monocytes and macrophages[379]. And a recent report showed HCV could also infect endothelial cells[380]. But a definitive proof that HCV could replicate in KCs and LSECs is still missing, and no virus infection was detected in isolated KCs or LSECs in the study presented here.

The third pathway appeared very likely for HCV based on the imaging analysis of virus localization in perfused liver tissue (Figure 3.7,3.8,3.9). The sequential up take of HCV first by non-parenchymal cells and later by hepatocytes under pulse chase perfusion setting conditions suggested that the virus entering into hepatocytes was derived from non-parenchymal cells. And the HCV staining pattern showed a series of dotted virus signals between neighboring KCs and hepatocytes (Figure 3.8.C) or LSECs and hepatocytes (Figure 3.8.D), and thus also fits to the scenario that viruses were transferred from KCs/LSECs to hepatocytes. In line with this, it was reported that DC-SIGN and L-SIGN that are expressed on the surface of liver macrophages and/or endothelial cells could capture HCV and facilitate hepatocytes infection in trans[331, 332, 344, 373, 374]. The mechanism proposed was that following "SIGN" receptors binding the virus was delivered via transferrin positive recycling endosomes to proximal hepatocytes[332]. Those researches were conducted mainly via HCVpp (pseudo particles) in cell lines *in vitro*[331, 332, 344, 373, 374]. In contrast to that, *Wai K. et al.* reported that L-SIGN and DC-SIGN expressed on primary LSECs only supported binding of HCVpp but not entry. Despite the inconsistency, it is very difficult to apply either conclusion to HCVcc or HCV from patient serum. HCVcc as well as blood-born HCV particles are characterized by lipoprotein association but HCVpp lack lipoprotein components[287] and thus may not be a suitable model.

Thus, in the presented study, transinfection was tested using HCVcc strain JC1-luci. No experiment on mix-cultured LSECs and Huh7.5 are shown in this study. This is because mouse LSEC is an inappropriate model in this context due to its low expression level of SIGN molecule[381-383]. And when our collaborator Prof. Jane Mckeating tested human LSECs, no transinfection was observed. However, when we co-cultured human KCs and Huh7.5, the result suggested that HCV could transinfect hepatocytes via binding to the C-type lectin DC-SIGN/L-SIGN of KCs, which is consistent with a model that DC-SIGN and L-SIGN on sinusoidal cells provide a mechanism for high affinity binding of circulating HCV within the liver sinusoids and this allows transfer of the virus to underlying hepatocytes, in a manner analogous to dendritic cell DC-SIGN presenting HIV to T lymphocytes[329, 330]. Viral capture at the cell surface can be rate limiting for infection, suggesting that expression of DC-SIGN on KCs may enhance the rate and efficiency of virus infection of hepatocytes expressing the virus receptors[384-386].

A growing number of such hepatocyte receptors have been identified including CD81, SRB1, Claudin-1 (CLDN1), occluding (OCLN), EGFR, NPC1L1 and more recently transferrin receptor 1 (TrR1)[203-209]. These receptors have varied distribution regions in polarized hepatocytes, for example CLDN1 and OCLN localize in tight junction in the apical domain of the hepatocytes while the others have distribution on basolateral domain facing the space of Disse. It is still not certainly known how they contribute to HCV entry in a sequential manner. In the study presented, it was observed that HCV in hepatocytes were first located in the cortical region close to the cell membrane, which implied that viral particles were in the early entry process (Figure 3.8). The strong actin staining on the apical domain indicated the existence of tight junctions of the hepatocytes. The localization of HCV particles to the tight junctions could be explained by the association of virus with CLDN1 and/or OCLN. These findings suggested rolling of HCV along the hepatocytes membrane to interact with different receptors, which represent a entry model similar to that described for Group B Coxsackieviruses, which access tight junction localized receptors via alternative receptor binding on the apical surface and relocalization to the junctional complex[387, 388]. Further staining of CLDN1 and OCLN will be helpful to prove the virus association with confidence.

3.2.4. Innate immune defense against HCV via non-parenchymal liver cells

The data obtained in this study have demonstrated that KCs and LSECs were sources of hepatic IFN-β in the early HCV infection (Figure 3.10). They actively collected HCV virus from circulation and elicited innate immune response in a dose dependent manner but irrelevant with viral transcription (Figure3.7, 3.13,3.16).

KCs and LSECs are vigorous scavengers in the liver. They express a large spectrum of receptors, which facilitate ligand binding and internalization[6, 323]. Besides DC/L-SIGN, they also express CD81, SRB1, LDLR, all of which are involved in HCV entry into hepatocytes[323, 389, 390]. Thus it is reasonable to suspect that those receptors are also involved in HCV internalization into KCs and LSECs as presented in the study (Figure 3.7). And this efficient “absorption” of virus into non-parenchymal cells contributed very likely to the rapid viremia decrease observed in HCV patients in the early time after reperfusion of the transplanted liver[372, 391]. The internalized virus did

not contribute to infecting hepatocytes in trans (Figure 3.11), thus the cells cleared them from blood representing an important mechanical barrier but may be also inducing innate immune defense.

Similar phenomena were studied in detail with *in vivo* administered adenoviral vectors. Adenovirus vectors have been widely used for gene therapy applications and as vaccine vehicles for treating infectious diseases. While these vectors are effectively targeted to chosen tissues, and in particular to the liver, the infection process is highly inefficient. When adenoviral vectors are administered systemically by intravenous injection, rapid removal of virions by KCs and LSECs in the liver greatly impaired the efficiency of gene delivery [392-394]. Associated with viral clearance was an immediately triggered innate immune response, which was characterized by secretion of inflammatory cytokines including type I IFN, IL6 and TNF[395, 396]. Contributions of both innate immune cells like KCs and non-innate immune cells like endothelial cells to this cytokine expression have been reported[397, 398].

Interestingly, HCV is also known for its early induction of innate immune defense. ISG could already be detected in the first few days after infection[243]. However, it is not certainly known which cells express IFN in early acute HCV infection. There have been several studies showing IFN induction in PHH after HCV infection[399, 400]. However, PHH isolation usually is not absolutely pure. Contamination of non-parenchymal cells that could be the source of IFN expression will lead to mis-interpretation. An argument in favor of non-parenchymal cells expresses IFN in the early HCV infection is that the viral NS3/4A serine protease, only expressed in infected hepatocytes, blocks the phosphorylation and effector action of interferon regulatory factor–3 (IRF-3), a transcription factor that is essential for IFN induction[401]. NS3/4A also interferes with both the TLR dependent and the cytosolic sensory pathways by cleaving and inactivating MAVS and TRIF[238, 239], which are essential component in RIG-1 and TLR-3 pathway, respectively. Since this cleavage occurs only in HCV infected hepatocytes, IFN induction in those cells should be prevented. In contrast, in non-parenchymal cells, which are not productively infected and thus do not express NS3/4A, IFN production would not be affected. In support of this, *Lau et al.* have reported that KCs were a local source of IFN that promoted expression of ISGs in hepatocytes[402]. However, the data shown in this study suggest not only KCs but

also LSECs contribute to innate immune response against HCV in the early virus infection (Figure 3.13,3.16).

Overall, the study presented here leads to a novel paradigm identifying both KC and LSEC as central to HCV initial clearance from blood, virus recognition and immunity.

3.2.5. IFN-β expression is mediated by a TLR3 dependent pathway

In the work described here, we have shown that the TLR3 signaling pathway is critical in mediating innate immunity activation after HCV sensing by non-parenchymal liver cells (Figure 3.17).

In most published studies about the HCV sensory pathway, *in vitro* transcribed HCV RNA was used to transfect cells. There are severe limitations of this approach. First of all, *in vitro* transcribed RNA has a 5' triphosphate, which is a well-known binding motive for RIG-I[403]. In addition, it is unknown if any of such RNA molecules would be exposed to the sensor naturally when infection occurs[404]. HCV induces a so called membranous web structures in the hepatocytes, which, among other things, most probably shields the replicating RNA from cellular sensors[405]. Therefore, in the presented study, all the virus stimulation experiments were performed using infectious viral particles.

In addition to RIG-I, a TLR3 mediated establishment anti-HCV innate immunity was reported for hepatoma cells. TLR3 recognizes double-stranded viral replication intermediates[228]. A previous study from our group showed that although PHHs, KCs and LSECs express comparably high levels of TLR3, its signaling pathway is less functional in PHHs due to lower adaptor proteins expression, like TRIF and RIP1. In the contrast, TLR3 in KCs and LSECs is highly functional[350]. It is well acknowledged that TLR3 recognizes double-stranded RNA (dsRNA) with minimum 40-50bp double-stranded region[406, 407]. DsRNA is a common signature linked to the viral replication cycle and lysis of virus-infected cells is hypothesized to release dsRNA[408]. However, in negative-strand RNA virus infections, such as influenza A virus and phlebovirus, which generate little dsRNA as intermediate replication products, TLR3-mediated inflammatory cytokine and chemokine production was documented[409, 410]. In addition, *Kariko´ et al.* reported that *in vitro* transcribed HIV gag mRNA complexed with lipofectin activates TLR3[411]. Recently, it was reported that the TLR3 signaling cascade could also be activated by incomplete stable stem structures in

single-stranded RNA[412]. Thus, it is attempting to speculate that after HCV enters into lysosomes in KCs or LSECs, acidic hydrolysis exposes the viral genome (Figure 3.15.), of which the relatively long stem structure with bulge and internal loops in 5' UTR region would bind with two TRL3 molecules. Following TLR3 oligomerization, TRIF is recruited to the TLR3–TIR domain that activates the transcription factors, IRF-3, NF-κB, leading to the production of IFN-β, IFN-λ and pro-inflammatory cytokines[413-417].

Indeed, IFN induction have been observed in human liver tissues and primary LSECs and KCs culture after exposure to HCV (Figure 3.10,3.12,3.15) in my study. Early investigations on IFN expression during the early acute phase of HCV infection in experimentally infected chimpanzees revealed induction of type I IFN-stimulated genes. The extent and duration of ISG induction showed a positive correlation with viral load [227, 418]. In 2009, polymorphisms of the IL28B were identified to be associated with clearance of HCV infection, which was suggested to be correlated with the antiviral function of the its product — IFN-λ[265]. Recently, increase of IFN-λ in the serum as well as up regulation of IFN-λ mRNA in experimentally infected chimpanzees were reported [400, 419].

In the study presented here using HCV perfused tissue, IFN-β and IFN-λ were both identified to have been hugely up regulated during initial exposure of the liver to the virus (Figure 3.10.). IFN-α was only modestly up regulated although it was similarly transcriptionally activated via interferon regulatory factor (IRF) 7 as IFN-β[420]. The differential up regulation can be explained by the cell type specific expression of the two type I IFNs. While IFN-α is expressed primarily in leukocytes, IFN-β is expressed primarily in non-immune cell[421]. Moreover, IFN-β expression could be induced by an extra pathway via activation of IRF3, which might also contribute to the higher up regulation of IFN-β. IFN-γ is considered to be mainly produced by NK cells and CD4+ T cells, explaining the minor up regulation in the study presented here focusing on the early infection. IFN-λ is expressed in both immune and non-immune cells[421]. Besides being induced by virus stimulation, it could also be induced by both type I (IFN-α/β) and type III IFN (IFN-λ)[421], identifying IFN-λs also as IFN-stimulated genes. This may explain the lacking of correlation of IFN-λ with HCV load but a strong correlation of IFN-β with HCV load (Figure 3.10. B, C.), despite that the type I IFN independent induction of the IFN-λ depends on the same signaling molecules as IFN-β [422].

Taken together, in this study, an *ex vivo* perfusion model permissive for HCV infection was developed. This model allows a time course tracking of HCV association with liver cells and revealed for the first time that non-parenchymal liver cells (LSECs and KCs) could selectively scavenge and remove HCV from perfusates. On one hand, the cell membrane associated HCV could efficiently infect hepatocytes in trans, on the other hand, the internalized virus was shown to be sensed by endosomal TLR3. This resulted in antiviral cytokine expression (e.g. IFN-β, IFN-λ) and induction of innate antiviral defense.

4. Materials and methods

4.1. Materials

4.1.1. Chemicals / reagents

Product	Supplier
Agarose	Peqlab
Alexa Fluor® 594	Life Technologies
Ampicillin	Roth
ANTI-FLAG® M1 Agarose Affinity Gel	Sigma-Aldrich
ATP	Sigma-Aldrich
Bafilomycin	Sigma-Aldrich
Biocoll Separation Reagent	Biochrome
Bovine Serum Albumin, BSA	Sigma-Aldrich
BSA-Fatty Acid Free	Sigma-Aldrich
CD146 (LSEC) MicroBead, mouse	Miltenyi Biotec
Chloroform	Roth
Collagen R	Serva
Cytochalasin D	Life Technologies
DEPC	Roth
DiI	Life Technologies
DMSO	Sigma-Aldrich
EDTA	Roch
EGTA	Roth
Ethanol	Roth
FCS	Gibco
Fetal Calf Serum	Life Technologies
Filipin	Sigma-Aldrich
Fluoromount-G® Mounting Media (+/-Dapi)	Sourthernbiotech
Formaldehyde	Roth
GBSS	Life Technologies

Gentamicin	Ratiopharm
Glucose	Roth
Glutamin 200mm	Gibco
Goat Serum	Life Technologies
Granulocyte-Macrophage Colony-Stimulating Factor (GMCSF)	Genzyme
HCL	Merck
Hepes	Sigma-Aldrich
HEPES pH7.4	Sigma-Aldrich
Human Serum	In house
Hydrocortison	Pfizer
Insulin	Sanofi Aventis
Isopropanol	Roth
L-Glutathione (GSH)	Merk
Mannan	Sigma-Aldrich
Methanol	Roth
Monopotassium Phosphate (KH_2PO_4)	Roth
NBD-Cholesterol	Life Technologies
Non-Essential Amino Acids 100x	Gibco
Optiprep™	Axis-Shield
PBS	Life Technologies
Penicillin/Streptomycin	Biochrom AG
Phorbol Myristate Acetate (PMA)	Sigma-Aldrich
Polyethylene Glycol (PEG) 8000	Promega
Potassium Chloride (KCL)	Merk
Recombinant Hbsag (Genotype D, Adw/Ayw)	Biotech
rNTP	Promega
Saponin	Roth
Sodium pyruvate	Gibco
Sodium Pyruvate 100mm	Gibco
Sucrose	Roth
Tissue-Tek O.C.T.	Sakura

Tritonx100	Roth
Trizol Reagent	Life Technologies
U18666A	Sigma-Aldrich
Versene	Life Technologies
Versene EDTA	Gibco
Yeast Extract	Gibco
β-Mercaptoethanol 50mM	Gibco

4.1.2. Antibodies

Primary antibodies			
Antigen	**Clone**	**Application and dilution**	**Supplier**
ApoA-1	EP1368Y	IF (1:200)	Acris Antibodies
NPC1	Polyclonal	IF (1:200)	Novus Biologicals
LAMP-1	H4A3	IF (1:500)	Abcam
Rab11	Polyclonal	IF (1:400)	Abcam
HCV-E2	A3R3	IF (1:500)	Dr. Mansun Law, Scripps Research Institute
HCV-E2	AP33	Neutralization (25 µg / ml)	Genentech
L-SIGN	604	IF (1:50)	R&D systems
CD68	PG-M1	IF (1:80)	DAKO
HCV-NS3	2E3	TCID50 (1:3000)	Biofront technologies
CD146	P1H12	IF (1:100)	eBioscience

Secondary antibodies			
Antigen	Conjugation	Application and dilution	Supplier
Human IgG	Alexa Fluor® 488	IF (1:1000)	Life technologies
Mouse IgG	Alexa Fluor® 488	IF (1:1000)	Life technologies
Rabbit IgG	Alexa Fluor® 488/594	IF (1:1000)	Life technologies
Mouse IgG	HRP	TCID50 (1:200)	Sigma-Aldrich

4.1.3. Enzymes

Product	Supplier
RQ1 DNase	Promega
T3 polymerase	Promega
T7 polymerase	Promega
RNase H	Life Technologies
ThermoScript™Reverse Transcriptase	Life Technologies
RNaseout™	Life Technologies
FastDigest FspAI	Thermo Scientific

4.1.4. Primers

Name	Sequence (5' to 3')
Virus primer	
HBV-1745	GTTGCCCGTTTGTCCTCTAATTC
HBV-1844	GGAGGGATACATAGAGGTTCCTTGA
HBV-cccDNA-92	GCCTATTGATTGGAAAGTATGT
HBV-cccDNA-2251	AGCTGAGGCGGTATCTA
HCV-fw	TCTGCGGAACCGGTGAGT
HCV-rev	GGGCATAGAGTGGGTTTATCC
HCV^{aq}-fw	GCT AGC CGA GTA GCG TTG GGT
HCV^{aq}-rev	TGC TCA TGG TGC ACG GTC TAC
HCV-tag-RC1	GGCCGTCATGGTGGCGAATAAGTCTAGCCATGGCGTTAG TA
HCV-tag	GGCCGTCATGGTGGCGAATAA
HCV-RC1	GTCTAGCCATGGCGTTAGTA
HCV-RC21	CTCCCGGGGCACTCGCAAGC
Human primer	
Prnp-fw	TGCTGGGAAGTGCCATGAG
Prnp-rev	CGGTGCATGTTTTCACGATAGTA
GAPDH-fw	AACGGATTTGGTCGTATTG

GAPDH-rev	AAAGGTGGAGGAGTGGGT
18sRNA-fw	AAACGGCTACCACATCCAAG
18sRNA-rev	CCTCCAATGGATCCTCGTTA
IFNA1-fw	GCCCTTTGCTTTACTGATGG
IFNA1-rev	TTATCCAGGCTGTGGGTCTC
IFNB1-fw	GCCGCATTGACCATCT
IFNB1-rev	AGTTTCGGAGGTAACCTG
IFNG-fw	GTTACTGCCAGGACCC
IFNG-rev	CTTGATGGTCTCCACACT
IFNL1-fw	GGGACCTGAGGCTTCTCC
IFNL1-rev	CCAGGACCTTCAGCGTCA
IL6-fw	GAGGAGACTTGCCTGGTGAAA
IL6-rev	GCCCATGCTACATTTGCCG
TNF-fw	GGCGCTCCCCAAGAAGACAGG
TNF-rev	CCAGGCACTCACCTCTTCCCT
Mouse primer	
mGAPDH-fw	ACCAACTGCTTAGCCC
mGAPDH-rev	CCACGACGGACACATT
mIFNA1-fw	GGACAGGAAGGACTTTGGATT
mIFNA1-rev	AGGACAGGGATGGCTTGAG
mIFNB-fw	CACAGCCCTCTCCATCAACTA
mIFNB-rev	CATTTCCGAATGTTCGTCCT
mIL6-fw	TGATGGATGCTACCAAACTGG
mIL6-rev	TTCATGTACTCCAGGTAGCTATGG
mTNF-fw	CGATGGGTTGTACCTTGTC
mTNF-rev	CGGACTCCGCAAAGTCTAAG
m2’5’OAS-fw	CCAGCAGGAGGTGGAATTT
m2’5’OAS-rev	GAATTGGGGTTCAGCATACG

4.1.5. Kits

Products	Supplier
Murex HBsAg Version 3	Abbott
NucleoBond Xtra Maxi Kit	Macherey & Nagel
Superscript III Kit	Life Technologies
SYBR Green I Master Mix	Roche
NucleoSpin®RNAII kit	Macherey & Nagel
NucleoSpin Tissue Kit	Macherey & Nagel
Pierce™ BCA Protein Assay Kit	Thermo Scientific
Luficerase assay system E1500	Promega
CD14 MicroBeads, human	Miltenyi Biotec
RNeasy mini kit	QIAGEN
RNase-Free DNase Set	QIAGEN

4.1.6. Media

DMEM complete medium	
DMEM	500 ml
FCS	50 ml
Pen/Strep (5000 I.U. / ml)	5.6 ml
L-Glutamine (200 mM)	5.6 ml
NEAA (100x)	5 ml
Sodium Pyruvate (100 mM)	5 ml

RPMI complete medium	
RPMI1640	500 ml
FCS	50 ml
Pen/Strep (5000 I.U. / ml)	5.6 ml

William's E basic medium	
William's E Medium	500 ml

Pen/Strep (5000 I.U. / ml)	5.6 ml
PHH culture medium	
William's E Medium	500 ml
FCS (FetalconeII)	50 ml
Pen/Strep (5000 I.U. / ml)	5.6 ml
L-Glutamine (200 mM)	5.6 ml
Insulin (40 IU / ml)	320 µl
Hydrocortisone (4.4 mg / ml)	600 µl
Gentamincin (40 mg / ml)	1 ml
DMSO	10 ml

PHH perfusion mediuma I	
HBSS, Ca^{2+}/Mg^{2+} free	500 ml
EGTA (100 mM)	2.5 ml
Heparin (5000 U / ml)	1 ml

PHH perfusion mediuma II	
William's E	250 ml
Calcium Chlorid (1 M)	0.9 ml
Gentamicin (10 ng / ml)	2.5 ml
Collagenase type IV	200 mg

PHH washing medium	
William's E	500 ml
*Glutamin (200 mM)	5.6 ml
*Glucose (5%)	6 ml
*Hepes (1M, pH 7.4)	11.5 ml
*Pen/Strep	5.6 ml
*Solutions were mixed and stored as premix at -20 °C	

***Ex vivo* Liver perfusion medium**	
William's E	500 ml

FCS (Heat inactivated)	50 ml
Pen/Strep (5000 I.U. / ml)	5.6 ml
L-Glutamine (200 mM)	5.6 ml
Insulin (40 IU / ml)	320 µl
Hydrocortisone (4.4 mg / ml)	600 µl
Gentamincin (40 mg / ml)	1 ml
NEAA (100x)	5 ml
Sodium Pyruvate (100 mM)	5 ml
EGF	1 nM

4.1.7. Plasmids / cell lines / mouse lines

Name	Description	Source
Plasmids		
pFK-Jc1	It is used to generate HCVcc JC1, which is J6-JFH1 chimera and produce high titer virus after infection	Ralf Bartenschlager, Heildelberg
pFK-luc-Jc1	it is used to generate JC1 derivative expressing firefly luciferase.	
pFK-Jc1-E2flag	Jc1 derivative encoding a FLAG-E2 fusion protein,	
Cell lines		
THP-1	human monocytic cell line; differentiate into macrophage in vitro upon PMA treatment	ATCC
Huh7.5	Hepatoma cell line; Subclone of Huh7; highly permissive for HCVcc infection	AG Protzer
Mouse lines		
C57BL/6	WT BL/6 mice	Harlan Laboratories
$TLR3^{-/-}$	BL/6 mice deficient for TLR3	Bernhard Holzmann, TUM

4.1.8. Technical equipments

Product	Supplier
incubator	Heraeus Holding GmbH
LightCycler® 480II	Roche Diagnostics
MACS separator	Mittenyl
Nanophotometer OD_{600}	IMPLEN GmbH
Sterile hood	Heraeus Holding GmbH
Thermocycler T300	Biometra
Cryostat CM3050S	Leica
ELISA Reader, Infinite F200	TECAN
LS 6500 Liquid Scintillation Counter	Beckman
Ultracentrifuge XL-70	Beckman
Thermo mixer	Eppendorf
Confocal microscope, FV10i	Olympus
Perfusion Pump, Masterflex L/S	Cole-Parmer Instrument Comapy
Fluorescence microscope CKX41	Olympus

4.1.9. Softwares

Name and supplier	Application
Microsoft Office (Microsoft)	Data presentation
Image J (NIH)	Image data processing
FV10-ASW (Olympus)	Image view
Graphpad Prism (GraphPad Software)	Graphic presentation and data analysis
LightCycler480 (Roche)	Analysis of qPCR
$TCID_{50}$ calculator	Molecular virology, Heidelberg

4.2. Methods

4.2.1. Cell culture

All cells were cultured at 37°C, 5% CO2 and 95% humidity.

4.2.1.1. Culture and differentiation of THP-1 cells

THP-1 monocytes were cultured in suspension with RPMI1640 complete medium plus 25mM β-mercaptoethanol. For flask culture, the cell number was maintained as 2-4x10^5/ml. For differentiation into macrophages, cells were grown for 48 h in culture medium added with 100ng/ml PMA in addition.

4.2.1.2. Culture of Huh7.5 cells

Huh7.5 cells were cultured with complete DMEM medium. For maintenance, cells were kept at 40% - 80% confluence..

4.2.1.3. Isolation and differentiation of monocyte derived macrophage

50ml peripheral blood was drawn from healthy individuals and collected in syringes containing 10 µl heparin (5000 I.U. / ml). 25ml of blood was then carefully pipetted on top of 20 ml Biocoll cell separation solution in a 50ml tube. Density centrifugation was performed for 18 min at 2000 rpm under 16°C with no brake. The PBMC layer, which was visible as a white ring, was collected carefully transferred into a new tube and washed twice with cold PBS by centrifuging for 10min at 300 g. Cells were resuspended and counted. Afterwards, cells were pelleted again by centrifugation. For every 1x10^7 cells, resuspesion was performed using 80ul blocking buffer plus 10 µl $CD14^+$ microbeads. And this cell suspension was directly stored in 4 °C for 10min. To remove the unbound antibody, the cell/microbead solution was centrifuge at 300 g for 6min. Afterwards, MACS separation column was used according to the manufacturer´s protocol to positively select $CD14^+$ monocyte. Isolated cells were seeded at density of 1x10^5 / cm^2 with RPMI complete medium. And 800 U / ml GM-CSF were added to culture for 6 days for differentiation.
For cholesterol loading, cells were incubated with 50 µg / ml acLDL in RPMI 1640 mock medium for 24h.

4.2.1.4. Isolation and culture of primary human hepatic cells

Two step perfusion for liver cell suspension

Surgical liver resections obtained from patients undergoing partial hepatectomy were used for cell isolation. Informed consent was obtained from each patient and the procedure was approved by the local Ethics Committee. All hepatic cells were isolated based on collagen two-step perfusion as described Schulze-Bergkamen[121]. Briefly, healthy liver tissue was first perfused with about 500 ml PHH perfusion-medium-I at a flow rate between 20 and 40 ml/min to wash out blood sticking in intrahepatic capillaries and vessels. Upon successful perfusion, the color of the resection tissue changed from red to brown after about 20 to 25 min. The second perfusion step was performed with 250ml PHH perfusion-medium-II containing the collagenase. Perfusion was stopped when liver cells appeared in the medium. Liver cell suspension was prepared by scratching small pieces of liver tissues and before the further cell purification, this cell suspension was filtrated through double-layer gaze.

Primary PHH isolation and culture

Raw PHH fraction was prepared by centrifuging the liver cell suspension at 50 g for 6 min. Supernatant was kept for non-parenchymal cell isolation and the pellet were resuspended and centrifuged again for 10 min at 50 g. Density gradient was prepared by placing 20 ml 18% OptiPrep (in PBS) carefully over 20 ml 9% OptiPrep. 10 ml cell suspension was carefully loaded on top and centrifuged for 25min at 800g with no break. The brownish cell ring in the middle was carefully collected and seeded on collagen treated substratum at density of $1.5x10^5/cm^2$ and cultured with PHH culture medium.

Primary KC isolation and culture

Non-parenchymal cell enriched supernatant from last step was collected in 50 ml falcon tubes and centrifuged for 10min with 300 g at 10°C. The cell pellet was further washed once using PHH washing medium. Then, cells were collected in 10 ml medium by centrifugation at 300 g for 10min and the resulting cell suspension was applied on top of gradient composed of 15 ml 9% OptiPrep (in PBS) and 15 ml 16% OptiPrep. And the density gradient was centrifuged in the same way as above. The

resulting cell band in-between 16% and 9% OptiPrep was the KCs enriched fraction and it was collected and washed once. After that, cells were resuspended and the total cell number was counted[##]. Cells were seeded at density of $1.14x10^6$ cells / well (24-well plate). Incubate the cells with serum free washing medium for 45 min at 37°C without the possibility of shaking. Afterward, wash the cell intensively for 3 times with PBS and further cultured with RPMI complete medium.

[##]Counting the KCs exactly is almost impossible. As it was calculated that approximately 15-20% of the cells are KCs. 6-fold number of cells in a well (24-well: 1,9 cm^2 = $1,9*10^5$ cells = $1,14*10^6$ cells to seed) was seeded to obtain a density of ≈$1*10^5$ cells pro cm^2. By this, constant cell number per well could be established from preparation to preparation.

4.2.1.5. Isolation and culture of primary murine liver sinusoidal endothelial cells

Mouse liver cell suspension was prepared similarly as human. 20 ml whole cell suspension was applied to 25 ml 30% (w/v) Nycodenz stock solution. Centrifugation was carried out at 1400 g for 20min with no brake at 20 °C. Cells in the top layer were recovered and washed once with cold MACS-Buffer. Number of the cell was counted and every $1x10^7$ cells was resuspended in 90 µl buffer plus 10 µl anti-LSEC beads. This cell/beads mixture were then incubated for 15 – 20 min at 4 °C. One time washing was performed in the end of 4 °C incubation. Afterwards, MACS separation columns were used according to the manufacturer´s protocol to positively select $CD146^+$ LSECs.

4.2.1.6. Mix-culture of virus loaded Kupffer cells with hepatocytes for virus transinfection

Pure KC culture was incubated with HBV or HCV at 4 °C or 37 °C as indicated. In the case of HCV, 20 µg / ml mannan was applied to cell culture 30min before virus loading and kept until wash in the group of mannan+HCV. Meanwhile, for HBV transinfection, PHH were detached from culture plate by incubation with trypsin and versene (1:1) solution for 5min at 37 °C and for HCV transinfection, Huh7.5 cells were trypsinized to prepare cell suspension. Detached PHH or Huh7.5 was washed once

using PBS and applied to virus loaded KC cultures for 12 days (HBV) or 3 days (HCV) mix-culture, respectively.

4.2.2. *Ex vivo* human liver perfusion

Fresh surgical human liver biopsies (5 to 10 g) were perfused in closed circuit at 37 °C / 5% CO_2 with liver perfusion medium via a catheter cannulated with portal vein branches. Flow rate was maintained at around 1 ml / min / g during virus containing pulse-perfusion and 3 ml / min / g during chase-perfusion. To visualize HCV localization during early entry into liver, perfusion-medium was pre-mixed with HCV stock to reach an inoculation around 0.1 MOI per hepatocyte (1 g liver is considered to contain approximately 10^8 hepatocytes). Perfusion was done for 1h with HCV-containing medium. For extended perfusion, tissue was chase perfused without virus for 15min with Williams E medium alone and then complete perfusion medium for indicated time length. Mock perfusion was done using mock control of virus stock. For immunofluorescence analysis, tissues pieces were first fixed for 5min via perfusion and then soaked into 4% PFA for 24h. The next day, completely fixed tissues were dehydrated using 30% sucrose solution for overnight. Tissue blocks were then embedded with Tissue-Tek O.C.T. and preserved in -80 °C until use.

4.2.3. Human TRL isolation and labeling

Plasma was collected from anti-HBsAg negative donor. TRL (density <1.006 g/ml) were isolated by a 45 minutes spin in a swing-out rotor (SW41, Beckman) at 280,000 g 4°C. For further purification, lipoproteins were dissolved in 2 ml of 15% sucrose solution (in PBS-EDTA, 10 mM, pH = 7.4) and sucrose was added to the lipoprotein to a final concentration of 15% and then layered under PBS and centrifuged for a second time as described above. The isolated TRL were stored in PBS-EDTA at 4 ° C for up to 14 days.

To label TRL with [^{3}H]-cholesterol or NBD-cholesterol, 100 µl of [^{3}H]-cholesterol (3.7 MBq) or 50 µg NBD-cholesterol was dried under liquid nitrogen, resuspended in 100 µl of DMEM+2% BSA, and incubated overnight in PBS-EDTA at 37 °C. Non-incorporated cholesterol was removed by ultracentrifugation as described in TRL isolation.

4.2.4. HBV resecretion and cholesterol efflux

THP macrophages, monocyte derived macrophages and Kupffer cells were preincubated for 2h with William's E basic medium supplemented with 2 mg / ml BSA (fatty acid free) before addition of concentrated supernatant of HepG2.2.15 cells. After 3 hours incubation with 10^8 genome copies / ml HBV virions, cells were washed three times and cultured for further 2h with medium free of HBV. Subsequently, cells were washed twice before chasing with William's E basic medium containing 10% human serum, 100 or 200 µg / ml HDL or 25 µg / ml ApoA-1 as indicated. Supernatant was collected for HBsAg quantification.

For efflux experiments, THP-macrophages were treated as described for HBV resecretion, except that additional 1 µg / ml [^{3}H]-cholesterol -TRL was added to 3h pulse incubation with HBV. Afterwards, cells were washed with heparin-containing medium to remove surface-bound lipoproteins. Supernatant was measured for [^{3}H]-cholesterol by liquid scintillation counting.

4.2.5. HCVcc production

JC1, JC1-luci or JC1-flag were produced as described[285, 286]. Briefly, plasmids were purified using phenol/chloroform method. RNA was transcribed in vitro using T7 polymerase and purified using phenol / chloroform. Huh7.5 cells were electroporated with purified RNA at 975 µF, 270 V and transferred into 150 cm^2 flasks with DMEM complete medium. Cell supernatant was collected every 24h for 5 to 7 days. Supernatant was filter through 0.45 µm filters before further preparation.

To purify the virus by ultracentrifugation, 20% sucrose cushion of at least 10% the total volume of the ultra tube was loaded in the bottom, then the virus stock was applied on top and spin at 100,000 g for 16h at 4 °C. Afterwards, the supernatant were poured off and virus pellet (might not be visible) was resuspend in 200 µl PBS + 0.2% BSA and stored in -80 °C.

4.2.5.1. Production of fluorescence labeled HCV virus

JC1-flag was prepared as mentioned above. Collected supernatant was concentrated 10 fold by Centricon Plus - 70 (Biomax 100, Millipore Corp). 1 ml anti-flag M1 agarose gel was placed into empty PD-1 (GE healthcare) chromatography column. The gel

was washed by loading 5 ml of 0.1 M glycine HCL (pH3.5) for three times, followed by three sequential aliquots of 5 ml TBS. HCV stock was mixed with 10 x TBS / Ca (0.5 M Tris, pH7.4, with 1.5 M NaCl and 100 mM $CaCl_2$). The column was filled completely with virus stock for JC1-flag binding. Multiple passes over the column will improve the binding efficiency. The column was washed three times by 12 ml of TBS / Ca solution. For elution, the column was incubated with 1 ml of TBS / EDTA (TBS containing 2 mM EDTA) for 30 minutes to chelate the calcium ions. Six rounds of elution were performed to elute the virus completely.

Virus was labeled by adding 10 µl (5 mM final concentration) of lipophilic dye DiI (Invitrogen, excitation 549 nm / emission 565 nm) to 1 mL of virus purified as above. Virus and dye were incubated for 1 hour with shaking at room temperature while protected from light. Labeled virus was enriched and purified first by Amicon® Pro Purification System (cutoff = 100 KD) and followed by Bio-spin-P30 (Biorad) to get rid of free dye.

4.2.6. HCV quantification

4.2.6.1. Quantification of HCV infectivity

TCID50 was determined as reported[285]. Huh7.5 cells were seeded at density of $1x10^4$/ well in 96 well plates 24 h before titration. Virus stock was serial diluted and added to cells with 6 replicate for 1 dilution. 72h post infection, cells were fixed and stained with anti-NS3 antibody followed by anti-mouse HRP antibody. Positive cells were counted and $TCID_{50}$ was calculated using the $TCID_{50}$ calculator.

4.2.6.2. Absolute quantification of HCV genome

Extract virus RNA from 100ul supernatant following protocol of Macherey Nagel NucleoSpin RNA II (DNA digestion can be skipped). Virus RNA standards were prepared by serial diluting HCV RNA transcribed *in vitro*. One step PCR was performed using HCV specific probe: 5' **FAM** TAC TGC CTG ATA GGG CGC TTG CGA GTG **TAMRA** 3'. PCR procedures were as following:

Programme		
Reverse transcription	50°C	20 min
Activation	95°C	5 min
Cycling (45x)	95°C	15 s
	60°C	45 s
Cooling	40°C	5 min

4.2.6.3. HCV (-)-strand specific qRT-PCR

HCV (-/+) RNA standard preparation: the sensitivity and specificity of the negative-strand HCV RNA qRT-PCR was assessed using negative and positive HCV RNA standards. (+)-strand RNA was produced using pFK-JC1 as described in secion 4.2.4. To prepare (-)-strand RNA, the same plasmid was first linearized by FspA1 and then *in vitro* transcribed using T3 polymerase. After degradation of the DNA template by RQ1 DNase treatment and RNA purification using phenol-chloroform extraction, the purity of synthetic RNA was evaluated by absorbance ratio of 260nm / 280nm and 260nm / 230nm. The integrity was checked by agarose gel electrophoresis. Concentrations were measured by absorbance at 260nm. The number of copies was obtained by calculation (1 µg (- / +) RNA=$1.8x10^{11}$ copies).

Reverse transcription was carried out using primer tag-RC1 or RC21 for (-) or (+) - strand RNA, respectively.

Taking (-) - strand RNA for example, the procedures were as following:

1) Denature 4 µl RNA template at 70°C for 8 min.
2) RNA template was incubated at 4°C for 5 min in the presence of 200 ng of tag-RC1 primer and 1.25 mM of each deoxynucleoside triphosphate (dNTP) in a total volume of 12 µl.
3) Reverse transcription was carried out for 60min at 60 °C in the presence of 20 U RNaseout™ and 7.5 U Thermoscript™ reverse transcriptase.
4) Adding 1 µl (2 U) RNase H for 20 min incubation at 37 °C

For qPCR, the resulting cDNA from last step was diluted 1:10. Under following program, primer pair (tag / RC21) or pair (RC1 / RC21) was used for minus-strand or plus-strand amplification, respectively.

Programme		
Initial denaturation	95 °C	120s
	95 °C	2s
Cycling (45x)	60 °C	5s
	72 °C	15s
Cooling	40 °C	5min

4.2.7. Molecular Biology

4.2.7.1. DNA extraction

Intracellular DNA has been extracted using the “NucleoSpin® Tissue”-kit. The standard protocol for cultured cells was used except that the silica membrane was dried for two minutes and incubation time before elution was increased to approximately five minutes.

4.2.7.2. RNA extraction

From cultured cell: Cell layers were washed with 1xPBS and RNA was extracted following the instruction of Macherey Nagel NucleoSpin RNA II.
From tissue: Fresh tissue or tissue stored in RNAlater solution was used for RNA extraction. Homogenization of tissue was performed on TissueLyser LT at 50 Hz for 5min. RNA extraction including on-column DNA digestion was performed following the instruction of RNeasy mini kit.

4.2.7.3. RT-PCR

For the synthesis of cDNA, “SuperScript® III First-Strand Synthesis SuperMix for qRT-PCR” was used. 5 µl of 2x RT reaction mix were combined with 1 µl of RT enzyme mix and 4 µl of extracted RNA. cDNA was transcribed in thermocycler with following temperature profile: 25 °C for 5 min, 50 °C for 30 min, 85 °C for 5 min, 4 °C. Then 0.5 µl of RNaseH (5 000 U / ml) were added to each well. After centrifugation, samples were incubated at 37 °C for 20min.

4.2.7.4. qPCR

qPCR was carried out as following unless specified differently: 4 µl of cDNA sample were mixed with 0.5 µl of reverse primer (20 µM), 0.5 µl of forward primer (20 µM) and 5 µl SYBR® Green Mix (Invitrogen, Karlsruhe, Germany). qPCR runs were performed using Prn-p, GAPDH or 18sRNA as reference gene.

4.2.8. Immunofluorescence staining

Cells grown on 4-well-glass slide (Lab-Tek II, Fisher Scientific - Germany, Schwerte, Germany) were fixed with 4% PFA (pH 7.4) for 10 min at room temperature and permeabilized with 0.5% saponin solution. Blocking was performed at room temperature for two hours using PBS buffer containing 0.5% saponin as well as 10% serum produced from species in which the secondary antibody was raised. Primary antibodies were diluted in fresh blocking buffer and incubated with cells overnight at 4 °C. After three times washing with PBS containing 0.5% saponin, the cells were incubated with secondary antibody with 2% blocking serum for 2 hours at room temperature in dark. Then the slide was mounted with Dapi Fluoromount-G (SouthernBiotech, Birmingham, Alabama, USA).

Filipin staining: Cells were fixed as above and washed 3 times with PBS. Following that, cells were incubated with 0.05 mg / ml filipin in PBS / 10% FBS solution for 2h at room temperature. Then slides should be mounted with Fluoromount-G DAPI free medium (SouthernBiotech, Birmingham, Alabama, USA).

5. References

1. Ishibashi H, Nakamura M, Komori A, et al. Liver architecture, cell function, and disease. Semin Immunopathol 2009;31:399-409.
2. Rouiller C. The Liver: Morphology, Biochemistry, Physiology. Academic Press Inc: Elsevier, 2013.
3. Taub R. Liver regeneration: from myth to mechanism. Nat Rev Mol Cell Biol 2004;5:836-47.
4. Kempka G, Kolb-Bachofen V. Binding, uptake, and transcytosis of ligands for mannose-specific receptors in rat liver: an electron microscopic study. Exp Cell Res 1988;176:38-48.
5. Seternes T, Sorensen K, Smedsrod B. Scavenger endothelial cells of vertebrates: a nonperipheral leukocyte system for high-capacity elimination of waste macromolecules. Proc Natl Acad Sci U S A 2002;99:7594-7.
6. Smedsrod B. Clearance function of scavenger endothelial cells. Comp Hepatol 2004;3 Suppl 1:S22.
7. Knolle PA, Germann T, Treichel U, et al. Endotoxin down-regulates T cell activation by antigen-presenting liver sinusoidal endothelial cells. J Immunol 1999;162:1401-7.
8. Wisse E. Observations on the fine structure and peroxidase cytochemistry of normal rat liver Kupffer cells. J Ultrastruct Res 1974;46:393-426.
9. Naito M, Hasegawa G, Ebe Y, et al. Differentiation and function of Kupffer cells. Med Electron Microsc 2004;37:16-28.
10. Friedman SL. Hepatic stellate cells: protean, multifunctional, and enigmatic cells of the liver. Physiol Rev 2008;88:125-72.
11. Senoo H, Kojima N, Sato M. Vitamin A-storing cells (stellate cells). Vitam Horm 2007;75:131-59.
12. Yin C, Evason KJ, Asahina K, et al. Hepatic stellate cells in liver development, regeneration, and cancer. J Clin Invest 2013;123:1902-10.
13. Hoekstra M, Out R, Kruijt JK, et al. Diet induced regulation of genes involved in cholesterol metabolism in rat liver parenchymal and Kupffer cells. J Hepatol 2005;42:400-7.

14. Ikonen E. Cellular cholesterol trafficking and compartmentalization. Nat Rev Mol Cell Biol 2008;9:125-38.
15. Hegele RA. Plasma lipoproteins: genetic influences and clinical implications. Nat Rev Genet 2009;10:109-21.
16. Havel RJ, Eder HA, Bragdon JH. The distribution and chemical composition of ultracentrifugally separated lipoproteins in human serum. J Clin Invest 1955;34:1345-53.
17. Hussain MM, Fatma S, Pan X, et al. Intestinal lipoprotein assembly. Curr Opin Lipidol 2005;16:281-5.
18. Dallinga-Thie GM, Franssen R, Mooij HL, et al. The metabolism of triglyceride-rich lipoproteins revisited: new players, new insight. Atherosclerosis 2010;211:1-8.
19. Ooi EM, Ng TW, Watts GF, et al. Dietary fatty acids and lipoprotein metabolism: new insights and updates. Curr Opin Lipidol 2013;24:192-7.
20. Diffenderfer MR, Schaefer EJ. The composition and metabolism of large and small LDL. Curr Opin Lipidol 2014;25:221-6.
21. Santos-Gallego CG, Badimon JJ, Rosenson RS. Beginning to Understand High-Density Lipoproteins. Endocrinol Metab Clin North Am 2014;43:913-947.
22. Zannis VI, Chroni A, Krieger M. Role of apoA-I, ABCA1, LCAT, and SR-BI in the biogenesis of HDL. J Mol Med (Berl) 2006;84:276-94.
23. Kwiterovich PO, Jr. The metabolic pathways of high-density lipoprotein, low-density lipoprotein, and triglycerides: a current review. Am J Cardiol 2000;86:5L-10L.
24. Lusa S, Heino S, Ikonen E. Differential mobilization of newly synthesized cholesterol and biosynthetic sterol precursors from cells. J Biol Chem 2003;278:19844-51.
25. Yamauchi Y, Reid PC, Sperry JB, et al. Plasma membrane rafts complete cholesterol synthesis by participating in retrograde movement of precursor sterols. J Biol Chem 2007;282:34994-5004.
26. Cruz JC, Chang TY. Fate of endogenously synthesized cholesterol in Niemann-Pick type C1 cells. J Biol Chem 2000;275:41309-16.

27. Mobius W, van Donselaar E, Ohno-Iwashita Y, et al. Recycling compartments and the internal vesicles of multivesicular bodies harbor most of the cholesterol found in the endocytic pathway. Traffic 2003;4:222-31.
28. Sturley SL, Patterson MC, Balch W, et al. The pathophysiology and mechanisms of NP-C disease. Biochim Biophys Acta 2004;1685:83-7.
29. Soccio RE, Breslow JL. Intracellular cholesterol transport. Arterioscler Thromb Vasc Biol 2004;24:1150-60.
30. Ouimet M, Marcel YL. Regulation of lipid droplet cholesterol efflux from macrophage foam cells. Arterioscler Thromb Vasc Biol 2012;32:575-81.
31. Gelissen IC, Harris M, Rye KA, et al. ABCA1 and ABCG1 synergize to mediate cholesterol export to apoA-I. Arterioscler Thromb Vasc Biol 2006;26:534-40.
32. Hassan HH, Denis M, Lee DY, et al. Identification of an ABCA1-dependent phospholipid-rich plasma membrane apolipoprotein A-I binding site for nascent HDL formation: implications for current models of HDL biogenesis. J Lipid Res 2007;48:2428-42.
33. Summers J, Smolec JM, Snyder R. A virus similar to human hepatitis B virus associated with hepatitis and hepatoma in woodchucks. Proc Natl Acad Sci U S A 1978;75:4533-7.
34. Lanford RE, Chavez D, Brasky KM, et al. Isolation of a hepadnavirus from the woolly monkey, a New World primate. Proc Natl Acad Sci U S A 1998;95:5757-61.
35. Mason WS, Seal G, Summers J. Virus of Pekin ducks with structural and biological relatedness to human hepatitis B virus. J Virol 1980;36:829-36.
36. Sprengel R, Kaleta EF, Will H. Isolation and characterization of a hepatitis B virus endemic in herons. J Virol 1988;62:3832-9.
37. David M. Knipe PPMH, MD; Diane E. Griffin, MD, PhD; Robert A. Lamb, PhD, ScD; Malcom A. Martin, MD; Bernard Roizman, ScD etc. Fields Virology: Lippincott Williams & Wilkins, 2007.
38. Locarnini S, Littlejohn M, Aziz MN, et al. Possible origins and evolution of the hepatitis B virus (HBV). Semin Cancer Biol 2013;23:561-75.
39. Gilbert C, Feschotte C. Genomic fossils calibrate the long-term evolution of hepadnaviruses. PLoS Biol 2010;8.

40. Suh A, Brosius J, Schmitz J, et al. The genome of a Mesozoic paleovirus reveals the evolution of hepatitis B viruses. Nat Commun 2013;4:1791.
41. Simmonds P. The origin and evolution of hepatitis viruses in humans. J Gen Virol 2001;82:693-712.
42. Hepatitis B vaccines. Weekly Epidemiological Record. Volume 84. http://www.who.int/wer: World Health Organization, 2009:405-420.
43. Hepatitis B. Global Alert and Response (GAR). http://www.who.int/csr/disease/hepatitis/whocdscsrlyo20022/en/index1.html: World Health Organization.
44. Custer B, Sullivan SD, Hazlet TK, et al. Global epidemiology of hepatitis B virus. J Clin Gastroenterol 2004;38:S158-68.
45. Lavanchy D. Hepatitis B virus epidemiology, disease burden, treatment, and current and emerging prevention and control measures. J Viral Hepat 2004;11:97-107.
46. Shepard CW, Simard EP, Finelli L, et al. Hepatitis B virus infection: epidemiology and vaccination. Epidemiol Rev 2006;28:112-25.
47. Weinbaum CM, Williams I, Mast EE, et al. Recommendations for identification and public health management of persons with chronic hepatitis B virus infection. MMWR Recomm Rep 2008;57:1-20.
48. Kondili LA, Osman H, Mutimer D. The use of lamivudine for patients with acute hepatitis B (a series of cases). J Viral Hepat 2004;11:427-31.
49. Roussos A, Koilakou S, Kalafatas I, et al. Lamivudine treatment for acute severe hepatitis B: report of a case and review of the literature. Acta Gastroenterol Belg 2008;71:30-2.
50. Hyams KC. Risks of chronicity following acute hepatitis B virus infection: a review. Clin Infect Dis 1995;20:992-1000.
51. Guidotti LG, Matzke B, Schaller H, et al. High-level hepatitis B virus replication in transgenic mice. J Virol 1995;69:6158-69.
52. Grimm D, Heeg M, Thimme R. Hepatitis B virus: from immunobiology to immunotherapy. Clin Sci (Lond) 2013;124:77-85.
53. Chisari FV. Rous-Whipple Award Lecture. Viruses, immunity, and cancer: lessons from hepatitis B. Am J Pathol 2000;156:1117-32.

54. Guidotti LG, Rochford R, Chung J, et al. Viral clearance without destruction of infected cells during acute HBV infection. Science 1999;284:825-9.
55. Thimme R, Wieland S, Steiger C, et al. CD8(+) T cells mediate viral clearance and disease pathogenesis during acute hepatitis B virus infection. J Virol 2003;77:68-76.
56. Ferrari C, Penna A, Bertoletti A, et al. Cellular immune response to hepatitis B virus-encoded antigens in acute and chronic hepatitis B virus infection. J Immunol 1990;145:3442-9.
57. Rehermann B. Intrahepatic T cells in hepatitis B: viral control versus liver cell injury. J Exp Med 2000;191:1263-8.
58. Wieland SF, Chisari FV. Stealth and cunning: hepatitis B and hepatitis C viruses. J Virol 2005;79:9369-80.
59. Guidotti LG, Chisari FV. Immunobiology and pathogenesis of viral hepatitis. Annu Rev Pathol 2006;1:23-61.
60. European Association For The Study Of The L. EASL clinical practice guidelines: Management of chronic hepatitis B virus infection. J Hepatol 2012;57:167-85.
61. Balsano C, Alisi A. Viral hepatitis B: established and emerging therapies. Curr Med Chem 2008;15:930-9.
62. Yuen MF, Lai CL. Treatment of chronic hepatitis B: Evolution over two decades. J Gastroenterol Hepatol 2011;26 Suppl 1:138-43.
63. Guan R. Treatment of chronic hepatitis B infection using interferon. Med J Malaysia 2005;60 Suppl B:28-33.
64. Perrillo R. Benefits and risks of interferon therapy for hepatitis B. Hepatology 2009;49:S103-11.
65. Lucifora J, Xia Y, Reisinger F, et al. Specific and nonhepatotoxic degradation of nuclear hepatitis B virus cccDNA. Science 2014;343:1221-8.
66. Guidotti LG, Chisari FV. Noncytolytic control of viral infections by the innate and adaptive immune response. Annu Rev Immunol 2001;19:65-91.
67. Thomas H, Foster G, Platis D. Mechanisms of action of interferon and nucleoside analogues. J Hepatol 2003;39 Suppl 1:S93-8.
68. Tseng TC, Kao JH, Chen DS. Peginterferon alpha in the treatment of chronic hepatitis B. Expert Opin Biol Ther 2014;14:995-1006.

69. Buti M. [Nucleoside and nucleotide analogs in the treatment of chronic hepatitis B]. Enferm Infecc Microbiol Clin 2008;26 Suppl 7:32-8.
70. Chien RN, Liaw YF. Nucleos(t)ide analogues for hepatitis B virus: strategies for long-term success. Best Pract Res Clin Gastroenterol 2008;22:1081-92.
71. Balsano C. Recent advances in antiviral agents: established and innovative therapies for viral hepatitis. Mini Rev Med Chem 2008;8:307-18.
72. Zoulim F, Locarnini S. Hepatitis B virus resistance to nucleos(t)ide analogues. Gastroenterology 2009;137:1593-608 e1-2.
73. Gripon P, Cannie I, Urban S. Efficient inhibition of hepatitis B virus infection by acylated peptides derived from the large viral surface protein. J Virol 2005;79:1613-22.
74. Petersen J, Dandri M, Mier W, et al. Prevention of hepatitis B virus infection in vivo by entry inhibitors derived from the large envelope protein. Nat Biotechnol 2008;26:335-41.
75. Volz T, Allweiss L, Ben MM, et al. The entry inhibitor Myrcludex-B efficiently blocks intrahepatic virus spreading in humanized mice previously infected with hepatitis B virus. J Hepatol 2013;58:861-7.
76. Spellman M MJ. Treatment of hronic hepatitis b infection with dv-601, a therapeutic vaccine. Journal of Hepatology 2011;54:S302.
77. Zhang F, Wang G. A review of non-nucleoside anti-hepatitis B virus agents. Eur J Med Chem 2014;75:267-81.
78. Corporation AR. ARC-520, 2014.
79. Bruss V. Envelopment of the hepatitis B virus nucleocapsid. Virus Res 2004;106:199-209.
80. Bruss V. Hepatitis B virus morphogenesis. World J Gastroenterol 2007;13:65-73.
81. Glebe D, Urban S. Viral and cellular determinants involved in hepadnaviral entry. World J Gastroenterol 2007;13:22-38.
82. Miller RH, Kaneko S, Chung CT, et al. Compact organization of the hepatitis B virus genome. Hepatology 1989;9:322-7.
83. Robinson WS. The genome of hepatitis B virus. Annu Rev Microbiol 1977;31:357-77.

84. Kay A, Zoulim F. Hepatitis B virus genetic variability and evolution. Virus Res 2007;127:164-76.

85. Beck J, Nassal M. Hepatitis B virus replication. World J Gastroenterol 2007;13:48-64.

86. Seeger C, Mason WS. Hepatitis B virus biology. Microbiol Mol Biol Rev 2000;64:51-68.

87. David M. Knipe PPMH, MD; Diane E. Griffin, MD, PhD; Robert A. Lamb, PhD, ScD; Malcom A. Martin, MD; Bernard Roizman, ScD etc. Fields Virology: Lippincott Williams & Wilkins, 2007.

88. Zlotnick A, Cheng N, Stahl SJ, et al. Localization of the C terminus of the assembly domain of hepatitis B virus capsid protein: implications for morphogenesis and organization of encapsidated RNA. Proc Natl Acad Sci U S A 1997;94:9556-61.

89. Gallina A, Bonelli F, Zentilin L, et al. A recombinant hepatitis B core antigen polypeptide with the protamine-like domain deleted self-assembles into capsid particles but fails to bind nucleic acids. J Virol 1989;63:4645-52.

90. Chang C, Enders G, Sprengel R, et al. Expression of the precore region of an avian hepatitis B virus is not required for viral replication. J Virol 1987;61:3322-5.

91. Milich D, Liang TJ. Exploring the biological basis of hepatitis B e antigen in hepatitis B virus infection. Hepatology 2003;38:1075-86.

92. Wang GH, Seeger C. The reverse transcriptase of hepatitis B virus acts as a protein primer for viral DNA synthesis. Cell 1992;71:663-70.

93. Weber M, Bronsema V, Bartos H, et al. Hepadnavirus P protein utilizes a tyrosine residue in the TP domain to prime reverse transcription. J Virol 1994;68:2994-9.

94. Lucifora J, Arzberger S, Durantel D, et al. Hepatitis B virus X protein is essential to initiate and maintain virus replication after infection. J Hepatol 2011;55:996-1003.

95. Zoulim F, Saputelli J, Seeger C. Woodchuck hepatitis virus X protein is required for viral infection in vivo. J Virol 1994;68:2026-30.

96. Schulze A, Gripon P, Urban S. Hepatitis B virus infection initiates with a large surface protein-dependent binding to heparan sulfate proteoglycans. Hepatology 2007;46:1759-68.

97. Yan H, Zhong G, Xu G, et al. Sodium taurocholate cotransporting polypeptide is a functional receptor for human hepatitis B and D virus. Elife 2012;1:e00049.

98. Ni Y, Lempp FA, Mehrle S, et al. Hepatitis B and D viruses exploit sodium taurocholate co-transporting polypeptide for species-specific entry into hepatocytes. Gastroenterology 2014;146:1070-83.

99. Iwamoto M, Watashi K, Tsukuda S, et al. Evaluation and identification of hepatitis B virus entry inhibitors using HepG2 cells overexpressing a membrane transporter NTCP. Biochem Biophys Res Commun 2014;443:808-13.

100. Yan H, Peng B, Liu Y, et al. Viral entry of hepatitis B and D viruses and bile salts transportation share common molecular determinants on sodium taurocholate cotransporting polypeptide. J Virol 2014;88:3273-84.

101. Watashi K, Sluder A, Daito T, et al. Cyclosporin A and its analogs inhibit hepatitis B virus entry into cultured hepatocytes through targeting a membrane transporter, sodium taurocholate cotransporting polypeptide (NTCP). Hepatology 2014;59:1726-37.

102. Yan H, Peng B, He W, et al. Molecular determinants of hepatitis B and D virus entry restriction in mouse sodium taurocholate cotransporting polypeptide. J Virol 2013;87:7977-91.

103. Cooper A, Shaul Y. Clathrin-mediated endocytosis and lysosomal cleavage of hepatitis B virus capsid-like core particles. J Biol Chem 2006;281:16563-9.

104. Macovei A, Radulescu C, Lazar C, et al. Hepatitis B virus requires intact caveolin-1 function for productive infection in HepaRG cells. J Virol 2010;84:243-53.

105. Huang HC, Chen CC, Chang WC, et al. Entry of hepatitis B virus into immortalized human primary hepatocytes by clathrin-dependent endocytosis. J Virol 2012;86:9443-53.

106. Z. G, M. L, W. H, et al. Hepatitis B virus may enter HepG2 cells complemented with human NTCP via macropinocytosis., In the International Meeting on

Molecular Biology of Hepatitis B Viruses, Shanghai, China, 20.10.2013-23.10.2013.

107. Macovei A, Petrareanu C, Lazar C, et al. Regulation of hepatitis B virus infection by Rab5, Rab7, and the endolysosomal compartment. J Virol 2013;87:6415-27.
108. Rabe B, Delaleau M, Bischof A, et al. Nuclear entry of hepatitis B virus capsids involves disintegration to protein dimers followed by nuclear reassociation to capsids. PLoS Pathog 2009;5:e1000563.
109. Kann M, Schmitz A, Rabe B. Intracellular transport of hepatitis B virus. World J Gastroenterol 2007;13:39-47.
110. Schmitz A, Schwarz A, Foss M, et al. Nucleoporin 153 arrests the nuclear import of hepatitis B virus capsids in the nuclear basket. PLoS Pathog 2010;6:e1000741.
111. Nassal M. Hepatitis B viruses: reverse transcription a different way. Virus Res 2008;134:235-49.
112. Terre S, Petit MA, Brechot C. Defective hepatitis B virus particles are generated by packaging and reverse transcription of spliced viral RNAs in vivo. J Virol 1991;65:5539-43.
113. Locarnini S. Molecular virology of hepatitis B virus. Semin Liver Dis 2004;24 Suppl 1:3-10.
114. Wei Y, Neuveut C, Tiollais P, et al. Molecular biology of the hepatitis B virus and role of the X gene. Pathol Biol (Paris) 2010;58:267-72.
115. Dandri M, Locarnini S. New insight in the pathobiology of hepatitis B virus infection. Gut 2012;61 Suppl 1:i6-17.
116. Patient R, Hourioux C, Sizaret PY, et al. Hepatitis B virus subviral envelope particle morphogenesis and intracellular trafficking. J Virol 2007;81:3842-51.
117. Lentz TB, Loeb DD. Roles of the envelope proteins in the amplification of covalently closed circular DNA and completion of synthesis of the plus-strand DNA in hepatitis B virus. J Virol 2011;85:11916-27.
118. Lazar C, Macovei A, Petrescu S, et al. Activation of ERAD pathway by human hepatitis B virus modulates viral and subviral particle production. PLoS One 2012;7:e34169.

119. Bhat P, Snooks MJ, Anderson DA. Hepatocytes traffic and export hepatitis B virus basolaterally by polarity-dependent mechanisms. J Virol 2011;85:12474-81.

120. Watanabe T, Sorensen EM, Naito A, et al. Involvement of host cellular multivesicular body functions in hepatitis B virus budding. Proc Natl Acad Sci U S A 2007;104:10205-10.

121. Schulze-Bergkamen H, Untergasser A, Dax A, et al. Primary human hepatocytes--a valuable tool for investigation of apoptosis and hepatitis B virus infection. J Hepatol 2003;38:736-44.

122. Gripon P, Diot C, Theze N, et al. Hepatitis B virus infection of adult human hepatocytes cultured in the presence of dimethyl sulfoxide. J Virol 1988;62:4136-43.

123. Hantz O, Parent R, Durantel D, et al. Persistence of the hepatitis B virus covalently closed circular DNA in HepaRG human hepatocyte-like cells. J Gen Virol 2009;90:127-35.

124. Gripon P, Rumin S, Urban S, et al. Infection of a human hepatoma cell line by hepatitis B virus. Proc Natl Acad Sci U S A 2002;99:15655-60.

125. Sells MA, Chen ML, Acs G. Production of hepatitis B virus particles in Hep G2 cells transfected with cloned hepatitis B virus DNA. Proc Natl Acad Sci U S A 1987;84:1005-9.

126. Sureau C, Romet-Lemonne JL, Mullins JI, et al. Production of hepatitis B virus by a differentiated human hepatoma cell line after transfection with cloned circular HBV DNA. Cell 1986;47:37-47.

127. Tuttleman JS, Pugh JC, Summers JW. In vitro experimental infection of primary duck hepatocyte cultures with duck hepatitis B virus. J Virol 1986;58:17-25.

128. Dandri M, Volz TK, Lutgehetmann M, et al. Animal models for the study of HBV replication and its variants. J Clin Virol 2005;34 Suppl 1:S54-62.

129. Walter E, Keist R, Niederost B, et al. Hepatitis B virus infection of tupaia hepatocytes in vitro and in vivo. Hepatology 1996;24:1-5.

130. Marion PL, Cullen JM, Azcarraga RR, et al. Experimental transmission of duck hepatitis B virus to Pekin ducks and to domestic geese. Hepatology 1987;7:724-31.

131. Guidotti LG, Matzke B, Pasquinelli C, et al. The hepatitis B virus (HBV) precore protein inhibits HBV replication in transgenic mice. J Virol 1996;70:7056-61.

132. Chisari FV, Pinkert CA, Milich DR, et al. A transgenic mouse model of the chronic hepatitis B surface antigen carrier state. Science 1985;230:1157-60.

133. Isogawa M, Kakimi K, Kamamoto H, et al. Differential dynamics of the peripheral and intrahepatic cytotoxic T lymphocyte response to hepatitis B surface antigen. Virology 2005;333:293-300.

134. Yang PL, Althage A, Chung J, et al. Hydrodynamic injection of viral DNA: a mouse model of acute hepatitis B virus infection. Proc Natl Acad Sci U S A 2002;99:13825-30.

135. Dandri M, Petersen J. Chimeric mouse model of hepatitis B virus infection. J Hepatol 2012;56:493-5.

136. Tsuge M, Hiraga N, Takaishi H, et al. Infection of human hepatocyte chimeric mouse with genetically engineered hepatitis B virus. Hepatology 2005;42:1046-54.

137. Meuleman P, Libbrecht L, De Vos R, et al. Morphological and biochemical characterization of a human liver in a uPA-SCID mouse chimera. Hepatology 2005;41:847-56.

138. Kapoor A, Simmonds P, Gerold G, et al. Characterization of a canine homolog of hepatitis C virus. Proc Natl Acad Sci U S A 2011;108:11608-13.

139. Stapleton JT, Foung S, Muerhoff AS, et al. The GB viruses: a review and proposed classification of GBV-A, GBV-C (HGV), and GBV-D in genus Pegivirus within the family Flaviviridae. J Gen Virol 2011;92:233-46.

140. Burbelo PD, Dubovi EJ, Simmonds P, et al. Serology-enabled discovery of genetically diverse hepaciviruses in a new host. J Virol 2012;86:6171-8.

141. Troesch M, Meunier I, Lapierre P, et al. Study of a novel hypervariable region in hepatitis C virus (HCV) E2 envelope glycoprotein. Virology 2006;352:357-67.

142. Neumann AU, Lam NP, Dahari H, et al. Hepatitis C viral dynamics in vivo and the antiviral efficacy of interferon-alpha therapy. Science 1998;282:103-7.

143. Gottwein JM, Scheel TK, Jensen TB, et al. Development and characterization of hepatitis C virus genotype 1-7 cell culture systems: role of CD81 and

scavenger receptor class B type I and effect of antiviral drugs. Hepatology 2009;49:364-77.

144. Simmonds P, Bukh J, Combet C, et al. Consensus proposals for a unified system of nomenclature of hepatitis C virus genotypes. Hepatology 2005;42:962-73.

145. Simmonds P. Genetic diversity and evolution of hepatitis C virus--15 years on. J Gen Virol 2004;85:3173-88.

146. Makuwa M, Souquiere S, Telfer P, et al. Hepatitis viruses in non-human primates. J Med Primatol 2006;35:384-7.

147. Quan PL, Firth C, Conte JM, et al. Bats are a major natural reservoir for hepaciviruses and pegiviruses. Proc Natl Acad Sci U S A 2013;110:8194-9.

148. Pol S, Vallet-Pichard A, Corouge M, et al. Hepatitis C: epidemiology, diagnosis, natural history and therapy. Contrib Nephrol 2012;176:1-9.

149. Shepard CW, Finelli L, Alter MJ. Global epidemiology of hepatitis C virus infection. Lancet Infect Dis 2005;5:558-67.

150. Lavanchy D. The global burden of hepatitis C. Liver Int 2009;29 Suppl 1:74-81.

151. Lavanchy D. Evolving epidemiology of hepatitis C virus. Clin Microbiol Infect 2011;17:107-15.

152. Kamal SM, Nasser IA. Hepatitis C genotype 4: What we know and what we don't yet know. Hepatology 2008;47:1371-83.

153. Frank C, Mohamed MK, Strickland GT, et al. The role of parenteral antischistosomal therapy in the spread of hepatitis C virus in Egypt. Lancet 2000;355:887-91.

154. Mohd Hanafiah K, Groeger J, Flaxman AD, et al. Global epidemiology of hepatitis C virus infection: new estimates of age-specific antibody to HCV seroprevalence. Hepatology 2013;57:1333-42.

155. Kohla M, Bonacini M. Pathogenesis of hepatitis C virus infection. Minerva Gastroenterol Dietol 2006;52:107-23.

156. Alberti A, Boccato S, Vario A, et al. Therapy of acute hepatitis C. Hepatology 2002;36:S195-200.

157. National Institutes of H. National Institutes of Health Consensus Development Conference Statement: Management of hepatitis C: 2002--June 10-12, 2002. Hepatology 2002;36:S3-20.

158. Heim MH. 25 years of interferon-based treatment of chronic hepatitis C: an epoch coming to an end. Nat Rev Immunol 2013;13:535-42.

159. Scheel TK, Rice CM. Understanding the hepatitis C virus life cycle paves the way for highly effective therapies. Nat Med 2013;19:837-49.

160. Catanese MT, Uryu K, Kopp M, et al. Ultrastructural analysis of hepatitis C virus particles. Proc Natl Acad Sci U S A 2013;110:9505-10.

161. Merz A, Long G, Hiet MS, et al. Biochemical and morphological properties of hepatitis C virus particles and determination of their lipidome. J Biol Chem 2011;286:3018-32.

162. Andre P, Komurian-Pradel F, Deforges S, et al. Characterization of low- and very-low-density hepatitis C virus RNA-containing particles. J Virol 2002;76:6919-28.

163. Nielsen SU, Bassendine MF, Burt AD, et al. Association between hepatitis C virus and very-low-density lipoprotein (VLDL)/LDL analyzed in iodixanol density gradients. J Virol 2006;80:2418-28.

164. Lindenbach BD, Meuleman P, Ploss A, et al. Cell culture-grown hepatitis C virus is infectious in vivo and can be recultured in vitro. Proc Natl Acad Sci U S A 2006;103:3805-9.

165. Icard V, Diaz O, Scholtes C, et al. Secretion of hepatitis C virus envelope glycoproteins depends on assembly of apolipoprotein B positive lipoproteins. PLoS One 2009;4:e4233.

166. Moradpour D, Penin F, Rice CM. Replication of hepatitis C virus. Nat Rev Microbiol 2007;5:453-63.

167. Bukh J, Purcell RH, Miller RH. Sequence analysis of the 5' noncoding region of hepatitis C virus. Proc Natl Acad Sci U S A 1992;89:4942-6.

168. Friebe P, Lohmann V, Krieger N, et al. Sequences in the 5' nontranslated region of hepatitis C virus required for RNA replication. J Virol 2001;75:12047-57.

169. Reynolds JE, Kaminski A, Carroll AR, et al. Internal initiation of translation of hepatitis C virus RNA: the ribosome entry site is at the authentic initiation codon. RNA 1996;2:867-78.

170. Yanagi M, St Claire M, Emerson SU, et al. In vivo analysis of the 3' untranslated region of the hepatitis C virus after in vitro mutagenesis of an infectious cDNA clone. Proc Natl Acad Sci U S A 1999;96:2291-5.

171. Kolykhalov AA, Feinstone SM, Rice CM. Identification of a highly conserved sequence element at the 3' terminus of hepatitis C virus genome RNA. J Virol 1996;70:3363-71.

172. Friebe P, Boudet J, Simorre JP, et al. Kissing-loop interaction in the 3' end of the hepatitis C virus genome essential for RNA replication. J Virol 2005;79:380-92.

173. Santolini E, Migliaccio G, La Monica N. Biosynthesis and biochemical properties of the hepatitis C virus core protein. J Virol 1994;68:3631-41.

174. Irshad M, Dhar I. Hepatitis C virus core protein: an update on its molecular biology, cellular functions and clinical implications. Med Princ Pract 2006;15:405-16.

175. McLauchlan J, Lemberg MK, Hope G, et al. Intramembrane proteolysis promotes trafficking of hepatitis C virus core protein to lipid droplets. EMBO J 2002;21:3980-8.

176. Branch AD, Stump DD, Gutierrez JA, et al. The hepatitis C virus alternate reading frame (ARF) and its family of novel products: the alternate reading frame protein/F-protein, the double-frameshift protein, and others. Semin Liver Dis 2005;25:105-17.

177. Bain C, Parroche P, Lavergne JP, et al. Memory T-cell-mediated immune responses specific to an alternative core protein in hepatitis C virus infection. J Virol 2004;78:10460-9.

178. Bartosch B, Cosset FL. Cell entry of hepatitis C virus. Virology 2006;348:1-12.

179. Pavlovic D, Neville DC, Argaud O, et al. The hepatitis C virus p7 protein forms an ion channel that is inhibited by long-alkyl-chain iminosugar derivatives. Proc Natl Acad Sci U S A 2003;100:6104-8.

180. Sakai A, Claire MS, Faulk K, et al. The p7 polypeptide of hepatitis C virus is critical for infectivity and contains functionally important genotype-specific sequences. Proc Natl Acad Sci U S A 2003;100:11646-51.

181. Pallaoro M, Lahm A, Biasiol G, et al. Characterization of the hepatitis C virus NS2/3 processing reaction by using a purified precursor protein. J Virol 2001;75:9939-46.

182. Lohmann V, Korner F, Koch J, et al. Replication of subgenomic hepatitis C virus RNAs in a hepatoma cell line. Science 1999;285:110-3.

183. Ma Y, Anantpadma M, Timpe JM, et al. Hepatitis C virus NS2 protein serves as a scaffold for virus assembly by interacting with both structural and nonstructural proteins. J Virol 2011;85:86-97.

184. Yi M, Ma Y, Yates J, et al. Trans-complementation of an NS2 defect in a late step in hepatitis C virus (HCV) particle assembly and maturation. PLoS Pathog 2009;5:e1000403.

185. Bazan JF, Fletterick RJ. Detection of a trypsin-like serine protease domain in flaviviruses and pestiviruses. Virology 1989;171:637-9.

186. Wardell AD, Errington W, Ciaramella G, et al. Characterization and mutational analysis of the helicase and NTPase activities of hepatitis C virus full-length NS3 protein. J Gen Virol 1999;80 (Pt 3):701-9.

187. Bartenschlager R, Lohmann V, Wilkinson T, et al. Complex formation between the NS3 serine-type proteinase of the hepatitis C virus and NS4A and its importance for polyprotein maturation. J Virol 1995;69:7519-28.

188. Lin C, Thomson JA, Rice CM. A central region in the hepatitis C virus NS4A protein allows formation of an active NS3-NS4A serine proteinase complex in vivo and in vitro. J Virol 1995;69:4373-80.

189. Bartenschlager R, Ahlborn-Laake L, Mous J, et al. Nonstructural protein 3 of the hepatitis C virus encodes a serine-type proteinase required for cleavage at the NS3/4 and NS4/5 junctions. J Virol 1993;67:3835-44.

190. Dumont S, Cheng W, Serebrov V, et al. RNA translocation and unwinding mechanism of HCV NS3 helicase and its coordination by ATP. Nature 2006;439:105-8.

191. Horner SM, Gale M, Jr. Regulation of hepatic innate immunity by hepatitis C virus. Nat Med 2013;19:879-88.

192. Egger D, Wolk B, Gosert R, et al. Expression of hepatitis C virus proteins induces distinct membrane alterations including a candidate viral replication complex. J Virol 2002;76:5974-84.

193. Tellinghuisen TL, Marcotrigiano J, Gorbalenya AE, et al. The NS5A protein of hepatitis C virus is a zinc metalloprotein. J Biol Chem 2004;279:48576-87.

194. Tellinghuisen TL, Foss KL, Treadaway JC, et al. Identification of residues required for RNA replication in domains II and III of the hepatitis C virus NS5A protein. J Virol 2008;82:1073-83.

195. Tellinghuisen TL, Foss KL, Treadaway J. Regulation of hepatitis C virion production via phosphorylation of the NS5A protein. PLoS Pathog 2008;4:e1000032.

196. Masaki T, Suzuki R, Murakami K, et al. Interaction of hepatitis C virus nonstructural protein 5A with core protein is critical for the production of infectious virus particles. J Virol 2008;82:7964-76.

197. Appel N, Zayas M, Miller S, et al. Essential role of domain III of nonstructural protein 5A for hepatitis C virus infectious particle assembly. PLoS Pathog 2008;4:e1000035.

198. Lohmann V, Korner F, Herian U, et al. Biochemical properties of hepatitis C virus NS5B RNA-dependent RNA polymerase and identification of amino acid sequence motifs essential for enzymatic activity. J Virol 1997;71:8416-28.

199. Cheng JC, Chang MF, Chang SC. Specific interaction between the hepatitis C virus NS5B RNA polymerase and the 3' end of the viral RNA. J Virol 1999;73:7044-9.

200. Germi R, Crance JM, Garin D, et al. Cellular glycosaminoglycans and low density lipoprotein receptor are involved in hepatitis C virus adsorption. J Med Virol 2002;68:206-15.

201. Monazahian M, Bohme I, Bonk S, et al. Low density lipoprotein receptor as a candidate receptor for hepatitis C virus. J Med Virol 1999;57:223-9.

202. Agnello V, Abel G, Elfahal M, et al. Hepatitis C virus and other flaviviridae viruses enter cells via low density lipoprotein receptor. Proc Natl Acad Sci U S A 1999;96:12766-71.

203. Martin DN, Uprichard SL. Identification of transferrin receptor 1 as a hepatitis C virus entry factor. Proc Natl Acad Sci U S A 2013;110:10777-82.

204. Sainz B, Jr., Barretto N, Martin DN, et al. Identification of the Niemann-Pick C1-like 1 cholesterol absorption receptor as a new hepatitis C virus entry factor. Nat Med 2012;18:281-5.

205. Lupberger J, Zeisel MB, Xiao F, et al. EGFR and EphA2 are host factors for hepatitis C virus entry and possible targets for antiviral therapy. Nat Med 2011;17:589-95.

206. Ploss A, Evans MJ, Gaysinskaya VA, et al. Human occludin is a hepatitis C virus entry factor required for infection of mouse cells. Nature 2009;457:882-6.

207. Evans MJ, von Hahn T, Tscherne DM, et al. Claudin-1 is a hepatitis C virus co-receptor required for a late step in entry. Nature 2007;446:801-5.

208. Scarselli E, Ansuini H, Cerino R, et al. The human scavenger receptor class B type I is a novel candidate receptor for the hepatitis C virus. EMBO J 2002;21:5017-25.

209. Pileri P, Uematsu Y, Campagnoli S, et al. Binding of hepatitis C virus to CD81. Science 1998;282:938-41.

210. Zahid MN, Turek M, Xiao F, et al. The postbinding activity of scavenger receptor class B type I mediates initiation of hepatitis C virus infection and viral dissemination. Hepatology 2013;57:492-504.

211. Dao Thi VL, Granier C, Zeisel MB, et al. Characterization of hepatitis C virus particle subpopulations reveals multiple usage of the scavenger receptor BI for entry steps. J Biol Chem 2012;287:31242-57.

212. Blanchard E, Belouzard S, Goueslain L, et al. Hepatitis C virus entry depends on clathrin-mediated endocytosis. J Virol 2006;80:6964-72.

213. Timpe JM, Stamataki Z, Jennings A, et al. Hepatitis C virus cell-cell transmission in hepatoma cells in the presence of neutralizing antibodies. Hepatology 2008;47:17-24.

214. Valli MB, Crema A, Lanzilli G, et al. Molecular and cellular determinants of cell-to-cell transmission of HCV in vitro. J Med Virol 2007;79:1491-9.

215. Tscherne DM, Jones CT, Evans MJ, et al. Time- and temperature-dependent activation of hepatitis C virus for low-pH-triggered entry. J Virol 2006;80:1734-41.

216. Li Y, Masaki T, Yamane D, et al. Competing and noncompeting activities of miR-122 and the 5' exonuclease Xrn1 in regulation of hepatitis C virus replication. Proc Natl Acad Sci U S A 2013;110:1881-6.

217. Yang F, Robotham JM, Nelson HB, et al. Cyclophilin A is an essential cofactor for hepatitis C virus infection and the principal mediator of cyclosporine resistance in vitro. J Virol 2008;82:5269-78.

218. Watashi K, Ishii N, Hijikata M, et al. Cyclophilin B is a functional regulator of hepatitis C virus RNA polymerase. Mol Cell 2005;19:111-22.

219. Binder M, Quinkert D, Bochkarova O, et al. Identification of determinants involved in initiation of hepatitis C virus RNA synthesis by using intergenotypic replicase chimeras. J Virol 2007;81:5270-83.

220. Bartenschlager R, Penin F, Lohmann V, et al. Assembly of infectious hepatitis C virus particles. Trends Microbiol 2011;19:95-103.

221. Miyanari Y, Atsuzawa K, Usuda N, et al. The lipid droplet is an important organelle for hepatitis C virus production. Nat Cell Biol 2007;9:1089-97.

222. Shavinskaya A, Boulant S, Penin F, et al. The lipid droplet binding domain of hepatitis C virus core protein is a major determinant for efficient virus assembly. J Biol Chem 2007;282:37158-69.

223. Counihan NA, Rawlinson SM, Lindenbach BD. Trafficking of hepatitis C virus core protein during virus particle assembly. PLoS Pathog 2011;7:e1002302.

224. Huang H, Sun F, Owen DM, et al. Hepatitis C virus production by human hepatocytes dependent on assembly and secretion of very low-density lipoproteins. Proc Natl Acad Sci U S A 2007;104:5848-53.

225. Ariumi Y, Kuroki M, Maki M, et al. The ESCRT system is required for hepatitis C virus production. PLoS One 2011;6:e14517.

226. Tellinghuisen TL, Evans MJ, von Hahn T, et al. Studying hepatitis C virus: making the best of a bad virus. J Virol 2007;81:8853-67.

227. Bigger CB, Brasky KM, Lanford RE. DNA microarray analysis of chimpanzee liver during acute resolving hepatitis C virus infection. J Virol 2001;75:7059-66.

228. Wang N, Liang Y, Devaraj S, et al. Toll-like receptor 3 mediates establishment of an antiviral state against hepatitis C virus in hepatoma cells. J Virol 2009;83:9824-34.

229. Seki E, Brenner DA. Toll-like receptors and adaptor molecules in liver disease: update. Hepatology 2008;48:322-35.

230. Loo YM, Owen DM, Li K, et al. Viral and therapeutic control of IFN-beta promoter stimulator 1 during hepatitis C virus infection. Proc Natl Acad Sci U S A 2006;103:6001-6.

231. Arnaud N, Dabo S, Akazawa D, et al. Hepatitis C virus reveals a novel early control in acute immune response. PLoS Pathog 2011;7:e1002289.

232. Ivashkiv LB, Donlin LT. Regulation of type I interferon responses. Nat Rev Immunol 2014;14:36-49.

233. Perry AK, Chen G, Zheng D, et al. The host type I interferon response to viral and bacterial infections. Cell Res 2005;15:407-22.

234. Schoggins JW, Rice CM. Interferon-stimulated genes and their antiviral effector functions. Curr Opin Virol 2011;1:519-25.

235. Stetson DB, Medzhitov R. Type I interferons in host defense. Immunity 2006;25:373-81.

236. Barrett S, Sweeney M, Crowe J. Host immune responses in hepatitis C virus clearance. Eur J Gastroenterol Hepatol 2005;17:1089-97.

237. Shoukry NH, Cawthon AG, Walker CM. Cell-mediated immunity and the outcome of hepatitis C virus infection. Annu Rev Microbiol 2004;58:391-424.

238. Meylan E, Curran J, Hofmann K, et al. Cardif is an adaptor protein in the RIG-I antiviral pathway and is targeted by hepatitis C virus. Nature 2005;437:1167-72.

239. Li K, Foy E, Ferreon JC, et al. Immune evasion by hepatitis C virus NS3/4A protease-mediated cleavage of the Toll-like receptor 3 adaptor protein TRIF. Proc Natl Acad Sci U S A 2005;102:2992-7.

240. Garaigorta U, Chisari FV. Hepatitis C virus blocks interferon effector function by inducing protein kinase R phosphorylation. Cell Host Microbe 2009;6:513-22.

241. Crotta S, Brazzoli M, Piccioli D, et al. Hepatitis C virions subvert natural killer cell activation to generate a cytokine environment permissive for infection. J Hepatol 2010;52:183-90.

242. Tseng CT, Klimpel GR. Binding of the hepatitis C virus envelope protein E2 to CD81 inhibits natural killer cell functions. J Exp Med 2002;195:43-9.

243. Heim MH. Innate immunity and HCV. J Hepatol 2013;58:564-74.

244. Kau A, Vermehren J, Sarrazin C. Treatment predictors of a sustained virologic response in hepatitis B and C. J Hepatol 2008;49:634-51.

245. Bowen DG, Walker CM. Adaptive immune responses in acute and chronic hepatitis C virus infection. Nature 2005;436:946-52.

246. Farci P, Alter HJ, Wong DC, et al. Prevention of hepatitis C virus infection in chimpanzees after antibody-mediated in vitro neutralization. Proc Natl Acad Sci U S A 1994;91:7792-6.

247. Zhang P, Zhong L, Struble EB, et al. Depletion of interfering antibodies in chronic hepatitis C patients and vaccinated chimpanzees reveals broad cross-genotype neutralizing activity. Proc Natl Acad Sci U S A 2009;106:7537-41.

248. Edwards VC, Tarr AW, Urbanowicz RA, et al. The role of neutralizing antibodies in hepatitis C virus infection. J Gen Virol 2012;93:1-19.

249. Lai ME, Mazzoleni AP, Argiolu F, et al. Hepatitis C virus in multiple episodes of acute hepatitis in polytransfused thalassaemic children. Lancet 1994;343:388-90.

250. Farci P, Alter HJ, Govindarajan S, et al. Lack of protective immunity against reinfection with hepatitis C virus. Science 1992;258:135-40.

251. Di Lorenzo C, Angus AG, Patel AH. Hepatitis C virus evasion mechanisms from neutralizing antibodies. Viruses 2011;3:2280-300.

252. Jo J, Aichele U, Kersting N, et al. Analysis of CD8+ T-cell-mediated inhibition of hepatitis C virus replication using a novel immunological model. Gastroenterology 2009;136:1391-401.

253. Park SH, Rehermann B. Immune responses to HCV and other hepatitis viruses. Immunity 2014;40:13-24.

254. Cooper S, Erickson AL, Adams EJ, et al. Analysis of a successful immune response against hepatitis C virus. Immunity 1999;10:439-49.

255. Gerlach JT, Diepolder HM, Jung MC, et al. Recurrence of hepatitis C virus after loss of virus-specific CD4(+) T-cell response in acute hepatitis C. Gastroenterology 1999;117:933-41.

256. Missale G, Bertoni R, Lamonaca V, et al. Different clinical behaviors of acute hepatitis C virus infection are associated with different vigor of the anti-viral cell-mediated immune response. J Clin Invest 1996;98:706-14.

257. Yerly D, Heckerman D, Allen TM, et al. Increased cytotoxic T-lymphocyte epitope variant cross-recognition and functional avidity are associated with hepatitis C virus clearance. J Virol 2008;82:3147-53.

258. Spangenberg HC, Viazov S, Kersting N, et al. Intrahepatic CD8+ T-cell failure during chronic hepatitis C virus infection. Hepatology 2005;42:828-37.

259. Soderholm J, Ahlen G, Kaul A, et al. Relation between viral fitness and immune escape within the hepatitis C virus protease. Gut 2006;55:266-74.

260. Seifert U, Liermann H, Racanelli V, et al. Hepatitis C virus mutation affects proteasomal epitope processing. J Clin Invest 2004;114:250-9.

261. Urbani S, Amadei B, Fisicaro P, et al. Outcome of acute hepatitis C is related to virus-specific CD4 function and maturation of antiviral memory CD8 responses. Hepatology 2006;44:126-39.

262. Kaplan DE, Sugimoto K, Newton K, et al. Discordant role of CD4 T-cell response relative to neutralizing antibody and CD8 T-cell responses in acute hepatitis C. Gastroenterology 2007;132:654-66.

263. Dolganiuc A, Chang S, Kodys K, et al. Hepatitis C virus (HCV) core protein-induced, monocyte-mediated mechanisms of reduced IFN-alpha and plasmacytoid dendritic cell loss in chronic HCV infection. J Immunol 2006;177:6758-68.

264. Thimme R, Binder M, Bartenschlager R. Failure of innate and adaptive immune responses in controlling hepatitis C virus infection. FEMS Microbiol Rev 2012;36:663-83.

265. Ge D, Fellay J, Thompson AJ, et al. Genetic variation in IL28B predicts hepatitis C treatment-induced viral clearance. Nature 2009;461:399-401.

266. Sugiyama M, Tanaka Y, Wakita T, et al. Genetic variation of the IL-28B promoter affecting gene expression. PLoS One 2011;6:e26620.

267. Neumann-Haefelin C, McKiernan S, Ward S, et al. Dominant influence of an HLA-B27 restricted CD8+ T cell response in mediating HCV clearance and evolution. Hepatology 2006;43:563-72.

268. Grimaldi V, Sommese L, Picascia A, et al. Association between human leukocyte antigen class I and II alleles and hepatitis C virus infection in high-risk hemodialysis patients awaiting kidney transplantation. Hum Immunol 2013;74:1629-32.

269. Vejbaesya S, Songsivilai S, Tanwandee T, et al. HLA association with hepatitis C virus infection. Hum Immunol 2000;61:348-53.

270. Houghton M. The long and winding road leading to the identification of the hepatitis C virus. J Hepatol 2009;51:939-48.

271. Pietschmann T, Lohmann V, Kaul A, et al. Persistent and transient replication of full-length hepatitis C virus genomes in cell culture. J Virol 2002;76:4008-21.

272. Kato N, Sugiyama K, Namba K, et al. Establishment of a hepatitis C virus subgenomic replicon derived from human hepatocytes infected in vitro. Biochem Biophys Res Commun 2003;306:756-66.

273. Zhu H, Elyar J, Foss R, et al. Primary human hepatocyte culture for HCV study. Methods Mol Biol 2009;510:373-82.

274. Blight KJ, McKeating JA, Rice CM. Highly permissive cell lines for subgenomic and genomic hepatitis C virus RNA replication. J Virol 2002;76:13001-14.

275. Lohmann V, Bartenschlager R. On the history of hepatitis C virus cell culture systems. J Med Chem 2014;57:1627-42.

276. Blight KJ, Kolykhalov AA, Rice CM. Efficient initiation of HCV RNA replication in cell culture. Science 2000;290:1972-4.

277. Blight KJ, McKeating JA, Marcotrigiano J, et al. Efficient replication of hepatitis C virus genotype 1a RNAs in cell culture. J Virol 2003;77:3181-90.

278. Lohmann V, Korner F, Dobierzewska A, et al. Mutations in hepatitis C virus RNAs conferring cell culture adaptation. J Virol 2001;75:1437-49.

279. Saeed M, Gondeau C, Hmwe S, et al. Replication of hepatitis C virus genotype 3a in cultured cells. Gastroenterology 2013;144:56-58 e7.

280. Krieger N, Lohmann V, Bartenschlager R. Enhancement of hepatitis C virus RNA replication by cell culture-adaptive mutations. J Virol 2001;75:4614-24.

281. Bartosch B, Dubuisson J, Cosset FL. Infectious hepatitis C virus pseudo-particles containing functional E1-E2 envelope protein complexes. J Exp Med 2003;197:633-42.

282. Hsu M, Zhang J, Flint M, et al. Hepatitis C virus glycoproteins mediate pH-dependent cell entry of pseudotyped retroviral particles. Proc Natl Acad Sci U S A 2003;100:7271-6.

283. Castet V, Moradpour D. A model for the study of hepatitis C virus entry. Hepatology 2003;38:771-4.

284. Zhong J, Gastaminza P, Cheng G, et al. Robust hepatitis C virus infection in vitro. Proc Natl Acad Sci U S A 2005;102:9294-9.

285. Wakita T, Pietschmann T, Kato T, et al. Production of infectious hepatitis C virus in tissue culture from a cloned viral genome. Nat Med 2005;11:791-6.

286. Lindenbach BD, Evans MJ, Syder AJ, et al. Complete replication of hepatitis C virus in cell culture. Science 2005;309:623-6.

287. Steinmann E, Pietschmann T. Cell culture systems for hepatitis C virus. Curr Top Microbiol Immunol 2013;369:17-48.

288. Muchmore E, Popper H, Peterson DA, et al. Non-A, non-B hepatitis-related hepatocellular carcinoma in a chimpanzee. J Med Primatol 1988;17:235-46.

289. Zhao X, Tang ZY, Klumpp B, et al. Primary hepatocytes of Tupaia belangeri as a potential model for hepatitis C virus infection. J Clin Invest 2002;109:221-32.

290. Amako Y, Tsukiyama-Kohara K, Katsume A, et al. Pathogenesis of hepatitis C virus infection in Tupaia belangeri. J Virol 2010;84:303-11.

291. Bissig KD, Wieland SF, Tran P, et al. Human liver chimeric mice provide a model for hepatitis B and C virus infection and treatment. J Clin Invest 2010;120:924-30.

292. Steenbergen RH, Joyce MA, Lund G, et al. Lipoprotein profiles in SCID/uPA mice transplanted with human hepatocytes become human-like and correlate with HCV infection success. Am J Physiol Gastrointest Liver Physiol 2010;299:G844-54.

293. Ploss A, Rice CM. Towards a small animal model for hepatitis C. EMBO Rep 2009;10:1220-7.

294. Legrand N, Ploss A, Balling R, et al. Humanized mice for modeling human infectious disease: challenges, progress, and outlook. Cell Host Microbe 2009;6:5-9.

295. Dorner M, Horwitz JA, Donovan BM, et al. Completion of the entire hepatitis C virus life cycle in genetically humanized mice. Nature 2013;501:237-41.

296. Dorner M, Horwitz JA, Robbins JB, et al. A genetically humanized mouse model for hepatitis C virus infection. Nature 2011;474:208-11.

297. Perlemuter G, Sabile A, Letteron P, et al. Hepatitis C virus core protein inhibits microsomal triglyceride transfer protein activity and very low density lipoprotein secretion: a model of viral-related steatosis. FASEB J 2002;16:185-94.

298. Esser K. Das Hepatitis B Virus folgt dem Transport der neutralen Lipide in die Leber und in die Hepatozyten, um seine Wirtszelle zu erreichen und zu infizieren: Universität zu Köln, 2012.

299. Asabe S, Wieland SF, Chattopadhyay PK, et al. The size of the viral inoculum contributes to the outcome of hepatitis B virus infection. J Virol 2009;83:9652-62.

300. Jilbert AR, Miller DS, Scougall CA, et al. Kinetics of duck hepatitis B virus infection following low dose virus inoculation: one virus DNA genome is infectious in neonatal ducks. Virology 1996;226:338-45.

301. Cuchel M, Rader DJ. Macrophage reverse cholesterol transport: key to the regression of atherosclerosis? Circulation 2006;113:2548-55.

302. Liu L, Bortnick AE, Nickel M, et al. Effects of apolipoprotein A-I on ATP-binding cassette transporter A1-mediated efflux of macrophage phospholipid and cholesterol: formation of nascent high density lipoprotein particles. J Biol Chem 2003;278:42976-84.

303. Bielicki JK, McCall MR, Forte TM. Apolipoprotein A-I promotes cholesterol release and apolipoprotein E recruitment from THP-1 macrophage-like foam cells. J Lipid Res 1999;40:85-92.

304. Schroeder F, Holland JF, Bieber LL. Fluorometric evidence for the binding of cholesterol to the filipin complex. J Antibiot (Tokyo) 1971;24:846-9.

305. Wustner D, Mondal M, Tabas I, et al. Direct observation of rapid internalization and intracellular transport of sterol by macrophage foam cells. Traffic 2005;6:396-412.

306. Mukherjee S, Zha X, Tabas I, et al. Cholesterol distribution in living cells: fluorescence imaging using dehydroergosterol as a fluorescent cholesterol analog. Biophys J 1998;75:1915-25.

307. Heeren J, Grewal T, Laatsch A, et al. Recycling of apoprotein E is associated with cholesterol efflux and high density lipoprotein internalization. J Biol Chem 2003;278:14370-8.

308. Wang N, Tall AR. Regulation and mechanisms of ATP-binding cassette transporter A1-mediated cellular cholesterol efflux. Arterioscler Thromb Vasc Biol 2003;23:1178-84.

309. Kamps JA, Kruijt JK, Kuiper J, et al. Characterization of the interaction of acetylated LDL and oxidatively modified LDL with human liver parenchymal and Kupffer cells in culture. Arterioscler Thromb 1992;12:1079-87.

310. Bolte S, Cordelieres FP. A guided tour into subcellular colocalization analysis in light microscopy. J Microsc 2006;224:213-32.

311. Dunn KW, Kamocka MM, McDonald JH. A practical guide to evaluating colocalization in biological microscopy. Am J Physiol Cell Physiol 2011;300:C723-42.

312. Babbey CM, Ahktar N, Wang E, et al. Rab10 regulates membrane transport through early endosomes of polarized Madin-Darby canine kidney cells. Mol Biol Cell 2006;17:3156-75.

313. Manders EM, Stap J, Brakenhoff GJ, et al. Dynamics of three-dimensional replication patterns during the S-phase, analysed by double labelling of DNA and confocal microscopy. J Cell Sci 1992;103 (Pt 3):857-62.

314. E. M. M. MANDERS FJVaAA. Measurement of co-localization of objects in dual-colour confocal images. 1993;169.

315. Ghosh S. Macrophage cholesterol homeostasis and metabolic diseases: critical role of cholesteryl ester mobilization. Expert Rev Cardiovasc Ther 2011;9:329-40.

316. Havel RJ. Triglyceride-rich lipoproteins and plasma lipid transport. Arterioscler Thromb Vasc Biol 2010;30:9-19.

317. Heeren J, Weber W, Beisiegel U. Intracellular processing of endocytosed triglyceride-rich lipoproteins comprises both recycling and degradation. J Cell Sci 1999;112 (Pt 3):349-59.

318. Heeren J, Grewal T, Jackle S, et al. Recycling of apolipoprotein E and lipoprotein lipase through endosomal compartments in vivo. J Biol Chem 2001;276:42333-8.

319. Heeren J, Grewal T, Laatsch A, et al. Impaired recycling of apolipoprotein E4 is associated with intracellular cholesterol accumulation. J Biol Chem 2004;279:55483-92.

320. Schneider WJ, Kovanen PT, Brown MS, et al. Familial dysbetalipoproteinemia. Abnormal binding of mutant apoprotein E to low density lipoprotein receptors of human fibroblasts and membranes from liver and adrenal of rats, rabbits, and cows. J Clin Invest 1981;68:1075-85.

321. Toniutto P, Fattovich G, Fabris C, et al. Genetic polymorphism at the apolipoprotein E locus affects the outcome of chronic hepatitis B. J Med Virol 2010;82:224-331.

322. Ahn SJ, Kim DK, Kim SS, et al. Association between apolipoprotein E genotype, chronic liver disease, and hepatitis B virus. Clin Mol Hepatol 2012;18:295-301.

323. Kolios G, Valatas V, Kouroumalis E. Role of Kupffer cells in the pathogenesis of liver disease. World J Gastroenterol 2006;12:7413-20.

324. Pepe G, Cifarelli A, Paradisi F, et al. HBsAg uptake by macrophages in vitro: an immunofluorescence study. Experientia 1979;35:382-4.

325. Hosel M, Quasdorff M, Wiegmann K, et al. Not interferon, but interleukin-6 controls early gene expression in hepatitis B virus infection. Hepatology 2009;50:1773-82.

326. Wu J, Meng Z, Jiang M, et al. Hepatitis B virus suppresses toll-like receptor-mediated innate immune responses in murine parenchymal and nonparenchymal liver cells. Hepatology 2009;49:1132-40.

327. Li H, Zheng HW, Chen H, et al. Hepatitis B virus particles preferably induce Kupffer cells to produce TGF-beta1 over pro-inflammatory cytokines. Dig Liver Dis 2012;44:328-33.

328. Kawai Y, Smedsrod B, Elvevold K, et al. Uptake of lithium carmine by sinusoidal endothelial and Kupffer cells of the rat liver: new insights into the classical vital staining and the reticulo-endothelial system. Cell Tissue Res 1998;292:395-410.

329. Geijtenbeek TB, Kwon DS, Torensma R, et al. DC-SIGN, a dendritic cell-specific HIV-1-binding protein that enhances trans-infection of T cells. Cell 2000;100:587-97.

330. Geijtenbeek TB, Torensma R, van Vliet SJ, et al. Identification of DC-SIGN, a novel dendritic cell-specific ICAM-3 receptor that supports primary immune responses. Cell 2000;100:575-85.

331. Cormier EG, Durso RJ, Tsamis F, et al. L-SIGN (CD209L) and DC-SIGN (CD209) mediate transinfection of liver cells by hepatitis C virus. Proc Natl Acad Sci U S A 2004;101:14067-72.

332. Ludwig IS, Lekkerkerker AN, Depla E, et al. Hepatitis C virus targets DC-SIGN and L-SIGN to escape lysosomal degradation. J Virol 2004;78:8322-32.

333. Breiner KM, Schaller H, Knolle PA. Endothelial cell-mediated uptake of a hepatitis B virus: a new concept of liver targeting of hepatotropic microorganisms. Hepatology 2001;34:803-8.

334. Pietschmann T, Kaul A, Koutsoudakis G, et al. Construction and characterization of infectious intragenotypic and intergenotypic hepatitis C virus chimeras. Proc Natl Acad Sci U S A 2006;103:7408-13.

335. Sainz B, Jr., Barretto N, Uprichard SL. Hepatitis C virus infection in phenotypically distinct Huh7 cell lines. PLoS One 2009;4:e6561.

336. Lan L, Gorke S, Rau SJ, et al. Hepatitis C virus infection sensitizes human hepatocytes to TRAIL-induced apoptosis in a caspase 9-dependent manner. J Immunol 2008;181:4926-35.

337. Deng L, Adachi T, Kitayama K, et al. Hepatitis C virus infection induces apoptosis through a Bax-triggered, mitochondrion-mediated, caspase 3-dependent pathway. J Virol 2008;82:10375-85.

338. Sileri P, Schena S, Morini S, et al. Pyruvate inhibits hepatic ischemia-reperfusion injury in rats. Transplantation 2001;72:27-30.

339. Michalopoulos GK, Bowen WC, Mule K, et al. Histological organization in hepatocyte organoid cultures. Am J Pathol 2001;159:1877-87.

340. Nichols RBDaM. THE ACTIN CYTOSKELETON IN LIVER FUNCTION. The Liver in Biology and Disease. Volume 15: Elsevier, 2004:49-79.

341. Sato M, Suzuki S, Senoo H. Hepatic stellate cells: unique characteristics in cell biology and phenotype. Cell Struct Funct 2003;28:105-12.

342. Makowska Z, Heim MH. Interferon signaling in the liver during hepatitis C virus infection. Cytokine 2012;59:460-6.

343. Gardner JP, Durso RJ, Arrigale RR, et al. L-SIGN (CD 209L) is a liver-specific capture receptor for hepatitis C virus. Proc Natl Acad Sci U S A 2003;100:4498-503.

344. Lozach PY, Lortat-Jacob H, de Lacroix de Lavalette A, et al. DC-SIGN and L-SIGN are high affinity binding receptors for hepatitis C virus glycoprotein E2. J Biol Chem 2003;278:20358-66.

345. Doyle S, Vaidya S, O'Connell R, et al. IRF3 mediates a TLR3/TLR4-specific antiviral gene program. Immunity 2002;17:251-63.

346. Lenardo MJ, Fan CM, Maniatis T, et al. The involvement of NF-kappa B in beta-interferon gene regulation reveals its role as widely inducible mediator of signal transduction. Cell 1989;57:287-94.

347. Thanos D, Maniatis T. Identification of the rel family members required for virus induction of the human beta interferon gene. Mol Cell Biol 1995;15:152-64.

348. Hoffmann JA, Kafatos FC, Janeway CA, et al. Phylogenetic perspectives in innate immunity. Science 1999;284:1313-8.

349. Lai WK, Sun PJ, Zhang J, et al. Expression of DC-SIGN and DC-SIGNR on human sinusoidal endothelium: a role for capturing hepatitis C virus particles. Am J Pathol 2006;169:200-8.

350. Broxtermann M. Die Erkennung viraler Partikel durch Rezeptoren des angeborenen Immunsystems am Beispiel des HBV und AAV: Technischen Universität München.

351. Eiseman B, Liem DS, Raffucci F. Heterologous liver perfusion in treatment of hepatic failure. Ann Surg 1965;162:329-45.

352. Abouna GM, Fisher LM, Still WJ, et al. Acute hepatic coma successfully treated by extracorporeal baboon liver perfusions. Br Med J 1972;1:23-5.

353. Abouna GM, Ganguly P, Jabur S, et al. Successful ex vivo liver perfusion system for hepatic failure pending liver regeneration or liver transplantation. Transplant Proc 2001;33:1962-4.

354. Butler AJ, Rees MA, Wight DG, et al. Successful extracorporeal porcine liver perfusion for 72 hr. Transplantation 2002;73:1212-8.

355. Abouna GM, Ganguly PK, Hamdy HM, et al. Extracorporeal liver perfusion system for successful hepatic support pending liver regeneration or liver

transplantation: a pre-clinical controlled trial. Transplantation 1999;67:1576-83.

356. Nakamura N, Kamiyama Y, Takai S, et al. Ex vivo liver perfusion with arterial blood from a pig with ischemic liver failure. Artif Organs 1999;23:153-60.

357. Alzaraa A, Al-Leswas D, Chung WY, et al. Contrast-enhanced ultrasound detects perfusion defects in an ex vivo porcine liver model: a useful tool for the study of hepatic reperfusion. J Artif Organs 2013;16:475-82.

358. Gravante G, Ong SL, Metcalfe MS, et al. The porcine hepatic arterial supply, its variations and their influence on the extracorporeal perfusion of the liver. J Surg Res 2011;168:56-61.

359. Harrington M. State of the (research) chimp. Lab Anim (NY) 2012;41:31.

360. Health NIo. Statement by NIH Director Dr. Francis Collins on the Institute of Medicine report addressing the scientific need for the use of chimpanzees in research, 2011.

361. de la Monte SM, Arcidi JM, Moore GW, et al. Midzonal necrosis as a pattern of hepatocellular injury after shock. Gastroenterology 1984;86:627-31.

362. Gravante G, Ong SL, McGregor A, et al. Histological changes during extracorporeal perfusions of the porcine liver: implications for temporary support during acute liver failures. J Artif Organs 2013;16:218-28.

363. Ganesan LP, Mohanty S, Kim J, et al. Rapid and efficient clearance of blood-borne virus by liver sinusoidal endothelium. PLoS Pathog 2011;7:e1002281.

364. Iio M, Wagner HN, Jr., Scheffel U, et al. Studies of the reticuloendothelial system (RES). I. Measurement of the phagocytic capacity of the RES in man and dog. J Clin Invest 1963;42:417-26.

365. Benacerraf B, Sebestyen MM, Schlossman S. A quantitative study of the kinetics of blood clearance of P32-labelled Escherichia coli and Staphylococci by the reticuloendothelial system. J Exp Med 1959;110:27-48.

366. Metchnikoff É. Lectures on the comparative pathology of inflammation, delivered at the Pasteur Instutute in 1891. Lectures on the comparative pathology of inflammation, delivered at the Pasteur Instutute in 1891: London, Kegan Paul, 1845-1916.

367. Brunner KT, Hurez D, Mc CR, et al. Blood clearance of P32-labeled vesicular stomatitis and Newcastle disease viruses by the reticuloendothelial system in mice. J Immunol 1960;85:99-105.

368. Gavosto F, Ficq A. Radioautographic study of the localization of tobacco mosaic virus antigen. Nature 1953;172:406-7.

369. Wisse E. An ultrastructural characterization of the endothelial cell in the rat liver sinusoid under normal and various experimental conditions, as a contribution to the distinction between endothelial and Kupffer cells. J Ultrastruct Res 1972;38:528-62.

370. Eriksson S, Fraser JR, Laurent TC, et al. Endothelial cells are a site of uptake and degradation of hyaluronic acid in the liver. Exp Cell Res 1983;144:223-8.

371. Fraser JR, Laurent TC, Pertoft H, et al. Plasma clearance, tissue distribution and metabolism of hyaluronic acid injected intravenously in the rabbit. Biochem J 1981;200:415-24.

372. Garcia-Retortillo M, Forns X, Feliu A, et al. Hepatitis C virus kinetics during and immediately after liver transplantation. Hepatology 2002;35:680-7.

373. Lozach PY, Amara A, Bartosch B, et al. C-type lectins L-SIGN and DC-SIGN capture and transmit infectious hepatitis C virus pseudotype particles. J Biol Chem 2004;279:32035-45.

374. Pohlmann S, Zhang J, Baribaud F, et al. Hepatitis C virus glycoproteins interact with DC-SIGN and DC-SIGNR. J Virol 2003;77:4070-80.

375. Schlepper-Schafer J, Hulsmann D, Djovkar A, et al. Endocytosis via galactose receptors in vivo. Ligand size directs uptake by hepatocytes and/or liver macrophages. Exp Cell Res 1986;165:494-506.

376. Mims CA. The response of mice to large intravenous injections of ectromelia virus. II. The growth of virus in the liver. Br J Exp Pathol 1959;40:543-50.

377. Meis JF, Verhave JP, Jap PH, et al. Malaria parasites--discovery of the early liver form. Nature 1983;302:424-6.

378. Mims CA. The response of mice to large intravenous injections of ectromelia virus. I. The fate of injected virus. Br J Exp Pathol 1959;40:533-42.

379. Revie D, Salahuddin SZ. Role of macrophages and monocytes in hepatitis C virus infections. World J Gastroenterol 2014;20:2777-84.

380. Fletcher NF, Wilson GK, Murray J, et al. Hepatitis C virus infects the endothelial cells of the blood-brain barrier. Gastroenterology 2012;142:634-643 e6.

381. Lech M, Susanti HE, Rommele C, et al. Quantitative expression of C-type lectin receptors in humans and mice. Int J Mol Sci 2012;13:10113-31.

382. Balch SG, Greaves DR, Gordon S, et al. Organization of the mouse macrophage C-type lectin (Mcl) gene and identification of a subgroup of related lectin molecules. Eur J Immunogenet 2002;29:61-4.

383. Park CG, Takahara K, Umemoto E, et al. Five mouse homologues of the human dendritic cell C-type lectin, DC-SIGN. Int Immunol 2001;13:1283-90.

384. Pohlmann S, Baribaud F, Lee B, et al. DC-SIGN interactions with human immunodeficiency virus type 1 and 2 and simian immunodeficiency virus. J Virol 2001;75:4664-72.

385. Lee B, Leslie G, Soilleux E, et al. cis Expression of DC-SIGN allows for more efficient entry of human and simian immunodeficiency viruses via CD4 and a coreceptor. J Virol 2001;75:12028-38.

386. Bashirova AA, Geijtenbeek TB, van Duijnhoven GC, et al. A dendritic cell-specific intercellular adhesion molecule 3-grabbing nonintegrin (DC-SIGN)-related protein is highly expressed on human liver sinusoidal endothelial cells and promotes HIV-1 infection. J Exp Med 2001;193:671-8.

387. Walters RW, Freimuth P, Moninger TO, et al. Adenovirus fiber disrupts CAR-mediated intercellular adhesion allowing virus escape. Cell 2002;110:789-99.

388. Bergelson JM, Cunningham JA, Droguett G, et al. Isolation of a common receptor for Coxsackie B viruses and adenoviruses 2 and 5. Science 1997;275:1320-3.

389. Koutsoudakis G, Herrmann E, Kallis S, et al. The level of CD81 cell surface expression is a key determinant for productive entry of hepatitis C virus into host cells. J Virol 2007;81:588-98.

390. Sorensen KK, McCourt P, Berg T, et al. The scavenger endothelial cell: a new player in homeostasis and immunity. Am J Physiol Regul Integr Comp Physiol 2012;303:R1217-30.

391. Charlton M. Liver biopsy, viral kinetics, and the impact of viremia on severity of hepatitis C virus recurrence. Liver Transpl 2003;9:S58-62.

392. Wolff G, Worgall S, van Rooijen N, et al. Enhancement of in vivo adenovirus-mediated gene transfer and expression by prior depletion of tissue macrophages in the target organ. J Virol 1997;71:624-9.

393. Alemany R, Suzuki K, Curiel DT. Blood clearance rates of adenovirus type 5 in mice. J Gen Virol 2000;81:2605-9.

394. Tao N, Gao GP, Parr M, et al. Sequestration of adenoviral vector by Kupffer cells leads to a nonlinear dose response of transduction in liver. Mol Ther 2001;3:28-35.

395. Zhang Y, Chirmule N, Gao GP, et al. Acute cytokine response to systemic adenoviral vectors in mice is mediated by dendritic cells and macrophages. Mol Ther 2001;3:697-707.

396. Zhu J, Huang X, Yang Y. Innate immune response to adenoviral vectors is mediated by both Toll-like receptor-dependent and -independent pathways. J Virol 2007;81:3170-80.

397. Liu Q, Muruve DA. Molecular basis of the inflammatory response to adenovirus vectors. Gene Ther 2003;10:935-40.

398. Muruve DA. The innate immune response to adenovirus vectors. Hum Gene Ther 2004;15:1157-66.

399. Marukian S, Andrus L, Sheahan TP, et al. Hepatitis C virus induces interferon-lambda and interferon-stimulated genes in primary liver cultures. Hepatology 2011;54:1913-23.

400. Thomas E, Gonzalez VD, Li Q, et al. HCV infection induces a unique hepatic innate immune response associated with robust production of type III interferons. Gastroenterology 2012;142:978-88.

401. Foy E, Li K, Wang C, et al. Regulation of interferon regulatory factor-3 by the hepatitis C virus serine protease. Science 2003;300:1145-8.

402. Lau DT, Negash A, Chen J, et al. Innate immune tolerance and the role of kupffer cells in differential responses to interferon therapy among patients with HCV genotype 1 infection. Gastroenterology 2013;144:402-413 e12.

403. Hornung V, Ellegast J, Kim S, et al. 5'-Triphosphate RNA is the ligand for RIG-I. Science 2006;314:994-7.

404. Stone AE, Giugliano S, Schnell G, et al. Hepatitis C virus pathogen associated molecular pattern (PAMP) triggers production of lambda-interferons by human plasmacytoid dendritic cells. PLoS Pathog 2013;9:e1003316.

405. Chatel-Chaix L, Bartenschlager R. Dengue virus- and hepatitis C virus-induced replication and assembly compartments: the enemy inside--caught in the web. J Virol 2014;88:5907-11.

406. Liu L, Botos I, Wang Y, et al. Structural basis of toll-like receptor 3 signaling with double-stranded RNA. Science 2008;320:379-81.

407. Alexopoulou L, Holt AC, Medzhitov R, et al. Recognition of double-stranded RNA and activation of NF-kappaB by Toll-like receptor 3. Nature 2001;413:732-8.

408. Karpala AJ, Doran TJ, Bean AG. Immune responses to dsRNA: implications for gene silencing technologies. Immunol Cell Biol 2005;83:211-6.

409. Le Goffic R, Balloy V, Lagranderie M, et al. mice TLR3 for influenza virus!!!Detrimental contribution of the Toll-like receptor (TLR)3 to influenza A virus-induced acute pneumonia. PLoS Pathog 2006;2:e53.

410. Gowen BB, Hoopes JD, Wong MH, et al. TLR3 deletion limits mortality and disease severity due to Phlebovirus infection. J Immunol 2006;177:6301-7.

411. Kariko K, Ni H, Capodici J, et al. mRNA is an endogenous ligand for Toll-like receptor 3. J Biol Chem 2004;279:12542-50.

412. Tatematsu M, Nishikawa F, Seya T, et al. Toll-like receptor 3 recognizes incomplete stem structures in single-stranded viral RNA. Nat Commun 2013;4:1833.

413. Wang Y, Li J, Wang X, et al. Hepatitis C virus impairs TLR3 signaling and inhibits IFN-lambda 1 expression in human hepatoma cell line. Innate Immun 2014;20:3-11.

414. Li J, Ye L, Wang X, et al. Induction of interferon-gamma contributes to Toll-like receptor 3-mediated herpes simplex virus type 1 inhibition in astrocytes. J Neurosci Res 2012;90:399-406.

415. Matsumoto M, Oshiumi H, Seya T. Antiviral responses induced by the TLR3 pathway. Rev Med Virol 2011;21:67-77.

416. Jenkins KA, Mansell A. TIR-containing adaptors in Toll-like receptor signalling. Cytokine 2010;49:237-44.

417. Blasius AL, Beutler B. Intracellular toll-like receptors. Immunity 2010;32:305-15.

418. Su AI, Pezacki JP, Wodicka L, et al. Genomic analysis of the host response to hepatitis C virus infection. Proc Natl Acad Sci U S A 2002;99:15669-74.

419. Park H, Serti E, Eke O, et al. IL-29 is the dominant type III interferon produced by hepatocytes during acute hepatitis C virus infection. Hepatology 2012;56:2060-70.

420. Honda K, Yanai H, Negishi H, et al. IRF-7 is the master regulator of type-I interferon-dependent immune responses. Nature 2005;434:772-7.

421. Ank N, West H, Bartholdy C, et al. Lambda interferon (IFN-lambda), a type III IFN, is induced by viruses and IFNs and displays potent antiviral activity against select virus infections in vivo. J Virol 2006;80:4501-9.

422. Onoguchi K, Yoneyama M, Takemura A, et al. Viral infections activate types I and III interferon genes through a common mechanism. J Biol Chem 2007;282:7576-81.

6. Publications and meetings

6.1. Publications

1. “Hepatitis B Virus targets Kupffer cell cholesterol transport to trans-infect hepatocytes.”
Knud Esser*, **Xiaoming Cheng***, Julie Lucifora, Dirk Wohlleber, Jochen Wettengel, Mathias Broxtermann, Daniel Hartmann, Norbert Hüser, Wolfgang E. Thasler, Mathias Heikenwälder, Georg Gasteiger, Axel Walch, Percy Knolle, and Ulrike Protzer (co-first author, *submitted)*

2. “Visualization of HCV host cell targeting in *ex vivo* perfused human liver. ”
Xiaoming Cheng, Knud Esser, Julia Graf, Jochen Weltengel, Norbert Hüser, Daniel Hartmann, Ulrike Protzer. Journal of Hepatology 2014, Volume 60, Supplement 1, Page S20

3. “Specific and Nonhepatotoxic Degradation of Nuclear Hepatitis B Virus cccDNA”
Julie Lucifora, Yuchen Xia, Florian Reisinger, Ke Zhang, Daniela Stadler, **Xiaoming Cheng**, Martin F. Sprinzl, Herwig Koppensteiner, Zuzanna Makowska, Tassilo Volz, Caroline Remouchamps, Wen-Min Chou, Wolfgang E. Thasler, Norbert Hüser, David Durantel, T. Jake Liang, Carsten Münk, Markus H. Heim, Jeffrey L. Browning, Emmanuel Dejardin, Maura Dandri, Michael Schindler, Mathias Heikenwalder, Ulrike Protzer. Science 2014, Volume. 343, no. 6176 Page 1221-1228

4. “Interferons induce degradation of HBV cccDNA.”
Yuchen Xia, Julie Lucifora, Ke Zhang, **Xiaoming Cheng**, Daniela Stadler, Florian Reisinger, Martin Feuerherd, Zuzanna Makowska, Daniel Hartmann, Wolfgang Thasler, Markus Heim, Mathias Heikenwaelder and Ulrike Protzer. Hepatology 2013, Volume 58, Issue S1, Page 277A

5. “Interferon-alpha elimilates HBV cccDNA via base excision repair pathway.”
Xia Y. J. Lucifora, K. Zhang, **X. Cheng**, F. Reisinger, M. Feuerherd, M. Heikenwaelder, U. Protzer. Journal of Hepatology 2013, Volume 58, Supplement 1,

Page S57

6.2. Meetings

September 3-6, 2014, Los Angeles, United States

International Meeting on Molecular Biology of Hepatitis B Viruses

-Young Investigator Award, Oral presentation: Tubular connection mediated HBV spreading between hepatocytes *in vitro*

April 9-13, 2014, London, United Kingdom

The International Liver Congress™ 2014, 49th annual meeting of the European Association for the Study of the Liver

-Young Investigator Award, Oral presentation: Visualization of HCV host cell targeting in *ex vivo* perfused human liver

August 25–30, 2013, Regensburg, Germany

Microscopy Conference 2013

-Poster presentation: Characterization of HBV transport pathways in macrophages

June 22-25, 2012, Shanghai, China

14th International Symposium on Viral Hepatitis and Liver Disease

- Poster presentation: Hepatitis B virus hijacks the neutral lipid transport to target and infect hepatocytes

7. Acknowledgements

I would never have been able to finish my dissertation without the guidance of my committee members, help from my co-workers and friends and support from my family.

I would like to give my deepest gratitude to my supervisor, Prof. Dr. Ulrike Protzer. Thanks her for providing me the opportunity to undertake PhD studies at the virology institute, for her kind support and invaluable wisdom in the last few years. I would also like to thank my other committee members, Prof. Dr. Mathias Heikenwälder and Prof. Dr. Markus Gehard, who have been guiding my studies by providing encouraging and constructive feedbacks.

I am grateful to Knud Esser, for introducing me the human liver perfusion model and always being ready to give his best help and suggestions. Many thanks go to him also for his considerable patience in correcting every single piece of my paperwork and for his continuous support and encouragement during my long study journey, without which I wouldn't survive easily. And thanks to Julia Graf for teaching me the HCV cell culture assays and for the feedback, discussions and proof reading of my work. Thanks to Hanaa Gaber, Wenmin-Chou and Lili Zhao for being here with me. Thanks to Romina Bester for sharing experimental work with me. Thanks to Mathias Broxtermann, Daniela Stadler, Frank Thiele, Karin Krebs, Nina Boettinger, Christian Bach, Theresa Asen, Natalie Röder, Stefanie Graf, Clemens Jaeger, Christina Dargel, Julie Lucifora, Kathrin Kappes, Jochen Wettengel and so on for sharing the technical expertise, discussions and for making my time in the lab very much enjoyable.

I also own a lot of thanks to the former Chinese fellows Dr. Ke Zhang and Dr. Yuchen Xia. They have left the group but they are sadly missed. I thank them for their constant care and help, not only in work as colleagues but also as elder brothers in a big family. I could not be luckier to have them in accompany since the first moment I arrived in Germany and hope that I can in turn pass the help and support that they have given to me. I would also want to thank Katrin, Harry, Silke and Ralph for their lovely food, the enjoyable talks and their help in solving difficulties in my life here. They opened many other windows of Germany to me and so that my experience in Germany is more enriched.

My study was funded by Chinese Scholarship Council (CSC). I would also like to express my thanks to all the members within this network for their support.
I would be extremely foolish to think any of this would have been possible without the love and support of my mom, who were always there for me, often unthanked, but always needed.

To those all I offer my sincerest gratitude.